

Climate change and fluvial flood peaks

FCERM Research & Development Programme research report

Date: March 2023

Version: SC150009/R2

We are the Environment Agency. We protect and improve the environment.

We help people and wildlife adapt to climate change and reduce its impacts, including flooding, drought, sea level rise and coastal erosion.

We improve the quality of our water, land and air by tackling pollution. We work with businesses to help them comply with environmental regulations. A healthy and diverse environment enhances people's lives and contributes to economic growth.

We can't do this alone. We work as part of the Defra group (Department for Environment, Food & Rural Affairs), with the rest of government, local councils, businesses, civil society groups and local communities to create a better place for people and wildlife.

Published by:

Environment Agency
Horizon House, Deanery Road,
Bristol, BS1 5AH

www.gov.uk/environment-agency

© Environment Agency 2023

All rights reserved. This document may be reproduced with prior permission of the Environment Agency.

Further copies of this report are available from our publications catalogue: [Flood and Coastal Erosion Risk Management Research and Development Programme](#) or our National Customer Contact Centre: 03708 506 506

Email: fcerm.evidence@environment-agency.gov.uk

Author(s):

Kay AL, Rudd AC, Fry M, Nash G

Keywords:

Flood, climate change, response surface, uplift, change factor

Research contractor:

UK Centre for Ecology & Hydrology
Maclean Building,
Benson Lane
Wallingford
Oxon
OX10 8BB
Tel: 01491 838800

Environment Agency's Project Manager:
Stuart Allen

Project number:
SC150009/R2

Citation:

Environment Agency (2023) Climate change and fluvial flood peaks.
Environment Agency, Bristol.

Executive summary

Climate change will alter future flood risk, so planners need information about how fluvial flood peaks may change. This report describes the most recent update to our projections of fluvial flood risk and builds on previous studies across Great Britain.

Earlier work (FD2020) developed a sensitivity framework for estimating the impacts of climate change on flood flows and applied it with hydrological models to 154 catchments across Great Britain. Typical flood response types were identified, along with decision trees to estimate the response type of other gauged but unmodelled catchments by using known catchment properties. A later study (FD2648) combined the response type information with the UK Climate Projections 2009 (UKCP09) (UKCP09) to estimate impacts of climate change on flood peaks for river basin regions across Great Britain.

This latest study reported here uses the sensitivity framework approach applied using a national-scale grid-based hydrological model that produces flood response surfaces for every gauged or ungauged 1km square. This provides a nationally consistent assessment of the sensitivity of flood peaks to climatic changes across Great Britain, and removes a number of steps from previous approaches, for example, the use of decision trees. This eliminates some sources of uncertainty resulting from those steps. We used the UK Climate Projections 2018 (UKCP18) for the study and compared the results with those from UKCP09.

The UKCP18 climate projections are overlaid on the modelled flood response surfaces to provide probabilistic impacts on flood peaks for any 1km river cell, for a range of future time slices and emissions scenarios. Therefore, impact ranges are location-specific, in contrast to results from FD2648, which provided regional average impact ranges. The range of impact uncertainty is large, as the climate projections cover a broad range of changes.

The overall method produces a large amount of data, because there are over 12,000 1km river cells in Great Britain, 3,000 ensembles of climate projections (for UKCP18), as well as combinations of future time slices, emissions scenarios, flood return periods and temperature/potential (T/PE) evaporation scenarios. A web tool that provides a convenient way to explore these data at individual locations is available at:

<https://eip.ceh.ac.uk/hydrology/cc-impacts/>

A number of regional summaries and comparisons show that climate modelling uncertainty and emissions scenario uncertainty are greater for later time slices, but that there is relatively little difference in impacts for different return period flood peaks and for different T/PE scenarios. The full set of results are provided through an interactive web tool for the purposes of this project. These results were subsequently amalgamated to [peak river flow climate change allowances](#) in England by management catchment for use within operational guidance and advice.

The regional changes to flood peaks under the UKCP18 projections are similar to those derived using the older UKCP09 projections with the new grid-based modelling, and to the existing guidance, based on UKCP09 and catchment-based modelling plus decision trees.

Contents

Executive summary	iii
1 Introduction	10
1.1 Background	10
1.2 Developments	13
2 Methods	14
2.1 Hydrological model and driving data	14
2.2 The sensitivity framework: definition	14
2.3 The sensitivity framework: application with G2G	16
2.4 Analysis of response surfaces and types	18
2.5 The climate change projections	20
2.6 Application of climate change projections	21
2.7 Sensitivity framework uncertainty	22
2.8 Hydrological model uncertainty	23
3 Results	26
3.1 Response types	26
3.2 Consistency of sensitivity domain with climate change projections	33
3.3 Impacts from UKCP18 projections	37
3.4 Comparing impacts from the UKCP18 and UKCP09 projections	50
3.5 Indicator of hydrological model uncertainty	59
4 Conclusions	62
4.1 Summary	62
4.2 Discussion	62
4.3 Possible future work	65
References	67
Appendix A: Indicator of hydrological model uncertainty	72
A.1 Modelled response types	72
A.2 Baseline model performance	78
Appendix B: Response types	83
B.1 Mapping response types	83
B.2 Checking for new response types	87
Appendix C: Consistency of sensitivity domain with climate change projections	92
C.1 Precipitation change projections	92
C.2 Temperature change projections	99
Appendix D: Web tool for exploring results	100

List of Figures

Figure 1.1 Schematic of the 9 flood response types of FD2020	10
Figure 1.2 Composite (average) flood response surfaces (first row) and standard deviation surfaces (second row) for each of the 9 flood response types of FD2020, for changes in 20-year return period flood peaks. The axes and colour key are shown at the bottom	11
Figure 1.4 Potential range of regional impacts (percentage change in 20-year return period flood peaks) for the 2080s time slice and high emissions scenario (lower end of range - left maps, middle - centre maps, higher end - right maps) (Kay and others, 2014a,b)	12
Figure 1.3 Estimated flood response family of each NRFA catchment in England and Wales (left) and Scotland (right), for changes in 20-year return period flood peaks (note that some response types were merged into groups) (from Kay and others, 2014a,b)	12
Figure 2.1 Example set of flood response surfaces for a single 1km river cell. Response surfaces are shown for 3 return periods (10, 20 and 50 years; left to right) and 3 T/PE scenarios (Medium-August, Low-August and High-January; top to bottom)	17
Figure 2.2 Example comparison of a modelled response surface (top) with each of the 9 average response surfaces (bottom) in terms of rmsd (given above each average response surface). In this case, the closest type (that with the lowest rmsd) is Mixed	18
Figure 2.3 Example Taylor diagram (right), showing the positions of 3 modelled response surfaces (bottom-left) when compared to a reference response surface (in this case, the Neutral average response surface, top-left)	19
Figure 2.4 The 19 river basin regions covering Great Britain from a) UKCP09 and b) UKCP18. The Orkney and Shetland region is excluded from both maps, as are the 3 regions covering Northern Ireland. Note that there are some differences between the UKCP09 and UKCP18 regions (highlighted). Some minor changes have also been made to the regions to make them consistent with the UK Centre for Ecology & Hydrology's (UKCEH's) 1km flow directions	20
Figure 2.5 Example of overlaying UKCP09 climate change projections on a modelled response surface (left). Blue dots show each of the 10,000 projections for one river basin region (North Highlands), emissions scenarios (A1B) and future time slice (2080s). The black contours delineate densities of 10, 100 and 500 projections per 5% \times 5% sensitivity domain square. Also shown is the cdf of the percentage changes in flood peaks extracted from the response surface using the projections (right). In this case, the changes are for 20-year return period flood peaks for a location in north-west Scotland.	22
Figure 3.1 Map showing the response type of the modelled response surface for each 1km river cell in GB, for changes in 20-year return period flood peaks using the Medium-August T/PE scenario	27
Figure 3.2 Stacked bar charts showing the balance of response types over the 19 river basin regions, for changes in flood peaks at 3 return periods (10-, 20 and 50- years), for the Medium-August T/PE scenario	28
Figure 3.3 Stacked bar charts showing the balance of response types over the 19 river basin regions, for each of the 3 T/PE scenarios (Medium-August, Low-August and High-January), for changes in 20-year return period flood peaks	29
Figure 3.4 Taylor diagrams comparing the modelled response surfaces for every 1km river cell (catchment area \geq 100km ²) with the FD2020 Neutral	

average response surface as reference. The points are coloured by their identified response type (section 3.1.1)	30
Figure 3.5 Example 'Extra-Sensitive' response surface (left) and the FD2020 average Sensitive response surface (right)	31
Figure 3.6 Comparison of rmsd for each response type, for each of the 3 return period and T/PE scenarios	32
Figure 3.7 Example Damped-Extreme response surface (left) and the FD2020 average Damped-Extreme response surface (right)	32
Figure 3.8 Contour plots showing UKCP18 P harmonic mean (X_0) versus amplitude (A) for each river basin region, for the 2020s, 2050s and 2080s (magenta, green and blue respectively) with RCP8.5 emissions. Contours delineate densities of 5 and 50 projections per 5% \times 5% sensitivity domain square (dotted and solid lines respectively)	34
Figure 3.9 Histograms showing the distribution of the UKCP18 P harmonic phase (Φ) for each river basin region, for the 2020s, 2050s and 2080s (magenta, green and blue respectively) with RCP8.5 emissions	35
Figure 3.10 Distribution of the 3 harmonic function parameters (top row; X_0 , A , Φ) from the UKCP18 probabilistic temperature change projections for the UK, for the 2080s with RCP6.0 emissions. The bottom row shows correlations between each pair of parameters	36
Figure 3.11 Map showing the 50th percentile of change in 20-year return period flood peaks for the 2080s under RCP8.5 emissions (Medium-August T/PE scenario)	38
Figure 3.12 Maps showing the regional means (top) and SDs (bottom) of 5 percentiles of change in 20-year return period flood peaks (10th, 25th, 50th, 75th and 90th; left to right) for 3 time slices (2020s, 2050s and 2080s) under RCP8.5 emissions (Medium-August T/PE scenario)	39
Figure 3.13 Plots comparing the regional means of changes in 20-year return period flood peaks using UKCP18 probabilistic projections for 3 time slices (2020s, 2050s and 2080s) under 4 emissions scenarios (RCP2.6, RCP4.5, RCP6.0 and RCP8.5) (Medium-August T/PE scenario). Each plot shows 5 percentiles of change (10th, 25th, 50th, 75th and 90th)	41
Figure 3.14 Plots comparing the regional SDs of changes in 20-year return period flood peaks using UKCP18 probabilistic projections for 3 time slices (2020s, 2050s and 2080s) under 4 emissions scenarios (RCP2.6, RCP4.5, RCP6.0 and RCP8.5) (Medium-August T/PE scenario). Each plot shows 5 percentiles of change (10th, 25th, 50th, 75th and 90th)	42
Figure 3.15 Plots comparing the regional means of changes in 10-, 20- and 50-year return period flood peaks using UKCP18 probabilistic projections for 3 time slices (2020s, 2050s and 2080s) under RCP8.5 emissions scenarios (Medium-August T/PE scenario). Each plot shows 5 percentiles of change (10th, 25th, 50th, 75th and 90th)	43
Figure 3.16 Plots comparing the regional SDs of changes in 10-, 20- and 50-year return period flood peaks using UKCP18 probabilistic projections for 3 time slices (2020s, 2050s and 2080s) under RCP8.5 emissions scenarios (Medium-August T/PE scenario). Each plot shows 5 percentiles of change (10th, 25th, 50th, 75th and 90th)	44
Figure 3.17 Plots comparing the regional means of changes in 20-year return period flood peaks using UKCP18 probabilistic projections for 3 time slices (2020s, 2050s and 2080s) under A1B emissions, for the 3 T/PE scenarios: High-January, Low-August, and Medium-August. Each plot shows 5 percentiles of change (10th, 25th, 50th, 75th and 90th)	45
Figure 3.18 Plots comparing the regional SDs of changes in 20-year return period flood peaks using UKCP18 probabilistic projections for 3 time slices (2020s, 2050s and 2080s) under A1B emissions, for the 3 T/PE	

	scenarios: High-January, Low-August, and Medium-August. Each plot shows 5 percentiles of change (10th, 25th, 50th, 75th and 90th)	46
Figure 3.19	Plots comparing the regional means of changes in 20-year return period flood peaks using UKCP18 probabilistic projections for 3 time slices (2020s, 2050s and 2080s) under RCP8.5 emissions, with and without the extra uncertainty allowances (Medium-August T/PE scenarios). Each plot shows 5 percentiles of change (10th, 25th, 50th, 75th and 90th)	48
Figure 3.20	Plots comparing the regional SDs of changes in 20-year return period flood peaks using UKCP18 probabilistic projections for 3 time slices (2020s, 2050s and 2080s) under RCP8.5 emissions, with and without the extra uncertainty allowances (Medium-August T/PE scenarios). Each plot shows 5 percentiles of change (10th, 25th, 50th, 75th and 90th)	49
Figure 3.21	Plots comparing the regional means of changes in 20-year return period flood peaks using UKCP18 and UKCP09 probabilistic projections for 3 time slices (2020s, 2050s and 2080s) under A1B emissions, without the extra uncertainty allowances (Medium-August T/PE scenario). Each plot shows 5 percentiles of change (10th, 25th, 50th, 75th and 90th)	51
Figure 3.22	Plots comparing the regional SDs of changes in 20-year return period flood peaks using UKCP18 and UKCP09 probabilistic projections for 3 time slices (2020s, 2050s and 2080s) under A1B emissions, without the extra uncertainty allowances (Medium-August T/PE scenario). Each plot shows 5 percentiles of change (10th, 25th, 50th, 75th and 90th)	52
Figure 3.23	Contour plots comparing the UKCP18 and UKCP09 projections in terms of P harmonic mean (X_0) versus amplitude (A) for each river basin region, for the 2080s (A1B emissions). Contours delineate densities of 0.2% and 1.8% of projections per 5% \times 5% sensitivity domain square (dotted and solid lines respectively), where there is an ensemble of 10,000 projections for UKCP09 and 3,000 for UKCP18	53
Figure 3.24	showing a) 94 modelled catchments (left) and b) regionalised for each 1km river cell, for the 20-year return period and Medium-August T/PE scenario (right)	60
Figure 3.25	Indicator of hydrological modelling uncertainty for the 94 modelled catchments (top) and regionalised for each 1km river cell (bottom), leaving out one set of model results in turn	61
Figure A.1	Comparison of G2G, PDM/CLASSIC (re-run), CLASSIC-GB and GR4J modelled response types (20-year return period flood peaks and Medium-August T/PE scenario) for 94 catchments	76
Figure A.2	The percentage of the 94 catchments with each response type, for each model (20-year return period and Medium-August T/PE scenario)	78
Figure A.3	The baseline model performance (NSE, volume bias and ffr) compared to the modelled response types (dot colour) and uncertainty indicator (right-hand panel) for 94 catchments, for G2G, PDM/CLASSIC (re-run), CLASSIC-GB and GR4J. The grey shading indicates very good (mid-grey) and good (light grey) performance bands for each performance measure	79
Figure B.1	Maps of the response type of modelled response surfaces, for changes in 10-, 20- and 50-year return period flood peaks (left to right) using the 3 T/PE scenarios (Medium-August, Low-August, High-January; top to bottom)	84
Figure B.2	Stacked bar charts showing the balance of response types over the 19 river basin regions, for changes in flood peaks at three return periods (10-, 20 and 50- years), for the Low-August T/PE scenario	85
Figure B.3	As Figure B.2 but for the High-January T/PE scenario	86

Figure B.4 Taylor diagrams comparing the modelled response surfaces for every 1km river cell identified as Damped-Extreme with the Damped-Extreme average response surface as reference.	87
Figure B.5 As Figure B.4 but for Damped-High	88
Figure B.6 As Figure B.4 but for Damped-Low	88
Figure B.8 As Figure B.4 but for Mixed	89
Figure B.7 As figure B.4 but for Neutral	89
Figure B.10 As Figure B.4 but for Enhanced-Medium	90
Figure B.9 As Figure B.4 but for Enhanced-Low	90
Figure B.12 As Figure B.4 but for Sensitive	91
Figure B.11 As Figure B.4 but for Enhanced-High	91
Figure C.1 Contour plots showing UKCP18 P harmonic mean ($X0$) versus amplitude (A) for each river basin region, for RCP2.6 emissions for the 2020s, 2050s and 2080s (magenta, green and blue respectively). Contours delineate densities of 5 and 50 projections per 5% \times 5% sensitivity domain square (dotted and solid lines respectively)	92
Figure C.2 As Figure C.1 but for RCP4.5	93
Figure C.3 As Figure C.1 but for RCP6.0	94
Figure C.4 Contour plots showing UKCP18 P harmonic mean ($X0$) versus amplitude (A) for each river basin region, for the 2080s under RCP2.6, RCP4.5, RCP6.0 and RCP8.5 emissions (magenta, green and blue respectively). Contours delineate densities of 5 and 50 projections per 5% \times 5% sensitivity domain square (dotted and solid lines respectively).	95
Figure C.5 Histograms showing the distribution of the UKCP18 P harmonic phase (Φ) for each river basin region, for RCP2.6 emissions for the 2020s, 2050s and 2080s (magenta, green and blue respectively)	96
Figure C.6 As Figure C.5 but for RCP4.	97
Figure C.7 As Figure C.5 but for RCP6.0	98
Figure C.9 As Figure C.8 but for RCP8.5 emissions	99
Figure C.8 Distribution of the 3 harmonic function parameters (top row; $X0$, A , Φ) from the UKCP18 probabilistic temperature change projections for the UK, for the 2080s under RCP2.6 emissions	99
Figure D.1 Components of the climate change impacts web tool	100
Figure D.3 Example graph, for the selected river cell, showing the cumulative distribution function of the percentage change in 10-year return period flood peaks for the 2020s under RCP2.6 emissions scenario	101
Figure D.2 Example Info, showing the Easting, Northing and catchment area of the selected river cell	101
Figure D.4 Example boxplots, for the selected river cell, comparing the range of percentage changes in flood peaks: a) grouped by RCP and fixed for 10-year RP return period flood peaks, b) grouped by horizon and fixed for 10-year return period flood peaks c) grouped by flood return period and fixed by 2050s horizon	101
Figure D.5 Example summary table, for the selected river cell, showing key percentiles for the percentage change in 10-year return period flood peaks for the 2020s under RCP2.6 emissions	101
Figure D.6 Example image, for the selected river cell, showing the modelled response surfaces and the hydrological model uncertainty indicator	101

List of Tables

Table 2.1	The 525 P scenarios used in FD2020, comprising 21 changes in the annual mean together with 25 changes in the seasonal amplitude. Note that where the combination of annual mean change and seasonal amplitude results in a monthly change <-100% for any month, this is reset to -100%	15
Table 2.2	The 8 T scenarios used in FD2020. The scenarios shaded in green are those used in the current project	15
Table 2.3	The number of 1km river cells that are contained within a river-basin region in UKCP18 compared to UKCP09	21
Table 2.4	The suggested extra uncertainty allowances from FD2020 (Reynard and others, 2009), for each response type and return period.	23
Table 2.5	Response type groups for hydrological model uncertainty analysis	24
Table 2.6	Uncertainty bands for hydrological model uncertainty analysis using response type groups (Table 2.5); <i>A</i> is the absolute difference between the PDM/CLASSIC and G2G response type group values, <i>B</i> is the absolute difference between GR4J and G2G response type group values, and <i>C</i> is the absolute difference between CLASSIC-GB and G2G response type group values	24
Table 3.1	The Spearman's rank correlation between the response type maps for each T/PE scenario (Medium-August, Low-August and High-January) and each return period (10-, 20- and 50-years). Correlations above 0.85 are shown in bold, while correlations below 0.80 are shown in italics	26
Table 3.2	Comparison of existing guidance for England and Wales with new regional values derived using grid-based modelling and the UKCP09 projections	56
Table 3.3	Comparison of existing guidance for Scotland with new regional values derived using grid-based modelling and the UKCP09 projections	57
Table 3.4	Comparison of existing guidance for England and Wales with new regional values derived using grid-based modelling and the UKCP18 projections	58
Table 3.5	Comparison of existing guidance for Scotland with new regional values derived using grid-based modelling and the UKCP18 projections	59
Table A.1	List of the 94 catchments, with the hydrological model used in FD2020 (CLASSIC, PDM daily or PDM hourly) and the response types both from FD2020 and when re-run with the new rainfall data. *PDM hourly was not re-run	73
Table A.2	List of modelled response types for the 94 catchments modelled with G2G, PDM/CLASSIC (re-run), CLASSIC-GB and GR4J (20-year return period and Medium-August T/PE scenario).	77
Table A.3	Median model performance, over the 94 catchments, for each model and each performance measure. Note that the PDM calibrations focused in part on flood frequency fit, therefore the better performance for ffr at the (marginal) expense of NSE	80

1 Introduction

This project, entitled 'Climate change and fluvial flood peaks', was commissioned to provide more locally-specific information on potential changes in flood peaks under climate change than is currently available. The research builds on projects FD2020 ('Regionalised impacts of climate change on flood flows in Britain', Reynard and others, 2009) and FD2648 ('Practicalities for implementing regionalised allowances for climate change on flood, Kay and others, 2011a), and equivalent work for Scotland (R10023PUR; 'An assessment of the vulnerability of Scotland's river catchments and coasts to the impacts of climate change', Kay and others, 2011b).

1.1 Background

Project FD2020 developed a sensitivity framework approach for estimating the impacts of climate change on flood flows (Prudhomme and others, 2010). This was used to model 154 catchments across Great Britain, from which 9 'flood response types' were identified (Figure 1.1; Prudhomme and others, 2013a), each with a composite (average) 'flood response surface' (and standard deviation surface) illustrating the sensitivity of flood peaks to climatic changes (Figure 1.2).

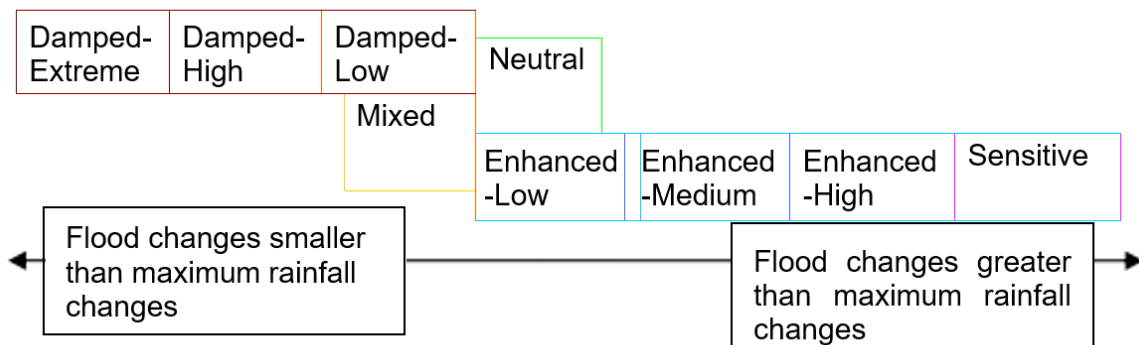


Figure 1.1 Schematic of the 9 flood response types of FD2020

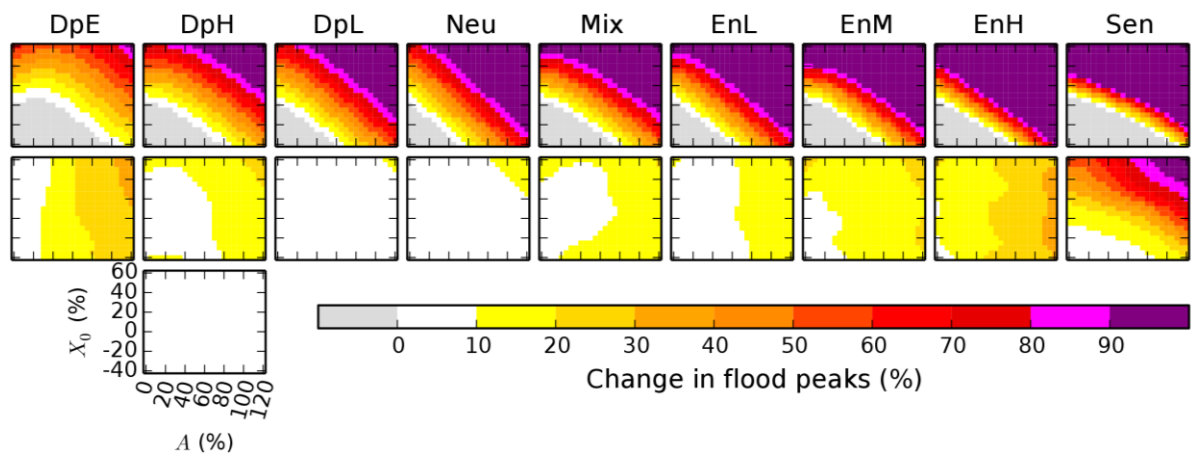


Figure 2.2 Composite (average) flood response surfaces (first row) and standard deviation surfaces (second row) for each of the 9 flood response types of FD2020, for changes in 20-year return period flood peaks. The axes and colour key are shown at the bottom

The project then developed ‘decision trees’, which enable a catchment’s flood response type to be estimated from its physical catchment properties (Prudhomme and others, 2013b). These properties, available from the [Flood Estimation Handbook](#) and the [Hydrometric Register](#), include standard annual average rainfall, mean altitude and fraction of high permeability bedrock. Uncertainty from this approach was also investigated (Kay and others, 2014c).

Project FD2648 applied the decision trees of FD2020 (after minor modification) to estimate the flood response type for each National River Flow Archive (NRFA) catchment (Figure 1.3a) (Kay and others, 2014a). It used the probabilistic projections for river basin regions from UK Climate Projections 2009 (UKCP09; Murphy and others, 2009), along with the average flood response surfaces corresponding to each flood response type, to estimate probabilistic response-type risk under climate change in each region. It then weighted this with the number of NRFA catchments of each type in the region to estimate regional risk (Kay and others, 2014a). Similar work was done for Scotland (Figure 1.3b; Kay and others, 2011b, 2014b). An example of the estimated range of potential impacts for each river basin region, for one time slice and emissions scenario, is shown in Figure 1.4.

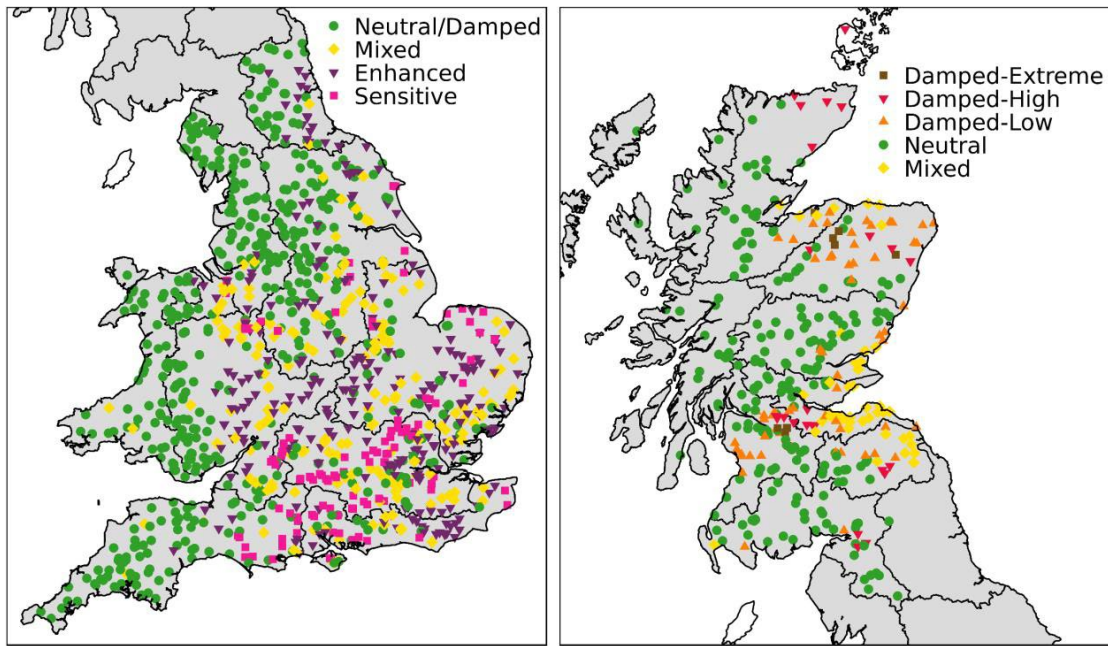


Figure 4.3 Estimated flood response family of each NRFA catchment in England and Wales (left) and Scotland (right), for changes in 20-year return period flood peaks (note that some response types were merged into groups) (from Kay and others, 2014a,b)

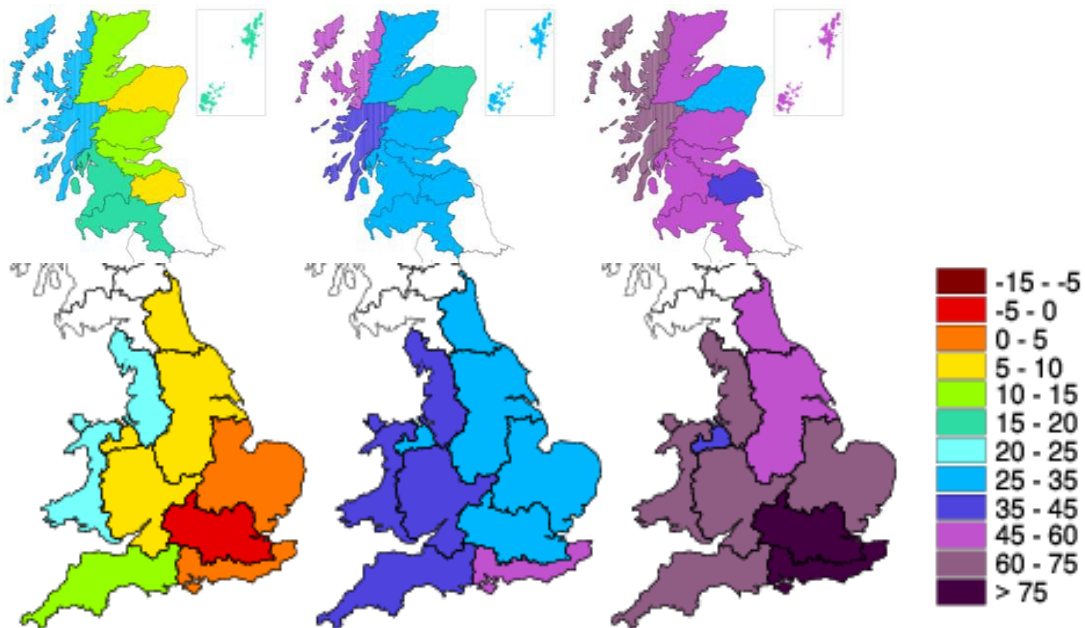


Figure 3.4 Potential range of regional impacts (percentage change in 20-year return period flood peaks) for the 2080s time slice and high emissions scenario (lower end of range - left maps, middle - centre maps, higher end - right maps) (Kay and others, 2014a,b)

One limitation of the work was that the FD2020/FD2648 decision trees do not readily apply to ungauged catchments, as one of the Hydrometric Register properties necessary in the characterisation procedure was ‘mean annual loss’ (defined by the NRFA as the difference between mean annual rainfall and mean annual run-off). This meant that location-specific impact estimates were only possible for gauged catchments, where the decision trees

could be used to estimate the response type. Therefore, the guidance subsequently derived for flood management authorities and flood risk assessments in England only provided regional average allowances (Environment Agency, 2016a,b), as did guidance similarly derived by the devolved administrations for Scotland (SEPA 2016, 2019) and Wales (Welsh Government 2016, 2017). Applying regional average values means that there is the risk of over- or under-adaptation, as the impact of climate change will inevitably vary between catchments within a region (sometimes significantly, depending on the response type of individual catchments relative to the dominance of alternative types within a region) (Reynard and others, 2017, Broderick and others, 2019).

1.2 Developments

The aim of this project was to apply the sensitivity framework of FD2020 with a grid-based hydrological model, therefore enabling a consistent assessment of the sensitivity and vulnerability of flood peaks to climate change across Great Britain. Such national-scale grid-based modelling produces modelled response surfaces for every point on the grid (with sufficiently large cumulative catchment area), which can be directly overlaid with climate change projections to estimate impact ranges for each location. By producing modelled response surfaces for grid cells across the country, a number of steps are removed from the previous approach, therefore eliminating the additional sources of uncertainty resulting from those steps. These are:

- a) use of average response surfaces (and the standard deviation of those surfaces)
- b) use of decision trees to estimate a catchment's response type from catchment properties

Note that, although outputs may be possible for every grid cell, they will only be saved/analysed for those cells with a sufficiently high catchment area given the spatial resolution of the hydrological model and the spatial and temporal resolution of the driving data (section 2.1).

This project also applies the most recent climate change projections for the country, UK Climate Projections 2018 (UKCP18; Lowe and others, 2018), and compares the results with those from UK Climate Projections 2009 (UKCP09 Murphy and others, 2009).

2 Methods

2.1 Hydrological model and driving data

It was decided to apply the Grid-to-Grid (G2G) model, which is a national-scale run-off-production and routing model that provides estimates of river flows on a 1km grid across Great Britain (Bell and others, 2009). G2G is used within the Flood Forecasting Centre - England and Wales (Price and others, 2012) and the Scottish Flood Forecasting Service (Cranston and others, 2012, Maxey and others, 2012). It has been used previously to assess the impact of climate change on floods (Bell and others, 2012, 2016) and droughts (Rudd and others, 2018). The model has been applied here using a 15-minute time step, with the optional snow module (Bell and others, 2016), and using one spatially consistent configuration for the whole model domain. G2G is able to represent a wide range of hydrological regimes due to using the spatial data sets of soil, terrain and land cover.

The G2G requires gridded time series of precipitation (P) and potential evaporation (PE) data, plus air temperature (T) data for the snow module. As yet, there is no national data set of gridded sub-daily P data, so 1km daily P from Gridded estimates of daily and monthly areal rainfall for the United Kingdom (CEH-GEAR) are used (Tanguy and others, 2015, Keller and others, 2015), divided equally over each 15-minute time step. The PE data comprises monthly 40km gridded estimates of short grass PE from Meteorological Office Rainfall and Evaporation Calculation System (MORECS) (Hough and Jones 1997), which is based on the Penman-Monteith formulation (Monteith 1965) and was previously used for G2G model calibration (Bell and others, 2009). The 40km monthly PE data were copied to each of the corresponding 1km grid boxes of the hydrological model grid and divided equally over each time step. As for P, there is, as yet, no national data set of gridded sub-daily T data, so 5km daily minimum and maximum T data are applied (Perry and others, 2009), interpolated through the day using a sine curve and downscaled to 1km using a lapse rate ($0.0059^{\circ}\text{C}/\text{m}$) and elevation data (Morris and Flavin, 1990). The river flow estimates produced by the model are natural flows and do not take into account surface or groundwater abstractions.

The threshold area for analysis of model outputs is set at 100km^2 . No results are produced for 1km grid cells with catchment areas below this threshold, as it is considered that the results will not be reliable for smaller catchments given the daily temporal resolution of the driving P data. The modelling therefore covers mainland Great Britain and the island of Lewis and Harris only, as there are no catchments with an area greater than 100km^2 within the smaller islands. In this report therefore, 1km grid cells with catchment areas of at least 100km^2 are termed '1km river cells'.

2.2 The sensitivity framework: definition

The sensitivity framework approach to climate impacts involves defining a regular sensitivity domain comprising a large number of plausible scenarios of climatic change. Modelling is then used to define the change in a given indicator for each scenario of the sensitivity domain, producing a 'response surface' (for example, Wetterhall and others, 2011, Weiß 2011, Bastola and others, 2011, Fronzek and others, 2010). The sensitivity domain developed in FD2020 uses a single harmonic function to represent the monthly pattern of changes in P and T, allowing the dimensionality of the domain to be greatly

reduced, while maintaining a seasonal variation (Prudhomme and others, 2010). The function is given by:

$$X(t) = X_0 + A \cos [2\pi (t - \Phi) / 12] \quad (1)$$

with $X(t)$ change for month t , annual mean change X_0 , seasonal amplitude A (height of peak above mean) and phase Φ (month of peak). Prudhomme and others (2010) analysed multi-model climate projections for Britain to determine appropriate values for the harmonic function parameters for P and T. For P, the majority of projections had a peak change in winter, so the phase Φ was set to 1 (January). Therefore, the sensitivity domain involved only 2 dimensions of P change (X_0 and A), each varied in increments between minimum and maximum values (Table 2.1). The analysis also showed no significant correlation between P and T changes, so T changes were treated independently and few scenarios were used, as floods in Britain are much less sensitive to T than P change. Therefore, the sensitivity domain involved 8 scenarios of T change; 3 with the peak change in January, 3 with the peak in August, and 2 non-seasonal (Table 2.2). Monthly PE changes were derived from monthly T changes using the Central England temperature series and the temperature-based PE formula of Oudin and others (2005). This gave a total of 4,200 scenarios in the sensitivity domain; 525 P scenarios for each of 8 T/PE scenarios.

Table 2.1 The 525 P scenarios used in FD2020, comprising 21 changes in the annual mean together with 25 changes in the seasonal amplitude. Note that where the combination of annual mean change and seasonal amplitude results in a monthly change <-100% for any month, this is reset to -100%

	annual mean (X_0)	seasonal amplitude (A)	Month of peak (Φ)
range	-40% to +60%	0% to 120%	1 (January)
increment	5%	5%	-
number of scenarios	21	25	1

Table 2.2 The 8 T scenarios used in FD2020. The scenarios shaded in green are those used in the current project

T/PE scenario		Description of T change pattern (deg C)			
Shorthand	Longhand	annual mean (X_0)	seasonal amplitude (A)	month of peak (Φ)	T change at peak
TPE1	Low-January	1.5	1.2	1 (January)	2.7
TPE2	Medium-January	2.5	0.8	1 (January)	3.3
TPE3	High-January	4.5	1.6	1 (January)	6.1
TPE4	Low-August	1.5	1.2	8 (August)	2.7
TPE5	Medium-August	2.5	0.8	8 (August)	3.3
TPE6	High-August	4.5	1.6	8 (August)	6.1
TPE7	Low-non-seasonal	0.5	0	None	0.5
TPE8	High-non-seasonal	4.5	0	None	4.5

Here, the same 525 P scenarios are applied, but only 3 of the 8 T/PE scenarios are applied, due to computing limitations with the fine-scale grid-based model. The choice of which T/PE scenarios were retained was based on:

- analysis of the modelled response types from FD2020, when using all 8 T/PE scenarios together and for each of the 8 individually (for 20-year return period flood peaks)
- comparison to the temperature changes suggested by UKCP18 climate change projections

The chosen scenarios are:

- medium-Aug (TPE5): most consistent with UKCP18 Representative Concentration Pathway 6.0 (RCP6.0) T changes
- low-Aug (TPE4): less likely than medium-Aug, but still within the bounds of UKCP18, both for RCP6.0 emissions and for lower emissions (RCP2.6)
- high-Jan (TPE3): less likely than medium-Aug, but still within the bounds of UKCP18, both for RCP6.0 emissions and for higher emissions (RCP8.5). In particular while scenarios with a January peak are much less likely than those with an August peak, they can have more extreme mean changes and amplitudes than some other months (except those around August), so it is a good idea to cover this possibility

These 3 T/PE scenarios are consistent with UKCP18 projections (section 3.2.2) and cover most of the variation in response types between the 8 T/PE scenarios of FD2020, while enabling the required sensitivity framework runs (525 P scenarios for each T/PE scenario) to be done with the 1km G2G hydrological model. Medium-August will be treated as the main T/PE scenario, with the others used to assess the sensitivity of the results to the choice of T/PE scenario.

The climatic changes given by the sensitivity domain are then applied to baseline climate time series using the change factor method, to provide adjusted driving data for the hydrological model. The change factor method involves applying monthly (percentage or absolute) changes in a variable to a baseline time series for that variable. In this case, the baseline comprises P, T and PE data for 1961 to 2001. The monthly change factors are applied equally to each day of the relevant month; monthly percentage changes for P (and PE) are applied to each day of the corresponding month in the observed P (and PE) time series, and monthly absolute changes for T are added to each day of the corresponding month in the observed T time series.

The baseline period is set to 1961 to 2001 (as used in FD2020), rather than a more standard 30-year period (for example, 1961 to 1990 used as the baseline in UKCP09; see section 2.5), as it allows for greater natural climatic variability and better estimation of flood peaks to higher return periods.

2.3 The sensitivity framework: application with G2G

G2G is run with the baseline driving data (section 2.1), and with the baseline data adjusted using each P scenario of the sensitivity domain (525) with each of the 3 T/PE scenarios of the sensitivity domain (section 2.2); 1,576 runs in total. For each run, 1km grids of the annual maxima (AM) of daily mean flows are saved, for each water year (October to September).

For each 1km river cell and for each model run, a flood frequency curve is fitted to the 40 AM, using L-moments and the generalised logistic distribution (Robson and Reed, 1999). The peak flows with return periods of 10, 20 and 50 years are then estimated. Changes in

these peak flows between the baseline run and each scenario run are then determined. This provides a set of 2-d response surfaces for each 1km river cell, where each response surface illustrates the percentage change in flood peaks (shown using a colour scale) for the 525 precipitation scenarios (21 annual mean changes X_0 on the y-axis by 25 seasonal amplitudes A on the x-axis), and separate surfaces are provided for each of the 3 return

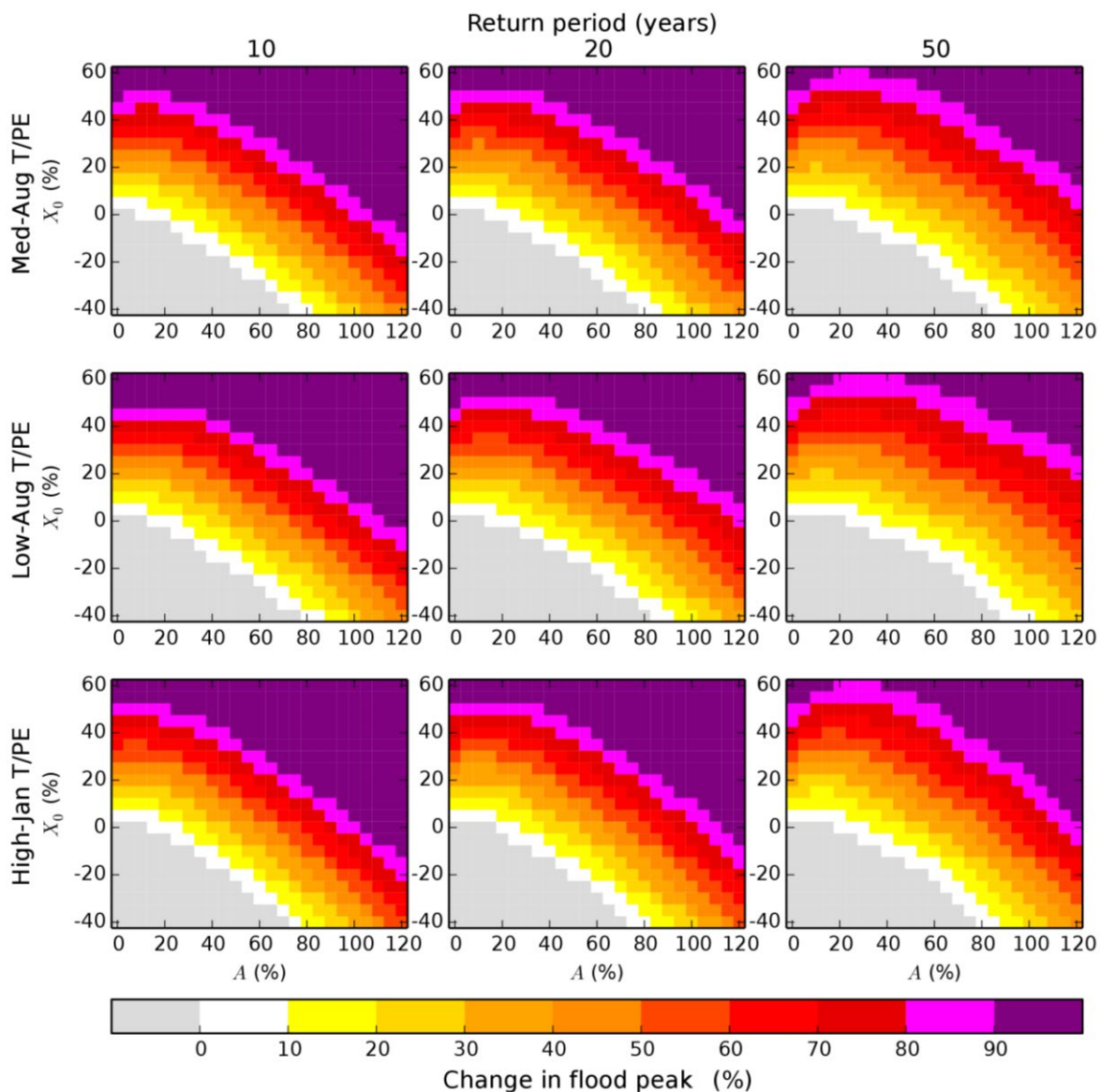


Figure 2.1 Example set of flood response surfaces for a single 1km river cell. Response surfaces are shown for 3 return periods (10, 20 and 50 years; left to right) and 3 T/PE scenarios (Medium-August, Low-August and High-January; top to bottom)

periods and 3 T/PE scenarios (Figure 2.1).

In FD2020, composite (average) response surfaces were calculated for each response type (Figure 1.2) by averaging the modelled response surfaces for each catchment of that type, including the surfaces for each of the 8 T/PE scenarios (Table 2.2) for a catchment (Reynard and others, 2009). These average response surfaces (and corresponding standard deviation surfaces) were those combined with climate change projections in FD2648 (section 1.1). Here, it is not necessary to calculate average response surfaces, as there are modelled response surfaces available for 1km river cells across the country. So, there is no need to use decision trees to estimate a catchment's response type from its

properties and then use the corresponding average response surface to represent the location (section 1.2). Therefore, the modelled surfaces for each of the 3 T/PE scenarios applied here (Table 2.2) will be kept separate and used to provide an indication of the influence of different T/PE changes on peak flow impacts (section 2.6).

2.4 Analysis of response surfaces and types

While application of climate change projections (section 2.5) will use the modelled response surfaces for each 1km river cell (section 2.6), it is useful for analysis purposes to classify the modelled response surfaces. This classification is based on the 9 response types derived in project FD2020 (Damped-Extreme, Damped-Low, Neutral, Mixed, Enhanced-Low, Enhanced-Medium, Enhanced-High, Sensitive), and the average response surfaces corresponding to each of these types (section 1.1). The classification is also required so uncertainty allowances can be included (section 2.7).

Classification involves comparing each modelled response surface with each of the 9 average response surfaces (for a given return period, and for the main part of the response surface; $A \leq 80$) and selecting the response type for which the root mean squared difference (rmsd) is the smallest (note that rmsd was also the similarity measure used by the clustering algorithm applied in FD2020 to delineate the response types). An example of this comparison is presented in Figure 2.2. The results of the response surface classification are presented in section 3.1.1.

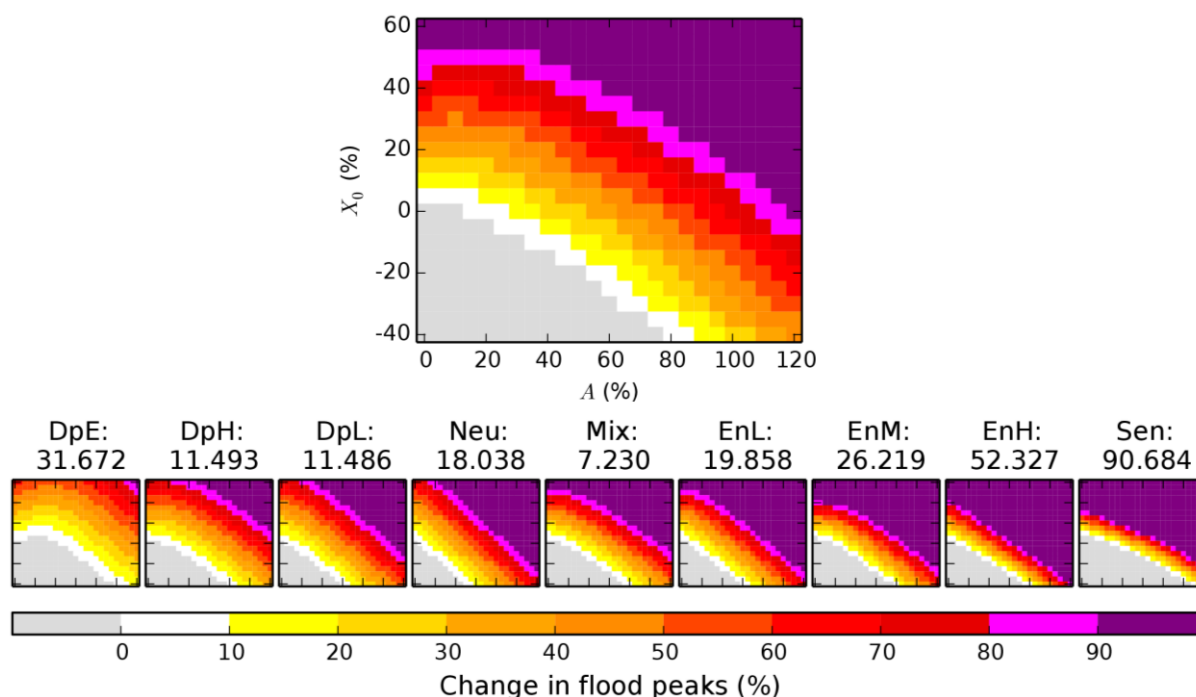


Figure 2.2 Example comparison of a modelled response surface (top) with each of the 9 average response surfaces (bottom) in terms of rmsd (given above each average response surface). In this case, the closest type (that with the lowest rmsd) is Mixed

The rmsd values are also used to check whether there are any modelled response surfaces significantly different from all 9 of the FD2020 average response surfaces, as these may indicate the presence of new response types not seen in the previous

catchment-based modelling. In addition, Taylor diagrams are produced comparing the modelled response surfaces with each of the average response surfaces. Taylor diagrams provide a graphical summary of how closely a modelled pattern (or set of patterns) matches a reference pattern. The similarity between 2 patterns is quantified using their centred root mean square difference (dissimilarity), their correlation, and the amplitude of their variations (represented by their standard deviation, SD). The modelled pattern SDs are scaled by the reference pattern SD; standardised SD is lower than 1 when the modelled pattern is less variable than the reference pattern, and greater than 1 when the modelled pattern is more variable than the reference pattern. Here, the patterns are the modelled response surfaces at each river cell (section 2.3) and the reference patterns are the 9 average response surfaces from FD2020 (Figure 1.2).

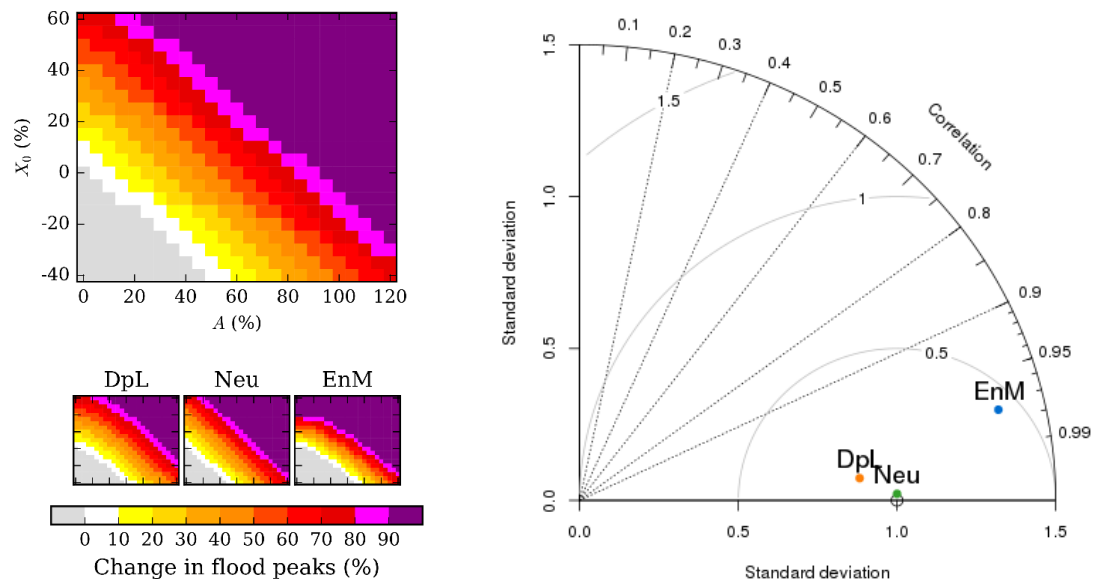


Figure 2.3 Example Taylor diagram (right), showing the positions of 3 modelled response surfaces (bottom-left) when compared to a reference response surface (in this case, the Neutral average response surface, top-left)

Figure 2.3 shows an example Taylor diagram using 3 modelled response surfaces, for river cells identified as Neutral, Damped-Low and Enhanced-High, compared to the Neutral average response surface. The closer the points are to the reference point (open circle at correlation one and standard deviation one), the more similar their pattern is to the reference pattern, and vice versa. In Figure 2.3, the closest point to the reference point is the one marked 'Neu'. This was expected as this river cell was identified as Neutral so its modelled response surface is very similar to the Neutral average response surface. The next closest point to the reference point is that marked 'DpL', which has a lower standard deviation and correlation with the reference surface. The point marked 'EnM' is the furthest away, with a higher standard deviation and lower correlation with the reference. Looking at the 3 modelled response surfaces, that for the river cell identified as having an Enhanced-Medium response type is clearly the least similar to the Neutral average response surface. The results of this analysis for all 1km river cells are presented in section 3.1.2.

2.5 The climate change projections

Both UKCP09 and UKCP18 provide probabilistic projections, consisting of N sets of changes in a number of climate variables where N is 10,000 for UKCP09 and 3,000 for UKCP18. The UKCP09 climate change projections are available as monthly changes from a baseline 30-year time slice (1961 to 1990) to a number of future 30-year time slices under 3 Special Report on Emissions Scenarios (SRES) emissions scenarios (equivalent to SRES B1, A1B and A1F1; IPCC 2000), on an approximately 25km grid over the UK or for 23 river basin regions. The river basin region data are used here as they are consistent across any river catchment; the grid data are not spatially coherent, so cannot provide spatial averages or different inputs to different parts of a catchment. The 19 river basin regions over Great Britain (excluding the Orkney and Shetland region) are shown in Figure 2.4a. Only the data for the A1B emissions are applied here, for the 3 non-overlapping future time slices; 2020s (2010 to 2039), 2050s (2040 to 2069), 2080s (2070 to 2099). Section 2.4.2 describes the differences in moving between catchment to gridded model, and between UKCP09 and UKCP18.

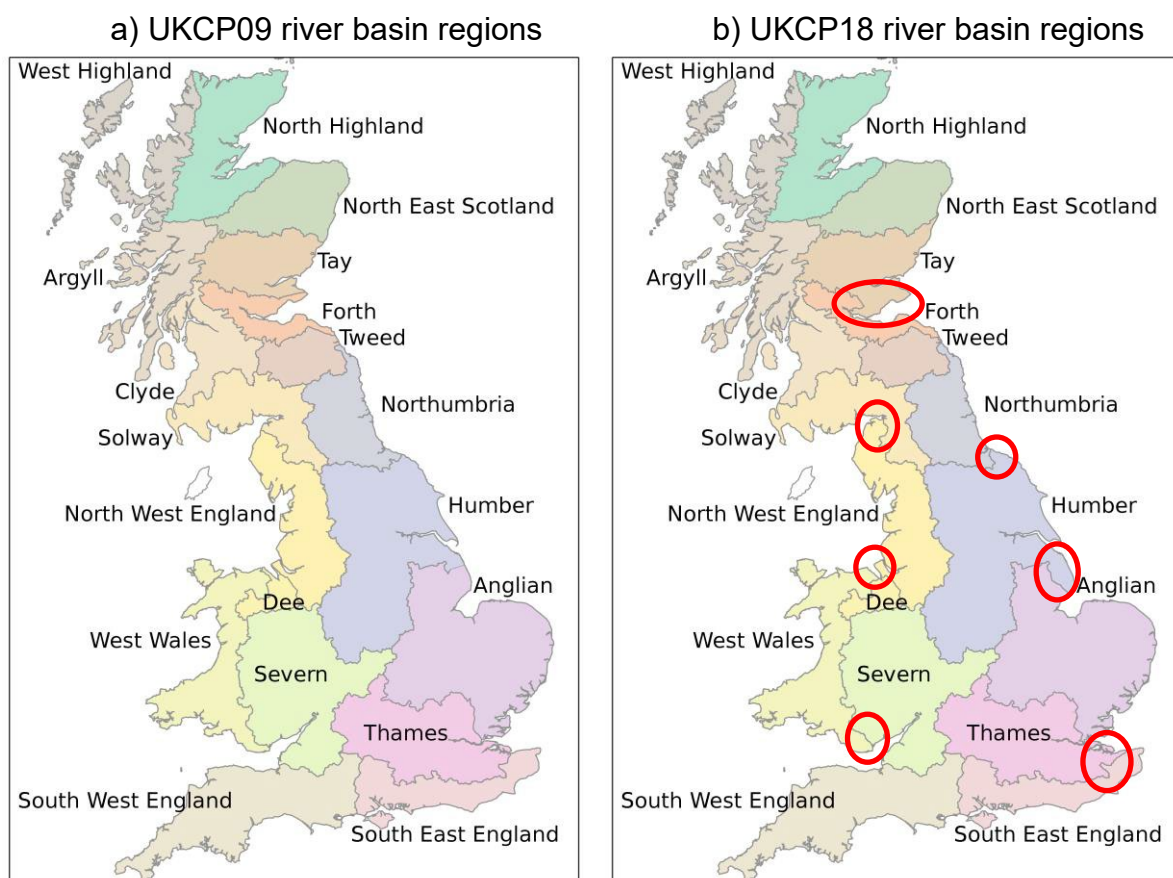


Figure 2.4 The 19 river basin regions covering Great Britain from a) UKCP09 and b) UKCP18. The Orkney and Shetland region is excluded from both maps, as are the 3 regions covering Northern Ireland. Note that there are some differences between the UKCP09 and UKCP18 regions (highlighted). Some minor changes have also been made to the regions to make them consistent with the UK Centre for Ecology & Hydrology's (UKCEH's) 1km flow directions

The UKCP18 climate change projections are similarly available on a 25km grid or for river basin regions (Figure 2.4b; Met Office Hadley Centre 2018), but under 4 Representative

Concentration Pathways (RCP2.6, 4.5, 6.0, 8.5; van Vuuren and others, 2011) as well as SRES A1B emissions. The data are available as time slice mean changes from 3 different baseline periods, but also as monthly anomalies in each individual year (from December 1960 to November 2099), calculated from a 20-year baseline (1981 to 2000). The river basin region data are used here, as time slice mean changes from a 1961 to 1990 baseline for the 3 future 30-year time slices used for UKCP09 (2020s, 2050s, 2080s). Data are applied for each emissions scenario (with SRES A1B only used for comparison with UKCP09).

Note that there are some differences between the UKCP09 and UKCP18 river basin regions (Figure 2.4). Table 2.3 summarises the number of 1km river cells (catchment area $\geq 100\text{km}^2$) affected by the different river basin region boundaries.

Table 2.3 The number of 1km river cells that are contained within a river-basin region in UKCP18 compared to UKCP09

UKCP09 river-basin region	UKCP18 river-basin region	Number of 1km river cells affected
Severn	West Wales	17
Anglian	Humber	12
Solway	NW England	19
Forth	Tay	33
Clyde	Argyll	13
NE Scotland	Tay	7

2.6 Application of climate change projections

The probabilistic climate change projections are applied by overlaying on the modelled response surfaces for each 1km river cell, and extracting the change in flood peaks corresponding to each projection. To do the overlaying, a single harmonic function (section 2.2) is fitted to each set of monthly P changes for the required region, emissions scenario and time slice. Two P harmonic parameters (mean X_0 and amplitude A) determine the position of each projection on the sensitivity domain, with the phase ϕ of the P harmonic ignored as the response surfaces assume a peak change in January. Checks are performed to ensure the sensitivity domain extents and assumptions for P changes are valid for the new UKCP18 projections (section 3.2.1).

The impact corresponding to each climate change projection is then extracted, to produce a cumulative distribution function (cdf) of the percentage changes in flood peaks resulting from the set of climate projections. The extraction uses bi-linear interpolation of the response surface values (only available at 5% \times 5% intervals; section 2.2) to give a smoother cdf. Figure 2.5 presents an example showing a set of climate projections overlaid on a modelled response surface, and the resulting cdf of change in flood peaks. Any required percentiles of change in flood peaks can be read from the cdf. [Note that interpolation was not applied in FD2020/FD2648, resulting in 'jumpy' cdfs; see, for example, Figure 2 of Reynard and others, 2017].

Sets of impacts are presented in section 3.3.1, comparing impacts from UKCP18 projections across time slices (2020s, 2050s, 2080s) and emissions scenarios (RCP2.6, 4.5, 6.0, 8.5), for the 20-year return period. A comparison across the 3 return periods (10, 20 and 50 years) is presented in section 3.3.2.

Only the P projections are used for overlaying; variations in T changes are much less important for changes in flood peaks in Britain (Prudhomme and others, 2013a), so the main results only use the response surfaces for the Medium-August T/PE scenario – the most consistent with UKCP18 projections (section 3.2.2). However, comparisons are made by overlaying sets of projections on response surfaces produced using the 2 alternative T/PE scenarios (section 2.2); these are presented in section 3.3.3.

A comparison of UKCP18 with UKCP09 for SRES A1B emissions is presented in section 3.4.1, for 3 time slices (2020s, 2050s, 2080s). All of the comparisons are done for 5 percentiles extracted from the impact cdfs for each 1km river cell; the 10th, 25th, 50th, 75th and 90th percentiles.

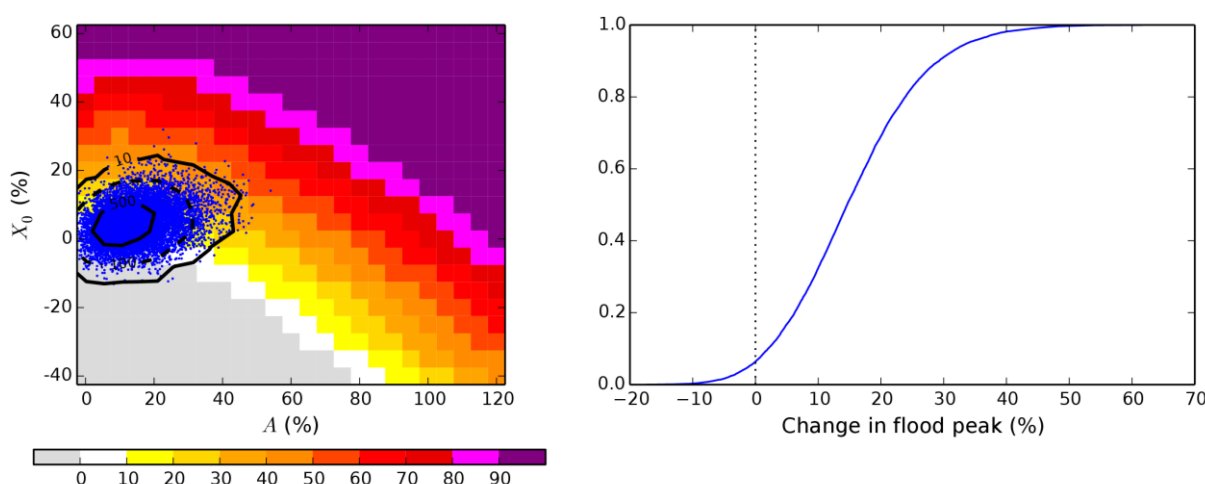


Figure 2.5 Example of overlaying UKCP09 climate change projections on a modelled response surface (left). Blue dots show each of the 10,000 projections for one river basin region (North Highlands), emissions scenarios (A1B) and future time slice (2080s). The black contours delineate densities of 10, 100 and 500 projections per 5% \times 5% sensitivity domain square. Also shown is the cdf of the percentage changes in flood peaks extracted from the response surface using the projections (right). In this case, the changes are for 20-year return period flood peaks for a location in north-west Scotland.

Note that application of climate change projections derived as changes from a particular baseline period (1961 to 1990; section 2.5) with response surfaces derived from a slightly different (but overlapping) baseline period (1961 to 2001; section 2.2), is not strictly consistent. However, it was deemed necessary to use a longer baseline in the hydrological modelling to allow changes in higher return period peak flows to be estimated. Shorter baselines are however preferable for the climate change projections in order to maximise the climate change signal and so that any changes during the baseline period itself can be considered negligible.

2.7 Sensitivity framework uncertainty

In project FD2020, 2 main sources of uncertainty were assessed and incorporated in the results (Reynard and others, 2009; Kay and others, 2014a,b). These were:

- representation of a catchment response surface by a composite (average) response surface
- the assumptions/simplifications necessary to develop/implement the sensitivity-based approach

The former was addressed by using standard deviation surfaces alongside the average response surfaces (Figure 1.2), but the availability here of modelled response surfaces for every 1km river cell means that standard deviation surfaces are no longer required. However, uncertainty from the sensitivity framework assumptions is still present, and can be addressed in the same way as previously.

Briefly, in FD2020 extra uncertainty allowances were developed to be able to correct mean bias in the impacts extracted from response surfaces (see section 7.2 of Reynard and others, 2009 for details). These extra allowances varied by response type and return period (Table 2.4), and can therefore be applied here using the response type classification for each 1km river cell (section 2.4). The relevant extra allowance is added to each value extracted from a response surface. Comparisons of regional impacts with and without these extra uncertainty allowances are presented in section 3.3.4. Note that the FD2020 uncertainty analysis also suggested the use of multiplication factors on the extra allowances for larger catchments (Area > 2,000km²), where uncertainty seemed to be larger, but these were not implemented in subsequent applications with UKCP09 projections (Kay and others, 2011a,b; Kay and others, 2014a,b) and are not implemented here.

Table 2.4 The suggested extra uncertainty allowances from FD2020 (Reynard and others, 2009), for each response type and return period.

Response type	Return periods (years)		
	10	20	50
DpE	11	11	11
DpH	11	12	16
DpL	6	7	8
Neu	3	3	3
Mix	13	11	10
EnL	6	7	8
EnM	12	15	18
EnH	12	9	6
Sen	20	20	20

2.8 Hydrological model uncertainty

Hydrological modelling is a further potential source of uncertainty. This has been discussed previously (for example, Reynard and others (2017) state "...a number of other potential sources of uncertainty are not currently accounted for, including hydrological model structure and parameterisation"), but it was not possible to fully investigate this in earlier research. Results are now available for a range of models (both catchment-based and grid-based) for a reasonably large number of catchments. These results are used to develop a simple indicator of potential hydrological model uncertainty for each 1km river cell.

For 94 catchments (Table A.1), the G2G modelled response types are compared to those from the original FD2020 catchment-based models (PDM and CLASSIC) re-run with updated input data, plus modelled response types from the grid-based model CLASSIC-GB (5km resolution; Crooks and others, 2014) and the catchment-based model GR4J (Perrin and others, 2003) (see Appendix A.1 and Table A.2 for further details). The response types are combined into 3 groups (Table 2.5), then each model result is compared to the G2G results; the G2G response types are considered as the ‘base’ results. Colours are assigned based on those differences, indicating different levels of uncertainty; low, medium and high (Table 2.6). Note that this simple algorithm assumes that the results from each hydrological model are equally valid, and does not take account of factors like model complexity or the performance of each model in simulating flows in a baseline period (see Appendix A.2).

Table 2.5 Response type groups for hydrological model uncertainty analysis

Group	Response types
1	DpE, DpH
2	DpL, Mix, Neu, EnL
3	EnM, EnH, Sen

Table 2.6 Uncertainty bands for hydrological model uncertainty analysis using response type groups (Table 2.5); *A* is the absolute difference between the PDM/CLASSIC and G2G response type group values, *B* is the absolute difference between GR4J and G2G response type group values, and *C* is the absolute difference between CLASSIC-GB and G2G response type group values

Uncertainty	Condition	Meaning	Colour
Low	If all (A,B,C) = 0	All models agree on response type group	Green
Medium	If all (A,B,C) < 2	The response type group of all models are less than 2 groups away from the G2G group (but they may not agree on direction)	Amber
High	Else	The response type group of at least one model is two groups away from the G2G group, and they may not all agree	Red

The indicator of hydrological model uncertainty is then regionalised to provide a value for each 1km river cell, by assuming that catchments are likely to have a consistent level of uncertainty with nearby catchments of a similar response type. The procedure is as follows:

- For each 1km river cell, find the nearest of the 94 catchments within the same response type group (Table 2.5) as that of the 1km river cell, and assign that catchment's uncertainty indicator value to the 1km river cell.

The uncertainty indicator results are presented in section 3.5, including an analysis of the effect of leaving out one model at a time.

3 Results

3.1 Response types

3.1.1 Mapping response types

The G2G modelled response types are mapped in Figure 3.1 for changes in 20-year return period flood peaks under the Medium-August T/PE scenario. Maps for the other return periods and T/PE scenarios are in Appendix B.1. There is significant variability in response types across the country, but with typically more Neutral/Damped types in the north/west and more Enhanced/Sensitive types in the south/east, while the Mixed type can be seen in almost all parts of the country (as for the FD2020 catchment-based modelling; Reynard and others, 2009, Prudhomme and others, 2013a).

Table 3.1 gives the Spearman’s rank correlation between the response type maps for each T/PE scenario and each return period. The correlations are generally high, indicating significant similarity between the maps for different T/PE scenarios and for different return periods. However, correlations are typically lower between the 10-year and 50-year return period maps than between either of these and the 20-year return period maps, indicating growing differences by return period. Correlations are also typically lower between the High- January and Low-August T/PE maps than between either of these and the Medium-August maps. This is unsurprising as both the High-January and Low-August T/PE scenarios are, by design, more extreme than the Medium-August T/PE scenario, and in different ways to each other (section 2.2). However, there is still significant similarity between maps for the High-January and Low-August T/PE scenarios; the lowest correlation (for matching return periods) is 0.763 (10-year return period) rising to 0.845 (50-year return period).

Table 3.1 The Spearman’s rank correlation between the response type maps for each T/PE scenario (Medium-August, Low-August and High-January) and each return period (10-, 20- and 50-years). Correlations above 0.85 are shown in bold, while correlations below 0.80 are shown in italics

Med-Aug T/PE	Med-Aug T/PE			Low-Aug T/PE			High-Jan T/PE			
	RP10	RP20	RP50	RP10	RP20	RP50	RP10	RP20	RP50	
Low-Aug T/PE	RP10	1	0.881	<i>0.787</i>	0.893	0.850	<i>0.790</i>	0.850	0.823	<i>0.741</i>
	RP20		1	0.86	0.836	0.907	0.854	0.822	0.902	0.82
	RP50			1	<i>0.748</i>	0.808	0.911	<i>0.766</i>	0.857	0.905
High-Jan T/PE	RP10				1	0.884	<i>0.791</i>	<i>0.763</i>	<i>0.762</i>	<i>0.689</i>
	RP20					1	0.866	<i>0.758</i>	0.821	<i>0.753</i>
	RP50						1	<i>0.742</i>	0.824	0.845
	RP10							1	0.855	<i>0.762</i>
	RP20								1	0.857
	RP50									1

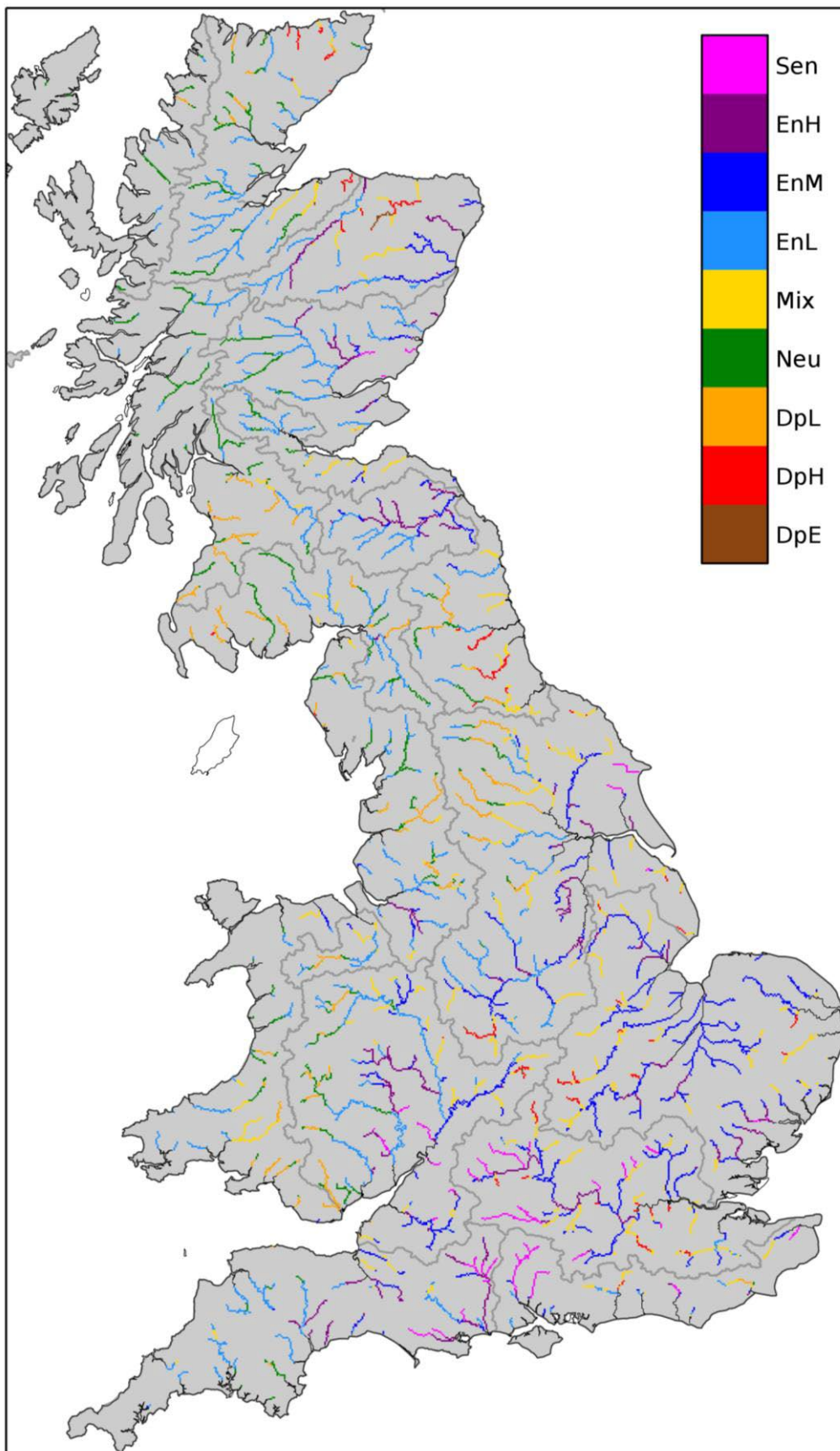


Figure 3.1 Map showing the response type of the modelled response surface for each 1km river cell in GB, for changes in 20-year return period flood peaks using the Medium-August T/PE scenario

These similarities and differences are also shown by bar charts summarising the balance of response types over each river basin region. Figure 3.2 compares return periods for the Medium-August T/PE scenario, and Figure 3.3 compares T/PE scenarios for the 20-year return period (other combinations are given in Appendix B.1).

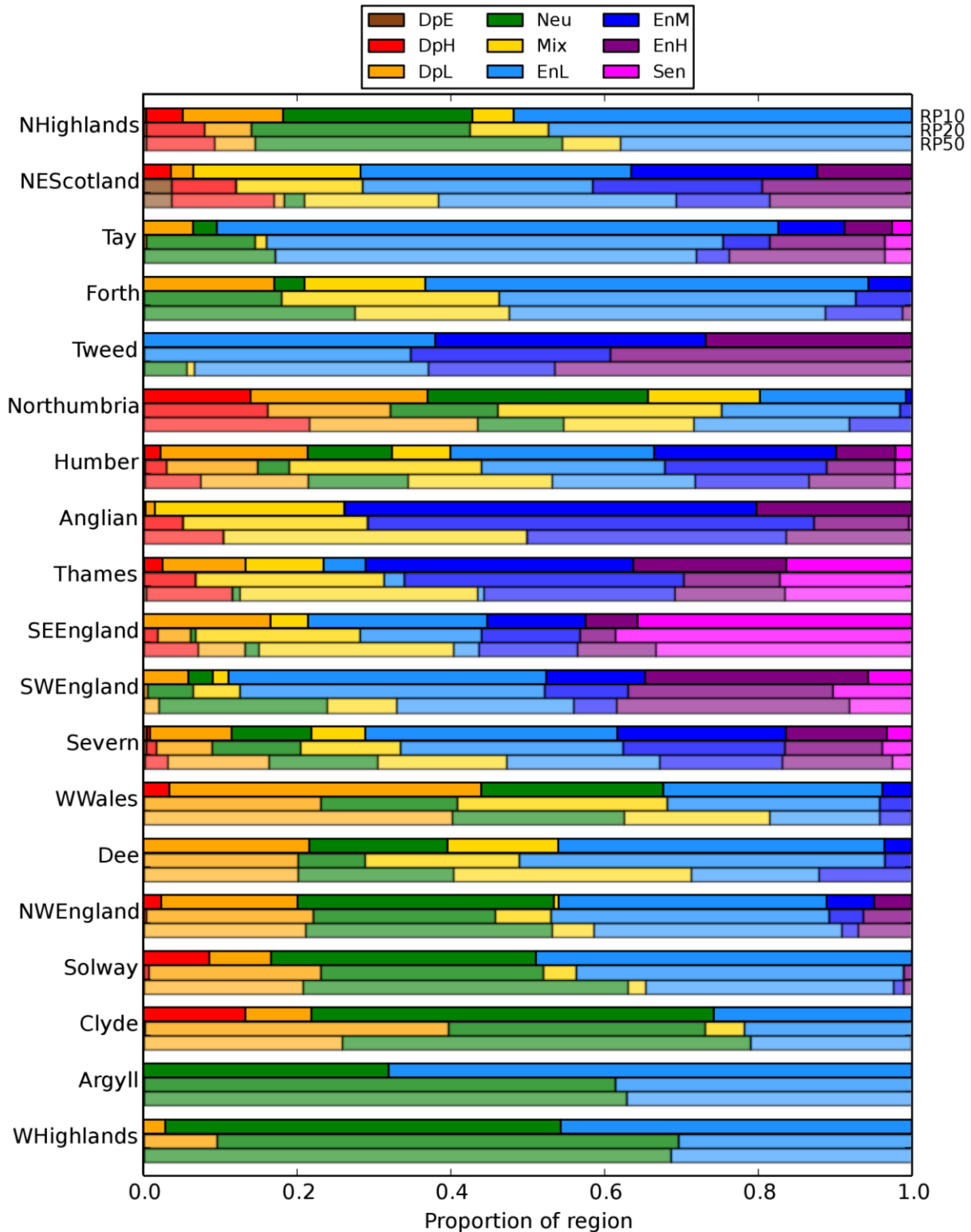


Figure 3.2 Stacked bar charts showing the balance of response types over the 19 river basin regions, for changes in flood peaks at 3 return periods (10-, 20 and 50- years), for the Medium-August T/PE scenario

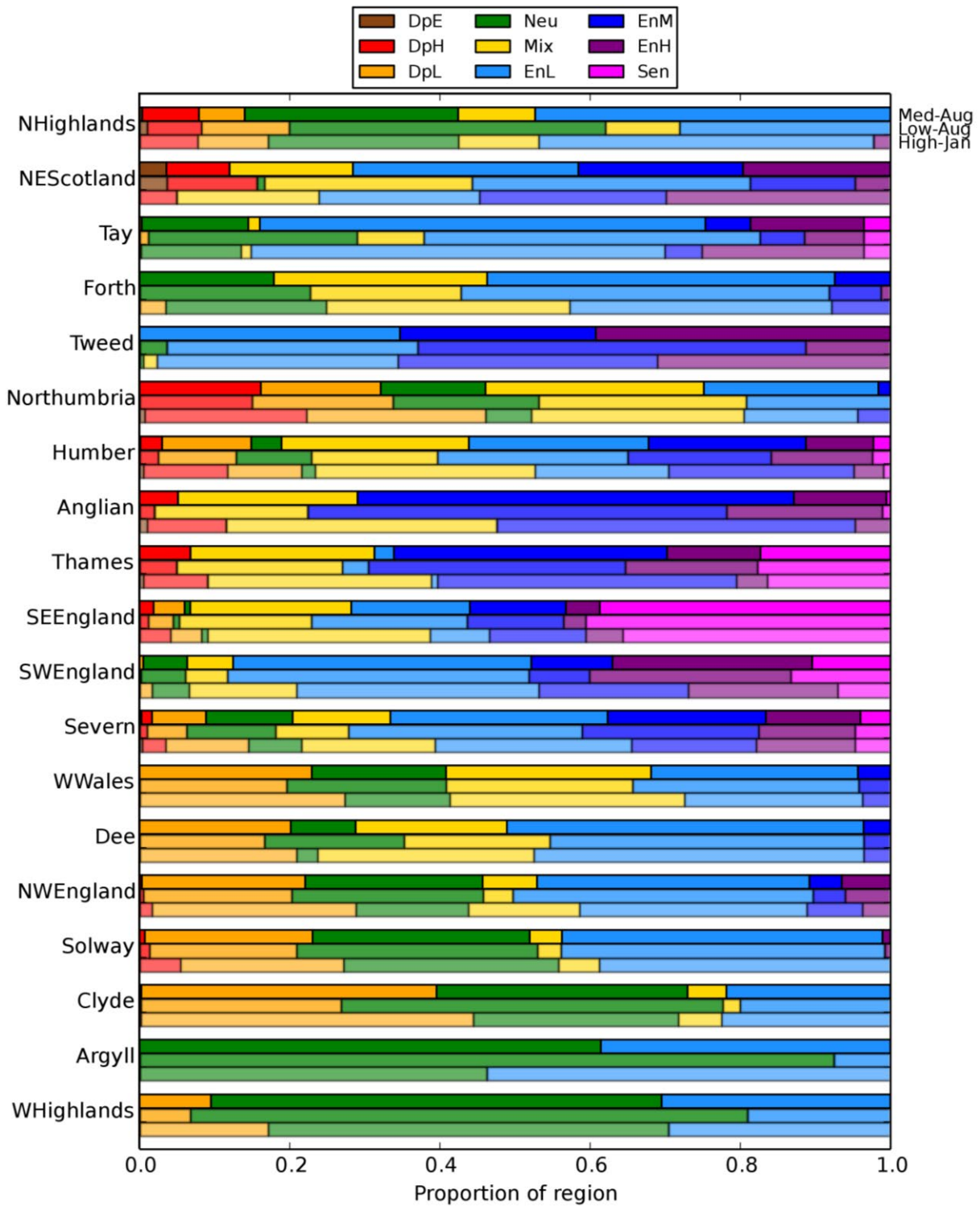


Figure 3.3 Stacked bar charts showing the balance of response types over the 19 river basin regions, for each of the 3 T/PE scenarios (Medium-August, Low-August and High-January), for changes in 20-year return period flood peaks

3.1.2 Checking for new response types

Figure 3.4 shows Taylor diagrams comparing the modelled response surfaces (for each 1km river cell) to the Neutral average response surface, for 3 return periods (10-, 20- and 50- years) and for the 3 T/PE scenarios (Medium-August, Low-August and High-January) – see section 2.4 for an explanation of Taylor diagrams. As expected, the river cells identified as having a Neutral response type (green) lie near where the correlation and standard deviation equal one. River cells identified as having a Sensitive response type (magenta) show the largest internal pattern variability (the points have the largest standardised standard deviation), and the largest intra-group variability (the points are not all very close to each other). The Taylor diagrams look similar across all return periods and T/PE scenarios, indicating consistency of response surface behaviour regardless of return period or T/PE scenario.

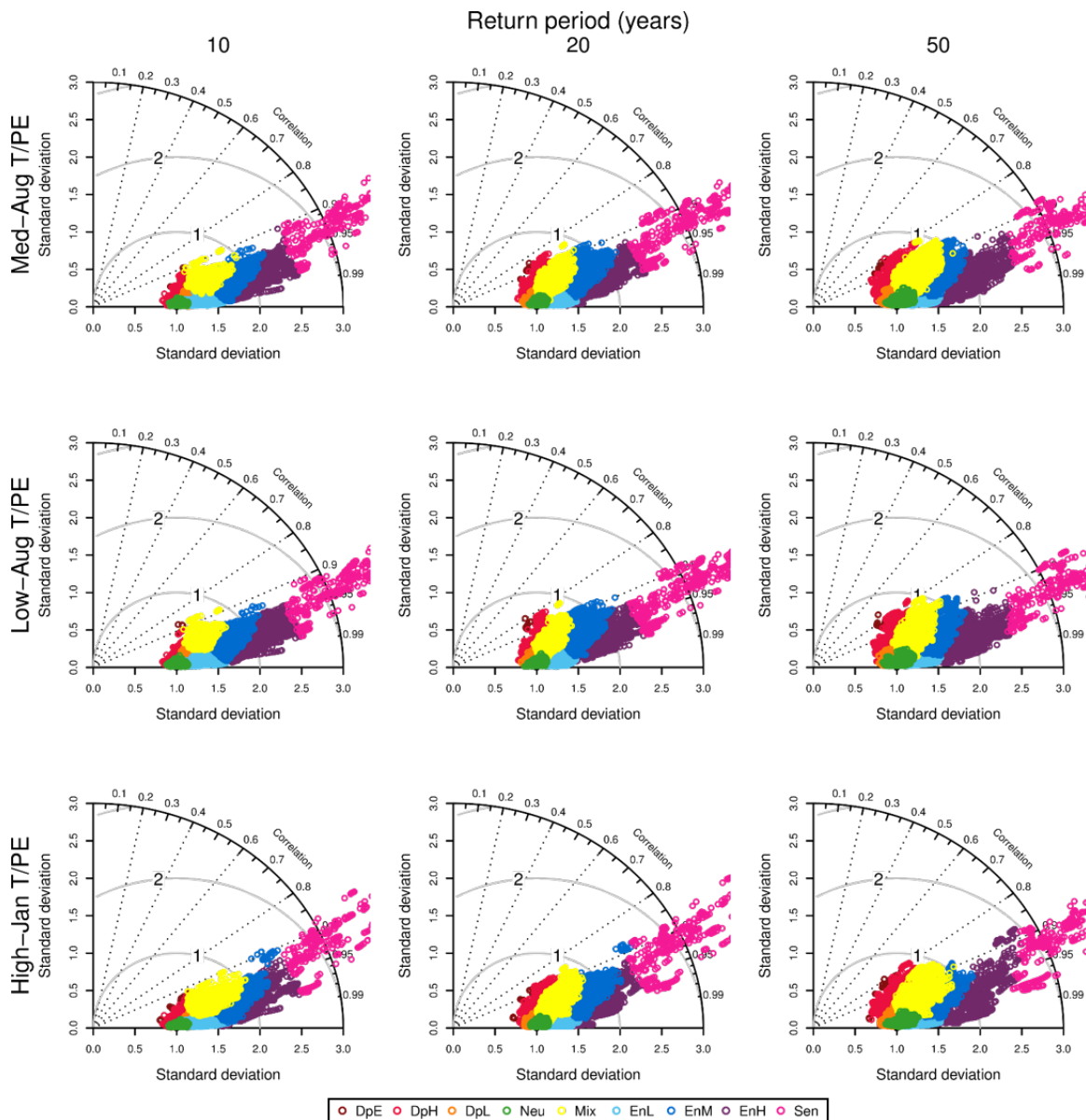


Figure 3.4 Taylor diagrams comparing the modelled response surfaces for every 1km river cell (catchment area $\geq 100\text{km}^2$) with the FD2020 Neutral average response surface as reference. The points are coloured by their identified response type (section 3.1.1)

For most of the response surfaces the points lie in a cluster around the reference surface of their respective type (see Appendix B.2), suggesting that there are no completely new response types. There are however some response surfaces that might be termed ‘Extra-Sensitive’; more extreme than the FD2020 Sensitive average response surface (see example in Figure 3.5).

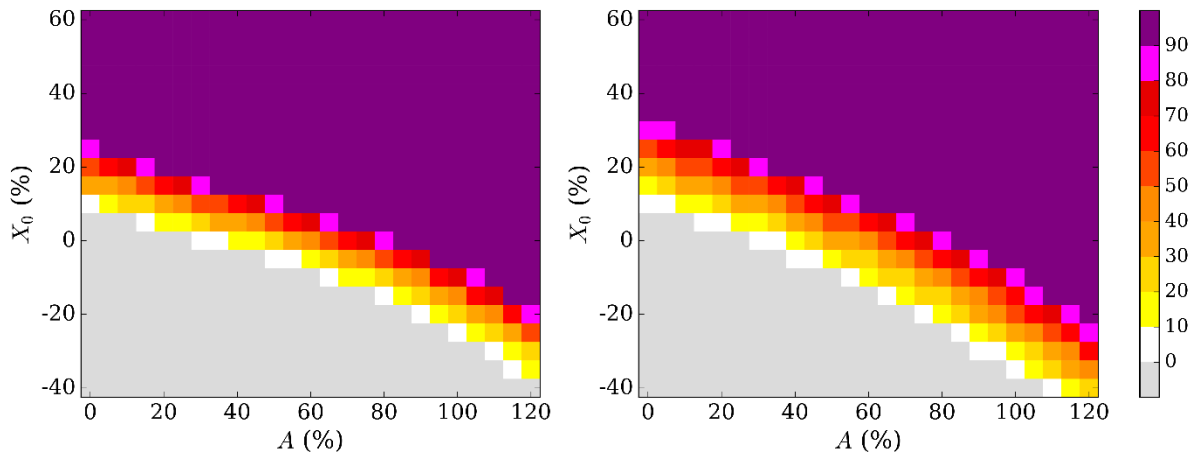


Figure 3.5 Example ‘Extra-Sensitive’ response surface (left) and the FD2020 average Sensitive response surface (right)

Another way to explore the difference between the modelled response surfaces and the FD2020 average response surfaces is to consider the rmsd between them (comparing each modelled response surface with the FD2020 average response surface of its identified response type). Plots of the rmsd distributions for each response type, for each return period and T/PE scenario (Figure 3.6) show that most 1km river cells have an rmsd of less than 40. However, the Sensitive river cells show rmsd values up to about 130; the 1km river cells in the tails of this distribution are ‘Extra-Sensitive’ like the example in Figure 3.5.

The Taylor diagrams and rmsd distributions also show that the Damped-Extreme modelled response surfaces are less similar to their corresponding FD2020 average response surface than is the case for the other response types (Appendix B.2 and Figure 3.6). The modelled response surfaces identified as Damped-Extreme here are generally less damped than the FD2020 Damped-Extreme average response surface (see example in Figure 3.7).

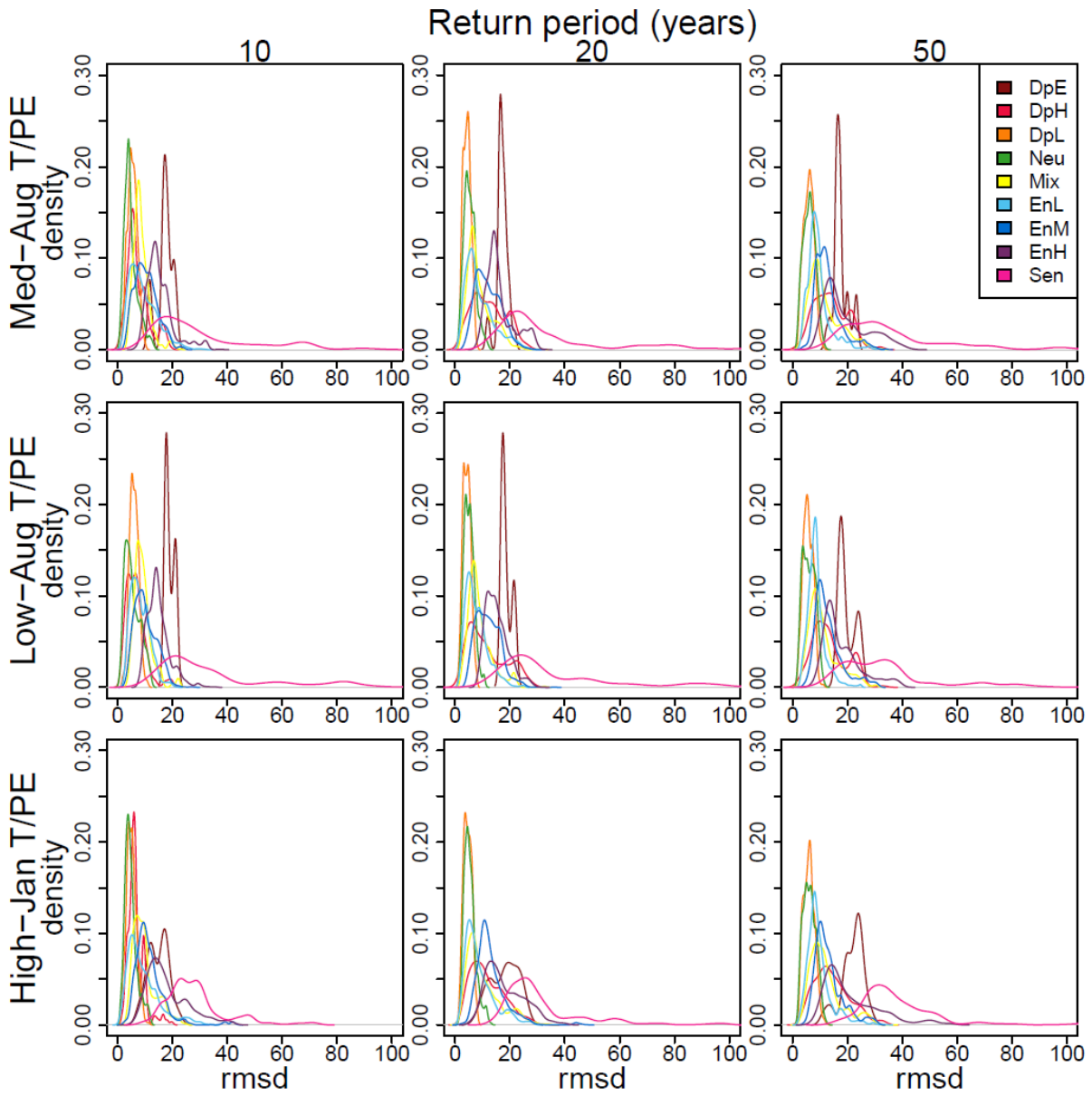


Figure 3.6 Comparison of rmsd for each response type, for each of the 3 return period and T/PE scenarios

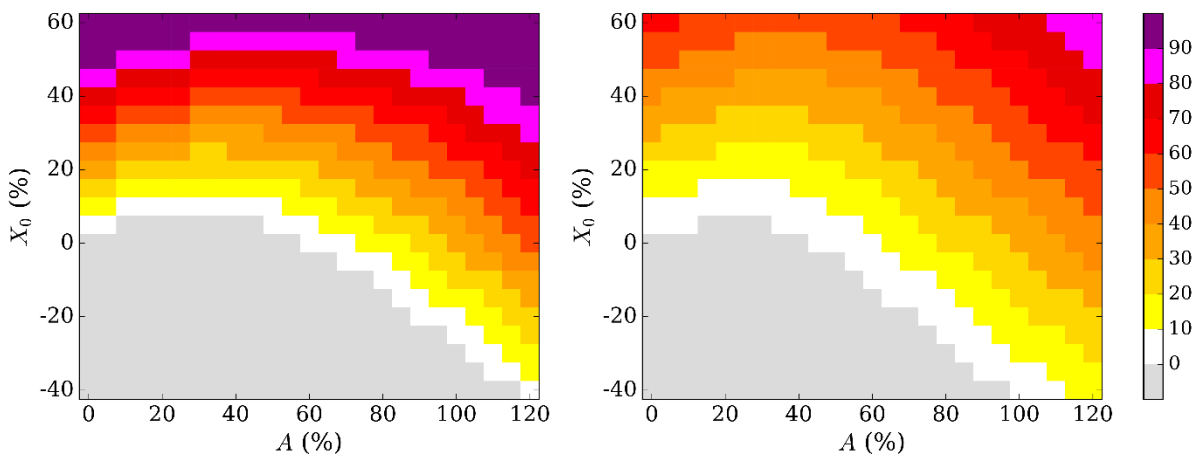


Figure 3.7 Example Damped-Extreme response surface (left) and the FD2020 average Damped-Extreme response surface (right)

3.2 Consistency of sensitivity domain with climate change projections

3.2.1 Precipitation change projections

Plots of the UKCP18 P harmonic mean (X_0) versus amplitude (A) for each river basin region (Figure 3.8 and Appendix C.1) show that although the distribution of the projections on the domain differs between regions and between emissions scenarios and time slices, the projections are generally consistent with the definition of the sensitivity framework (section 2.2), in terms of the extent set for the harmonic mean (X_0) and amplitude (A). Projections generally extend further across the X_0 vs A domain both for later time slices (Figure 3.8 and Figures B.1-B.3) and for higher emissions scenarios (Figure B.4). Similar plots for the UKCP09 projections are available in previous research reports (Kay and others, 2011a,b).

As for UKCP09, a very small number of the UKCP18 projections fall outside the sensitivity domain (with $A > 120\%$ or with $X_0 < -40\%$ or $X_0 > 60\%$), but only for the latest time slice (2080s) and highest emissions scenario (RCP8.5). In fact, this only affects one of the probabilistic projections in each of 2 regions, where $X_0 > 60\%$ in each case (specifically, one 2080s RCP8.5 projection has $X_0 = 64.2\%$ in the Argyll region and one projection has $X_0 = 63.7\%$ in the West Highland region, so these are not very far outside the extent of the sensitivity domain). For the A1B emissions scenario, none of the projections fall outside the sensitivity domain, either for UKCP09 or UKCP18. Where projections lie beyond the extent of the sensitivity domain, linear extrapolation is used to estimate the changes in flood peaks.

Plots of the UKCP18 P harmonic phase (Φ) for each river basin region (Figure 3.9 and Appendix C.1) show that while there is some variation in the month of the peak change, the predominant months are in winter, consistent with the peak month set for the single harmonic (January). Although more of the projections for the earlier time slices can peak in summer, the projections in these time slices generally have low amplitude (A , Figure 3.8), so the month is much less important. Even for later time slices, the small proportion of projections that peak in summer rather than winter generally have low amplitude compared to those projections peaking in winter (not shown). Therefore, the assumption of a winter peak will not make much difference to the extracted impacts on flood peaks. Similar plots for the UKCP09 projections are available in previous research reports (Kay and others, 2011a,b).

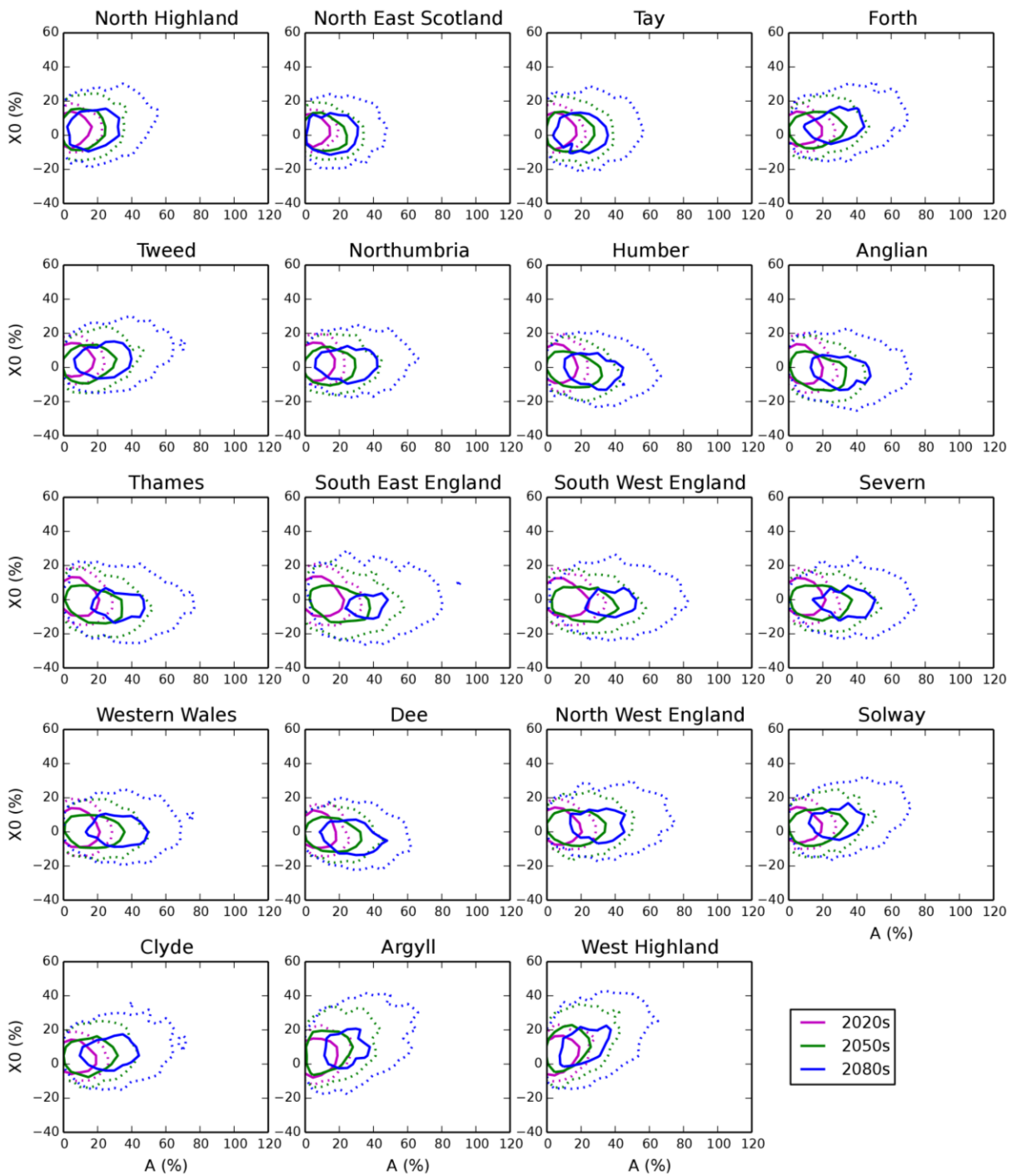


Figure 3.8 Contour plots showing UKCP18 P harmonic mean (X_0) versus amplitude (A) for each river basin region, for the 2020s, 2050s and 2080s (magenta, green and blue respectively) with RCP8.5 emissions. Contours delineate densities of 5 and 50 projections per 5% \times 5% sensitivity domain square (dotted and solid lines respectively)

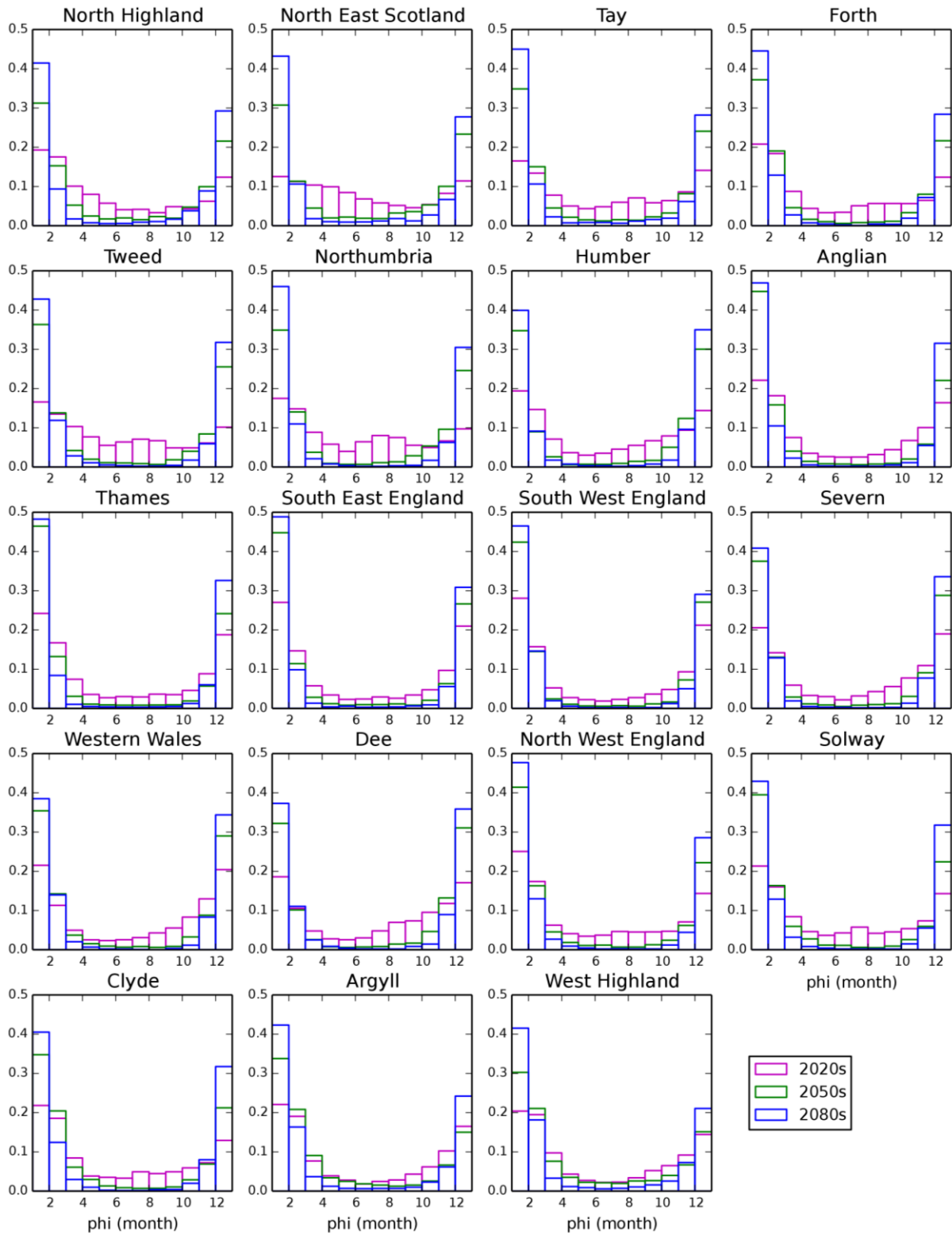


Figure 3.9 Histograms showing the distribution of the UKCP18 P harmonic phase (Φ) for each river basin region, for the 2020s, 2050s and 2080s (magenta, green and blue respectively) with RCP8.5 emissions

3.2.2 Temperature change projections

Figure 3.10 shows the distributions of the 3 harmonic function parameters (X_0 , A , Φ) from the UKCP18 probabilistic temperature change projections for the UK for the 2080s under RCP6.0 emissions. This shows that August is the predominant month of peak, with the most likely mean annual change in the range 2.5 to 3.0°C, and the most likely amplitude in the range 0.6 to 0.8°C (with no strong correlations between any pair of parameters). Therefore, the choice of the main T/PE scenario as ‘Medium-August’ is highly consistent with UKCP18, as it has a mean change of 2.5°C and an amplitude of 0.8°C, peaking in August (Table 2.2).

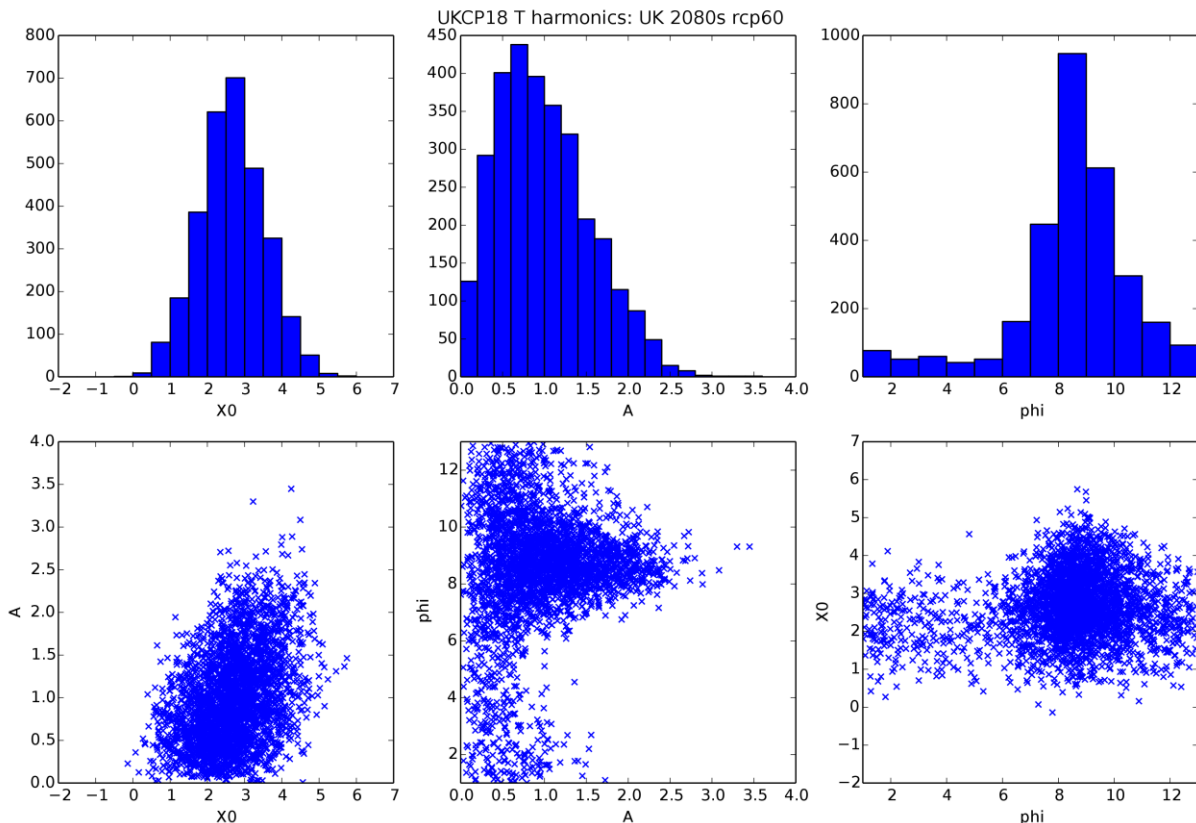


Figure 3.10 Distribution of the 3 harmonic function parameters (top row; X_0 , A , Φ) from the UKCP18 probabilistic temperature change projections for the UK, for the 2080s with RCP6.0 emissions. The bottom row shows correlations between each pair of parameters

The second chosen T/PE scenario is ‘Low-August’, which has a mean change of 1.5°C and an amplitude of 1.2°C, again peaking in August (Table 2.2). While this is less likely than Medium-August, it is still within the bounds of UKCP18, both for RCP6.0 emissions (Figure 3.10) and for lower emissions (RCP2.6; see Appendix C.2).

The third chosen T/PE scenario is ‘High-January’, which has a mean change of 4.5°C and an amplitude of 1.6°C, peaking in January. Again, this is less likely than Medium-August, but is still within the bounds of UKCP18, both for RCP6.0 emissions (Figure 3.10) and for higher emissions (RCP8.5; see Appendix C.2). In particular, while scenarios with a January peak are much less likely than those with an August peak, they can have more extreme mean changes and amplitudes (as shown by the plots of Φ against X_0 and A) than some other months (except those around August), so it is sensible to cover this possibility.

3.3 Impacts from UKCP18 projections

As an example, Figure 3.11 shows the UKCP18 50th percentile of change in 20-year return period flood peaks for the 2080s under RCP8.5 emissions (Medium-August T/PE scenario). This shows significant spatial variation, with impacts typically higher in the west than the east. However, the scale required for good visualisation of 1km rivers on such maps means that it is not possible to show all possible combinations of percentile of change, return period, time slice and emissions scenario in this way. The best way to explore the results for individual 1km river cells is through the UK CEH web tool (Appendix D). Instead, subsequent results are presented as the regional mean and standard deviation of the change in flood peaks, for each of the 19 UKCP18 river basin regions (Figure 2.4b).

Maps of regional means for 5 percentiles of change in 20-year return period flood peaks, for 3 future time slices under RCP8.5 emissions (Figure 3.12 top), generally show increases in flood peaks, which are typically higher for later time slices. The maps show clear differences between regions, with regional mean changes generally smaller in the south-east than in the north-west for the lower percentiles, although the differences become less pronounced for higher percentiles. In fact, some regions show decreases in flood peaks for lower percentiles, and these can either increase or decrease for later time slices.

The maps of regional standard deviations (SDs) (Figure 3.12 bottom) generally show higher SD for later time slices and higher percentiles, but with less clear spatial variation than for the regional means. However, north-east Scotland shows higher SD for all percentiles and time slices, and southern Britain shows higher SD for the 90th percentile in the 2080s. These regional differences are related to the range of response types in each region; a region with both damped and enhanced/sensitive types (Figure 3.1) will have a higher SD, especially for the higher percentile changes and when the climate projections extend to cover more of the sensitivity domain (Figure 3.8).

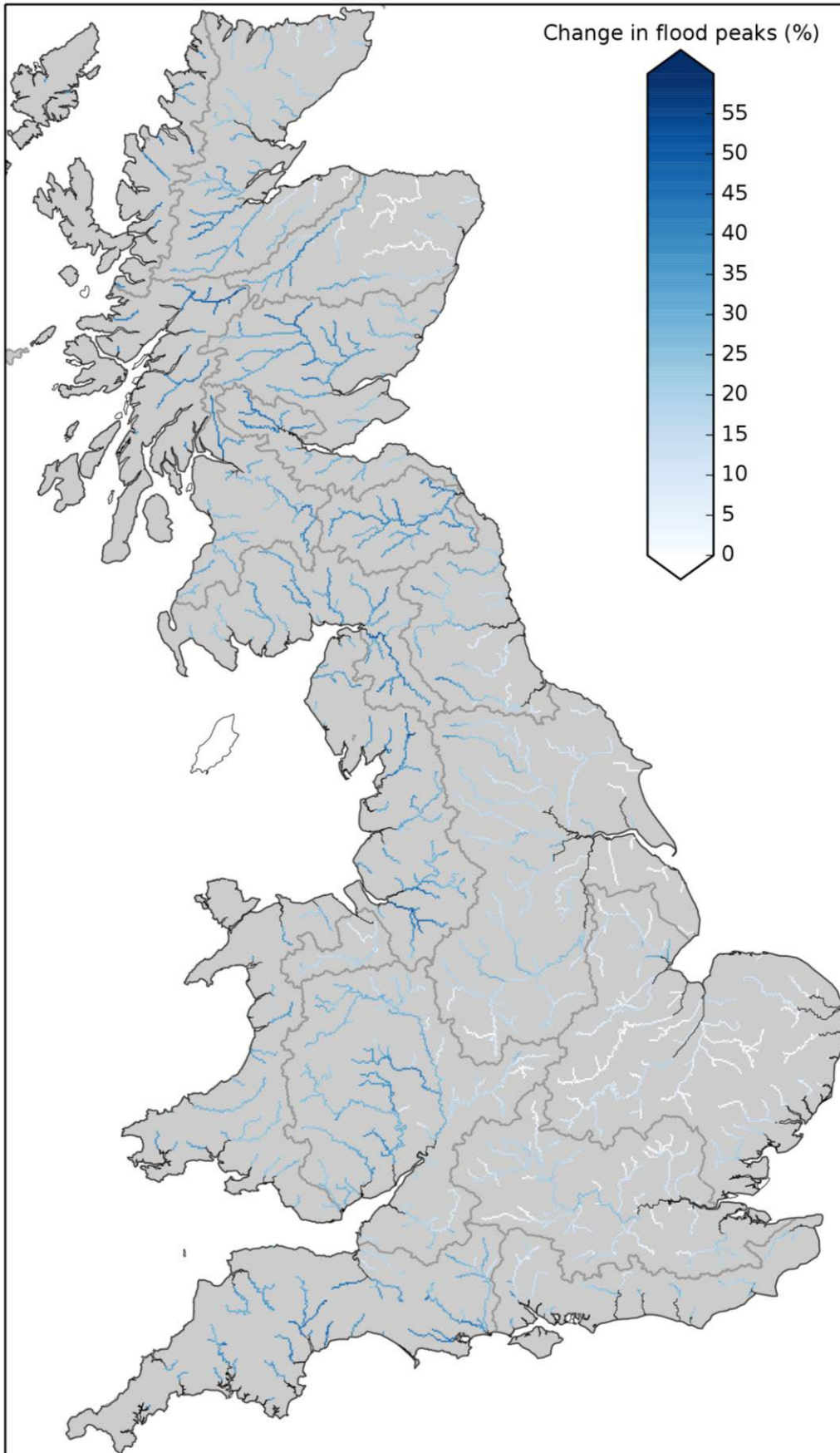


Figure 3.11 Map showing the 50th percentile of change in 20-year return period flood peaks for the 2080s under RCP8.5 emissions (Medium-August T/PE scenario)

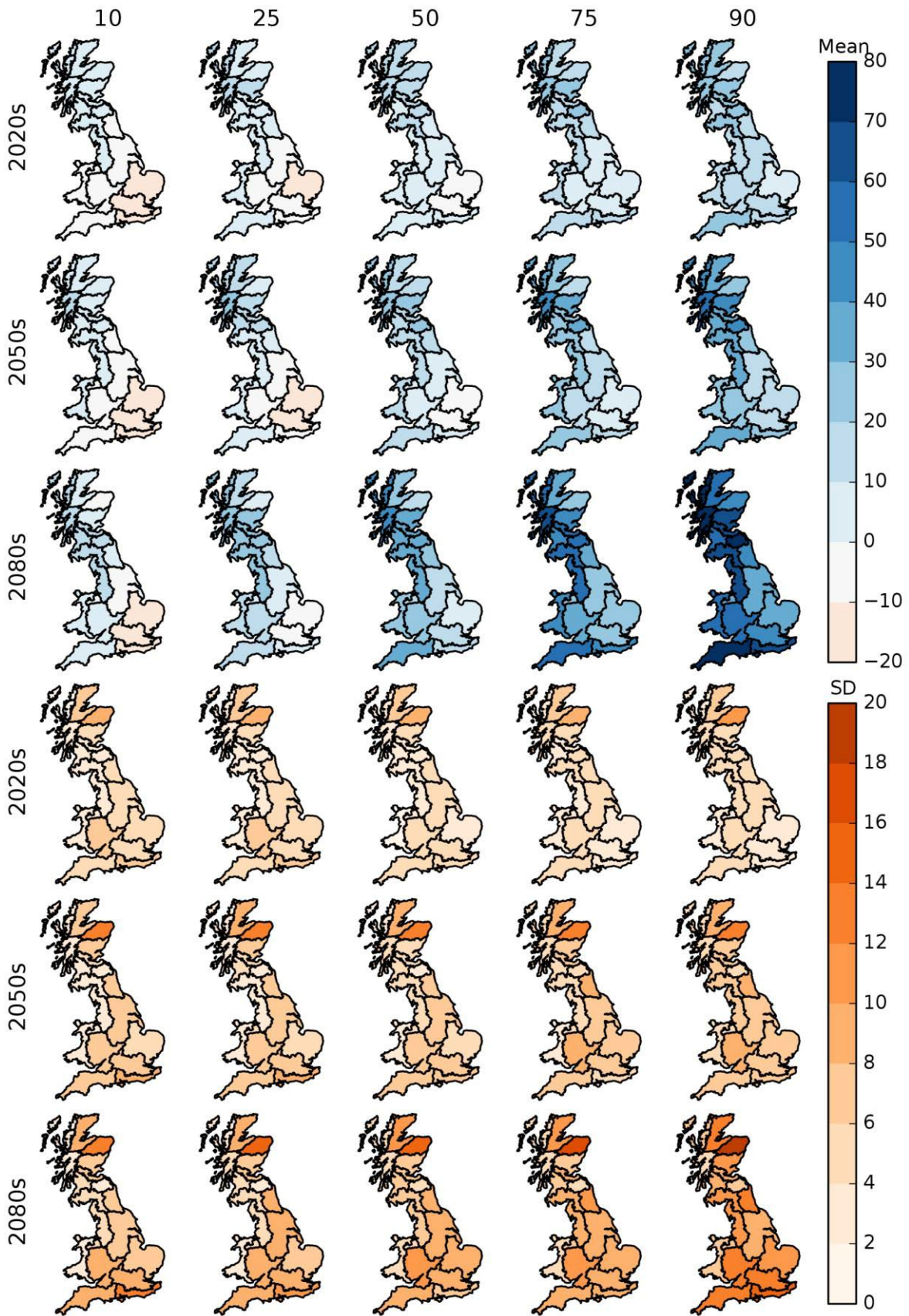


Figure 3.12 Maps showing the regional means (top) and SDs (bottom) of 5 percentiles of change in 20-year return period flood peaks (10th, 25th, 50th, 75th and 90th; left to right) for 3 time slices (2020s, 2050s and 2080s) under RCP8.5 emissions (Medium-August T/PE scenario)

3.3.1 Comparing regional values across emissions scenarios

Plots comparing the regional means across 3 time slices for the 4 emissions scenarios (Figure 3.13) show that both climate modelling uncertainty (the percentile range for a given emission scenario) and emissions scenario uncertainty (the range covered by different emissions scenarios for a given percentile of change) are greater for later time slices.

Plots comparing the regional SDs across 3 time slices for the 4 emissions scenarios (Figure 3.14) show that the SD (regional variation in impacts) is greater for higher emissions scenarios. This is particularly the case for the 90th percentile changes in most regions, and occurs because the response surfaces vary most for more extreme changes in precipitation.

3.3.2 Comparing regional values across periods

Plots comparing the regional means across 3 time slices for the 3 return periods (Figure 3.15) show that there is relatively little difference with return period, whatever percentile impact is selected.

Plots comparing the regional SDs across 3 time slices for the 3 return periods (Figure 3.16) show that some regions have greater variation in impacts for higher return periods than lower return periods. The variation is particularly clear in north-east Scotland. Differences in regional SDs with return period are due to a differing balance of response types in some regions for different return periods (Figure 3.2). For example, north-east Scotland gets more cells with Damped-Extreme/Damped-High types and more cells with Enhanced-High types for higher return periods, therefore has a greater spread of impacts across the region for higher return periods.

3.3.3 Comparing regional values across T/PE scenarios

Plots comparing the regional means across 3 time slices for the 3 T/PE scenarios (Figure 3.17) show that there is relatively little difference with T/PE scenario in most regions, whatever percentile impact is selected. There are some differences in southern and eastern parts of England, where the effect of potential evaporation on flows is typically larger, but the differences are relatively small compared to the range of climate modelling uncertainty, and the Medium-August T/PE scenario (the main T/PE scenario; section 2.2) gives impacts between those of the High-January and Low-August T/PE scenarios.

Plots comparing the regional SDs across 3 time slices for the 3 T/PE scenarios (Figure 3.18) show that some regions have greater variation in impacts for the High-January T/PE scenario, and less variation for the Low-August T/PE scenario, compared to the Med-August T/PE scenario. This is particularly the case in north-eastern parts of Scotland (possibly related to the varying effects of snow in different catchments) and in southern England (probably related to the varying influence of PE in different catchments).

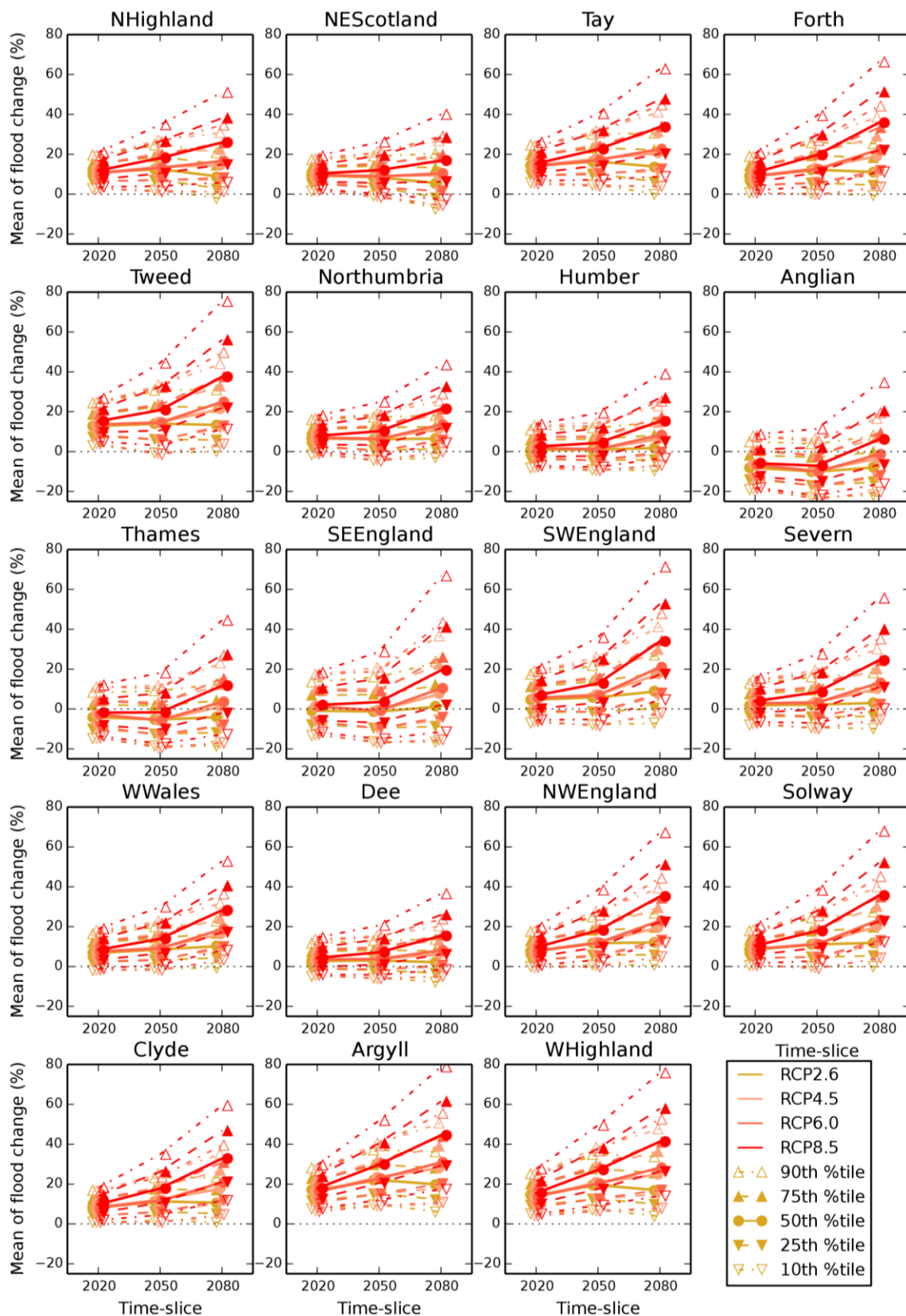


Figure 3.13 Plots comparing the regional means of changes in 20-year return period flood peaks using UKCP18 probabilistic projections for 3 time slices (2020s, 2050s and 2080s) under 4 emissions scenarios (RCP2.6, RCP4.5, RCP6.0 and RCP8.5) (Medium-August T/PE scenario). Each plot shows 5 percentiles of change (10th, 25th, 50th, 75th and 90th)

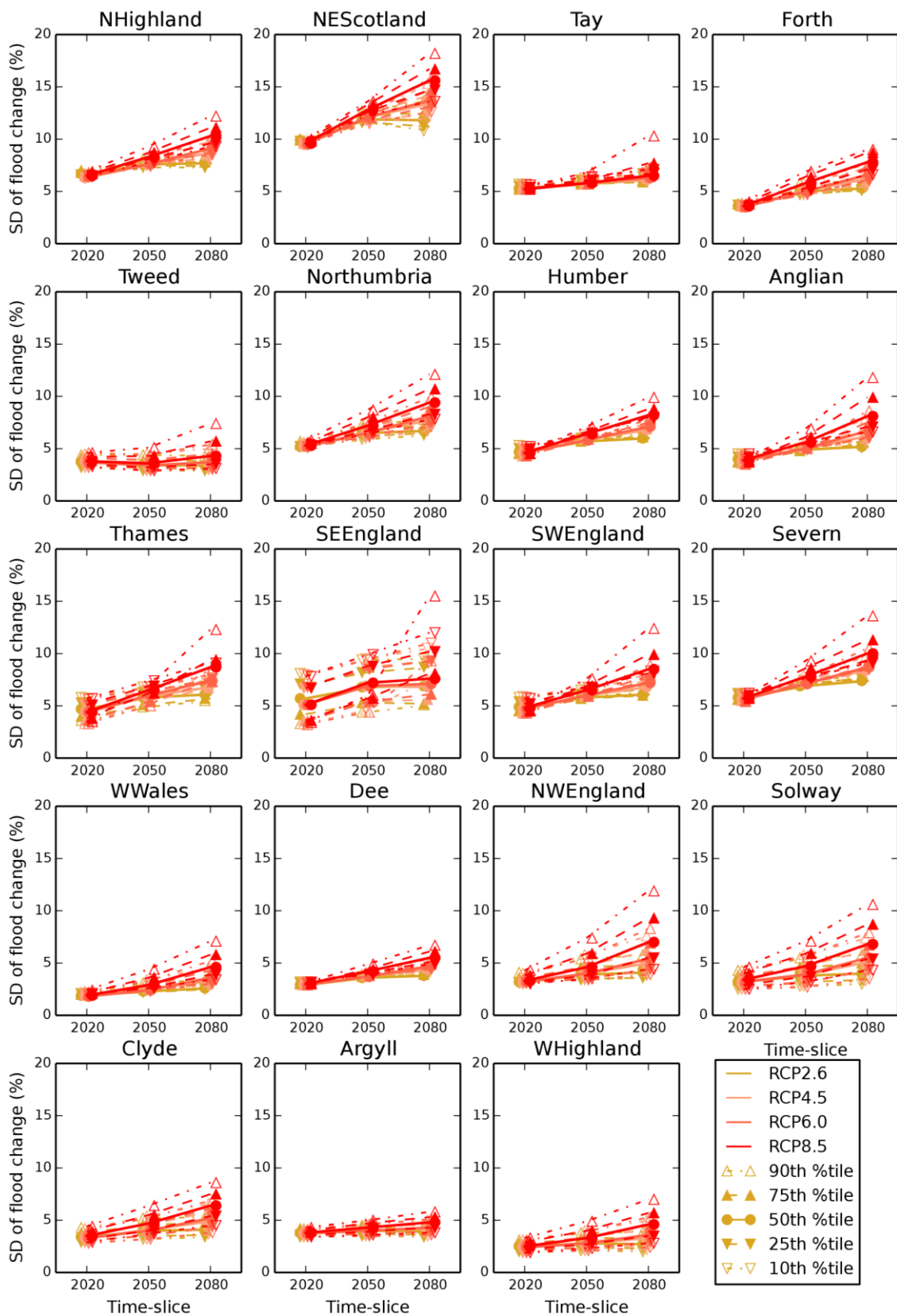


Figure 3.14 Plots comparing the regional SDs of changes in 20-year return period flood peaks using UKCP18 probabilistic projections for 3 time slices (2020s, 2050s and 2080s) under 4 emissions scenarios (RCP2.6, RCP4.5, RCP6.0 and RCP8.5) (Medium-August T/PE scenario). Each plot shows 5 percentiles of change (10th, 25th, 50th, 75th and 90th)

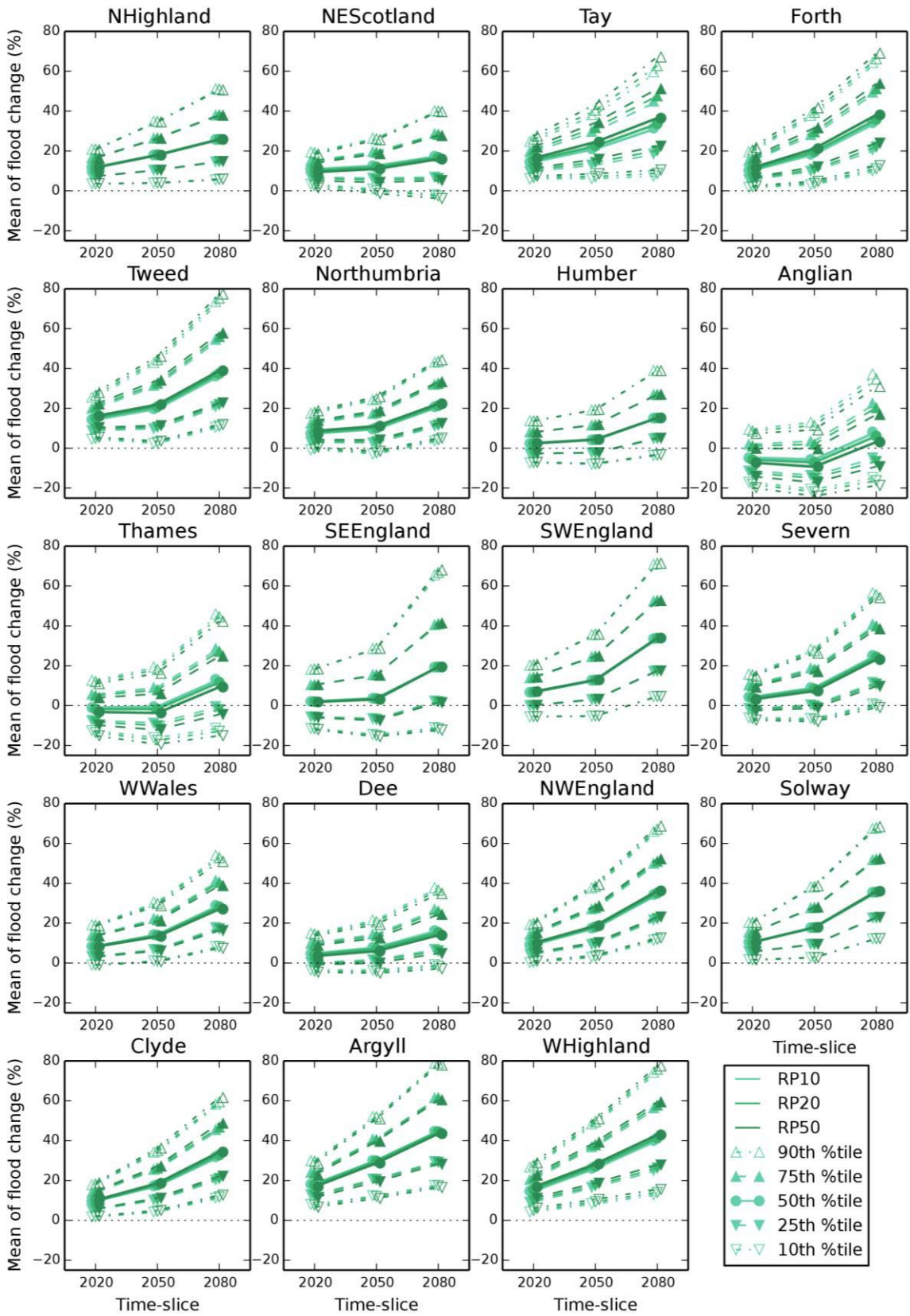


Figure 3.15 Plots comparing the regional means of changes in 10-, 20- and 50-year return period flood peaks using UKCP18 probabilistic projections for 3 time slices (2020s, 2050s and 2080s) under RCP8.5 emissions scenarios (Medium-August T/PE scenario). Each plot shows 5 percentiles of change (10th, 25th, 50th, 75th and 90th)

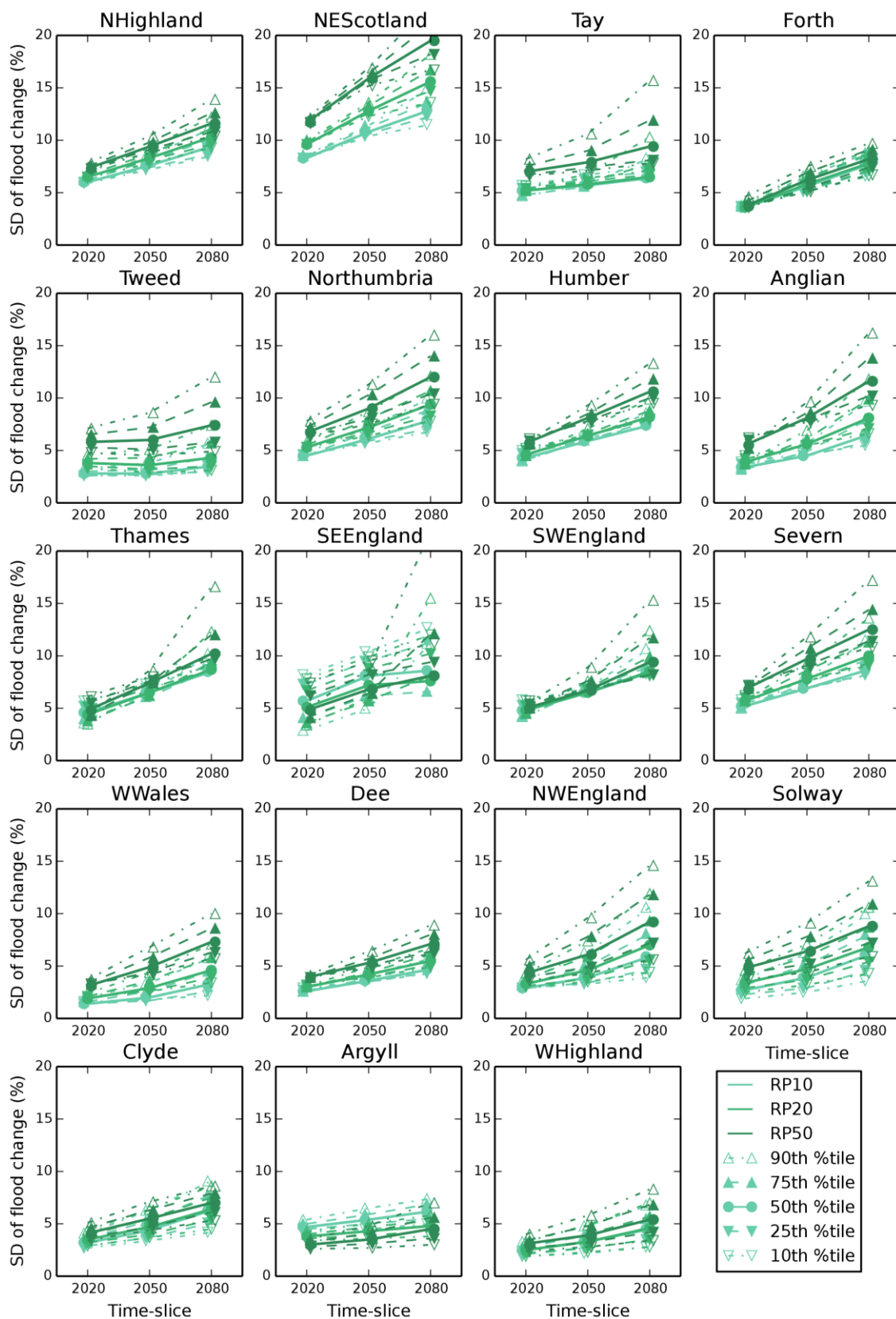


Figure 3.16 Plots comparing the regional SDs of changes in 10-, 20- and 50-year return period flood peaks using UKCP18 probabilistic projections for 3 time slices (2020s, 2050s and 2080s) under RCP8.5 emissions scenarios (Medium-August T/PE scenario). Each plot shows 5 percentiles of change (10th, 25th, 50th, 75th and 90th)

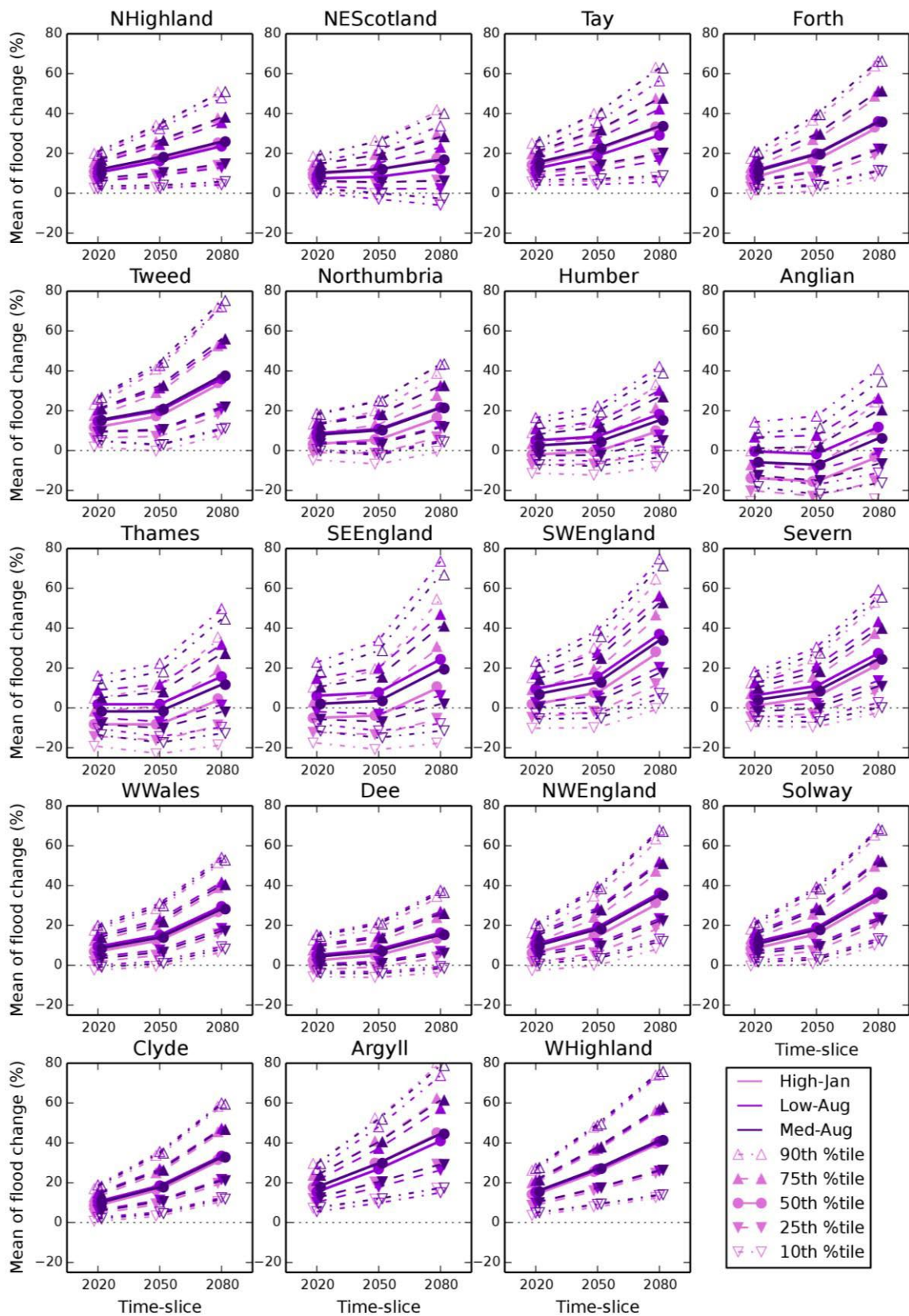


Figure 3.17 Plots comparing the regional means of changes in 20-year return period flood peaks using UKCP18 probabilistic projections for 3 time slices (2020s, 2050s and 2080s) under A1B emissions, for the 3 T/PE scenarios: High-January, Low-August, and Medium-August. Each plot shows 5 percentiles of change (10th, 25th, 50th, 75th and 90th)

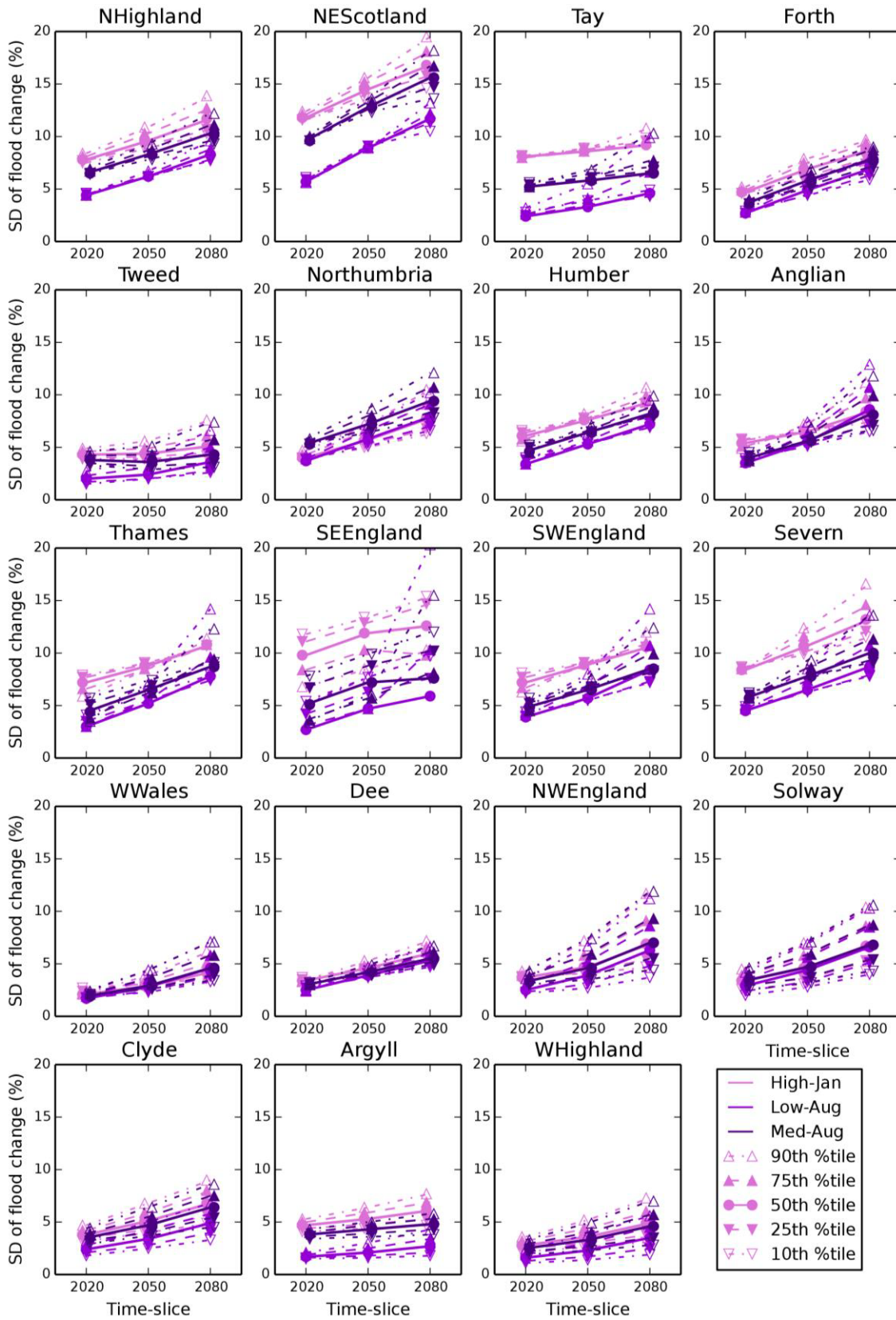


Figure 3.18 Plots comparing the regional SDs of changes in 20-year return period flood peaks using UKCP18 probabilistic projections for 3 time slices (2020s, 2050s and 2080s) under A1B emissions, for the 3 T/PE scenarios: High-January, Low-August, and Medium-August. Each plot shows 5 percentiles of change (10th, 25th, 50th, 75th and 90th)

3.3.4 Comparing regional values with and without extra uncertainty allowances

Plots comparing the regional means across 3 time slices for the UKCP18 projections with and without the extra uncertainty allowances (Figure 3.19) show that, unsurprisingly, the values with the extra uncertainty allowances are greater than those without. The amount of difference will depend on the balance of different response types within each region, as the uncertainty allowances differ by response type (Table 2.4). The differences do not depend on the percentile or the time slice, as neither the balance of the response types in a region nor the extra uncertainty allowances vary by percentile or time slice. The differences are likely to vary by return period though (not shown), as the balance of response types in a region varies by return period (Figure 3.2) and the extra uncertainty allowances vary by return period (Table 2.4).

Plots comparing the regional SDs across 3 time slices for the UKCP18 projections with and without the extra uncertainty allowances (Figure 3.20) show that using the extra uncertainty allowances generally causes relatively little difference in the regional variation in impacts, particularly for the 50th percentile impacts. In regions where there is some difference even for the 50th percentile impacts, the direction of the difference depends on the balance of response types in the region and the allowances for those types. For example, Northumbria has nearly the full range of response types, from Damped-High to Enhanced-Medium (Figure 3.2). Therefore, because the extra uncertainty allowances for the more extreme types are typically larger than those for intermediate types (Table 2.4), including them reduces the regional variation in impacts. In contrast, Argyll has just 2 similar response types, Neutral and Enhanced-Low, the latter of which has higher extra uncertainty allowances than the former, so including the allowances increases the regional variation in impacts. Differences at other percentiles in some regions (for example, 90th percentile for SE England) will similarly depend on the balance of response types in the region, and the allowances for those types.

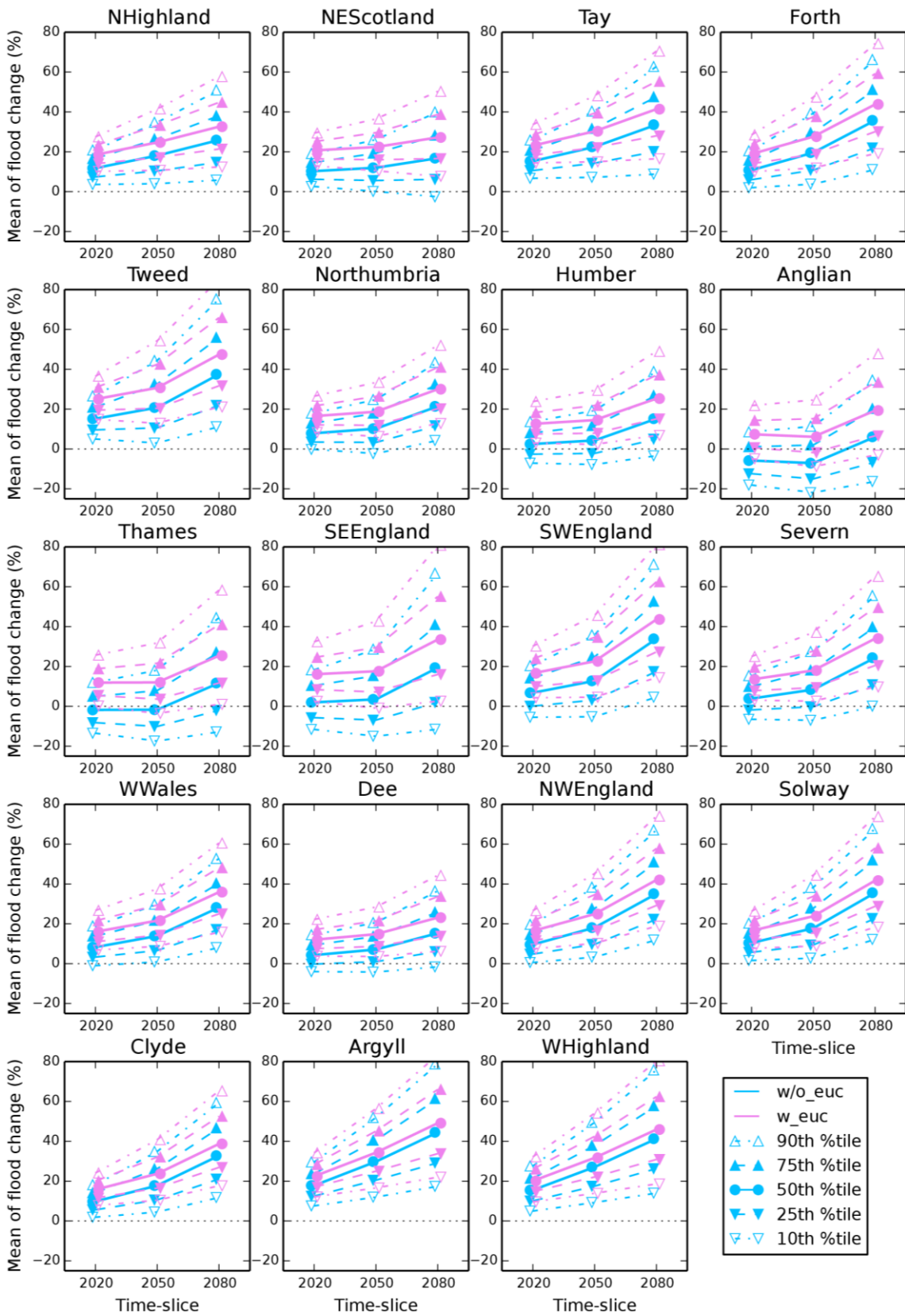


Figure 3.19 Plots comparing the regional means of changes in 20-year return period flood peaks using UKCP18 probabilistic projections for 3 time slices (2020s, 2050s and 2080s) under RCP8.5 emissions, with and without the extra uncertainty allowances (Medium-August T/PE scenarios). Each plot shows 5 percentiles of change (10th, 25th, 50th, 75th and 90th)

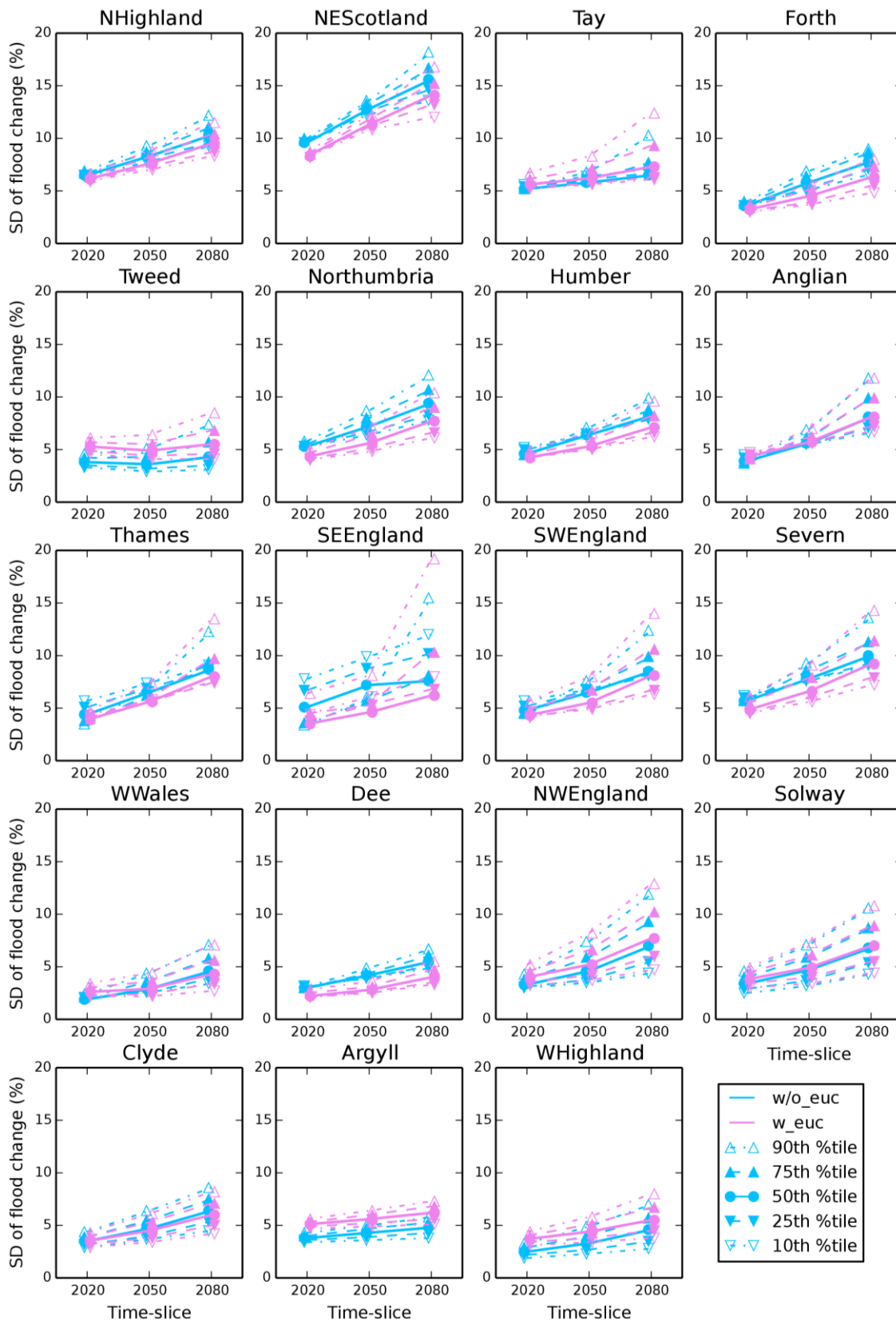


Figure 3.20 Plots comparing the regional SDs of changes in 20-year return period flood peaks using UKCP18 probabilistic projections for 3 time slices (2020s, 2050s and 2080s) under RCP8.5 emissions, with and without the extra uncertainty allowances (Medium-August T/PE scenarios). Each plot shows 5 percentiles of change (10th, 25th, 50th, 75th and 90th)

3.4 Comparing impacts from the UKCP18 and UKCP09 projections

3.4.1 Comparing regional values under UKCP18 and UKCP09

Plots comparing the regional means across 3 time slices for the UKCP18 and UKCP09 projections under A1B emissions (Figure 3.21) show that there is relatively little difference between the impacts from the new and old projections, especially for the 50th percentile impacts. However, the impact range under UKCP18 is often wider than under UKCP09. This is because the 10th percentile impact under UKCP18 is generally less than under UKCP09, and the 90th percentile impact under UKCP18 is often higher than, or at least similar to, that for UKCP09.

Plots comparing the regional SDs across 3 time slices for the UKCP18 and UKCP09 projections under A1B emissions (Figure 3.22) show relatively little difference, particularly for 50th percentile impacts.

Any differences in impacts from UKCP18 and UKCP09 occur due to the comparative positioning of the UKCP18 and UKCP09 probabilistic projections on the response surfaces. The UKCP18 projections are typically concentrated slightly further right (higher seasonal amplitude A), but also slightly lower (lower annual mean change X_0) (Figure 3.23), therefore not giving very different median impacts on flood peaks. The UKCP18 projections also typically have a greater spread than the UKCP09 projections, particularly in terms of potential reductions in X_0 (Figure 3.23), therefore giving a greater range of impacts, especially in terms of lower 10th percentile impacts.

Note that, for this comparison, the regional impact summaries for both the UKCP18 and UKCP09 projections use the UKCP18 river basin regions, for spatial consistency of the averages and SDs. However, overlaying the projections on response surfaces uses the river basin regions corresponding to each respective set of projections, for consistency with the calculation of the projections. This is considered to be the fairest way of comparing the impacts from the respective projections, given the (relatively small) differences in the river basin regions (Figure 2.4 and Table 2.3).

It is not particularly surprising that the range of impacts from UKCP18 is wider than that from UKCP09. Reynard and others (2017) highlight that “Climate modelling uncertainty is potentially reducible (Deser and others, 2012), for example, through improved process representation, but it is also possible that the inclusion of new processes, or refinement of existing ones, could lead to greater uncertainty (Maslin and Austin 2012; Murphy and others, 2009: Section 2.5).”

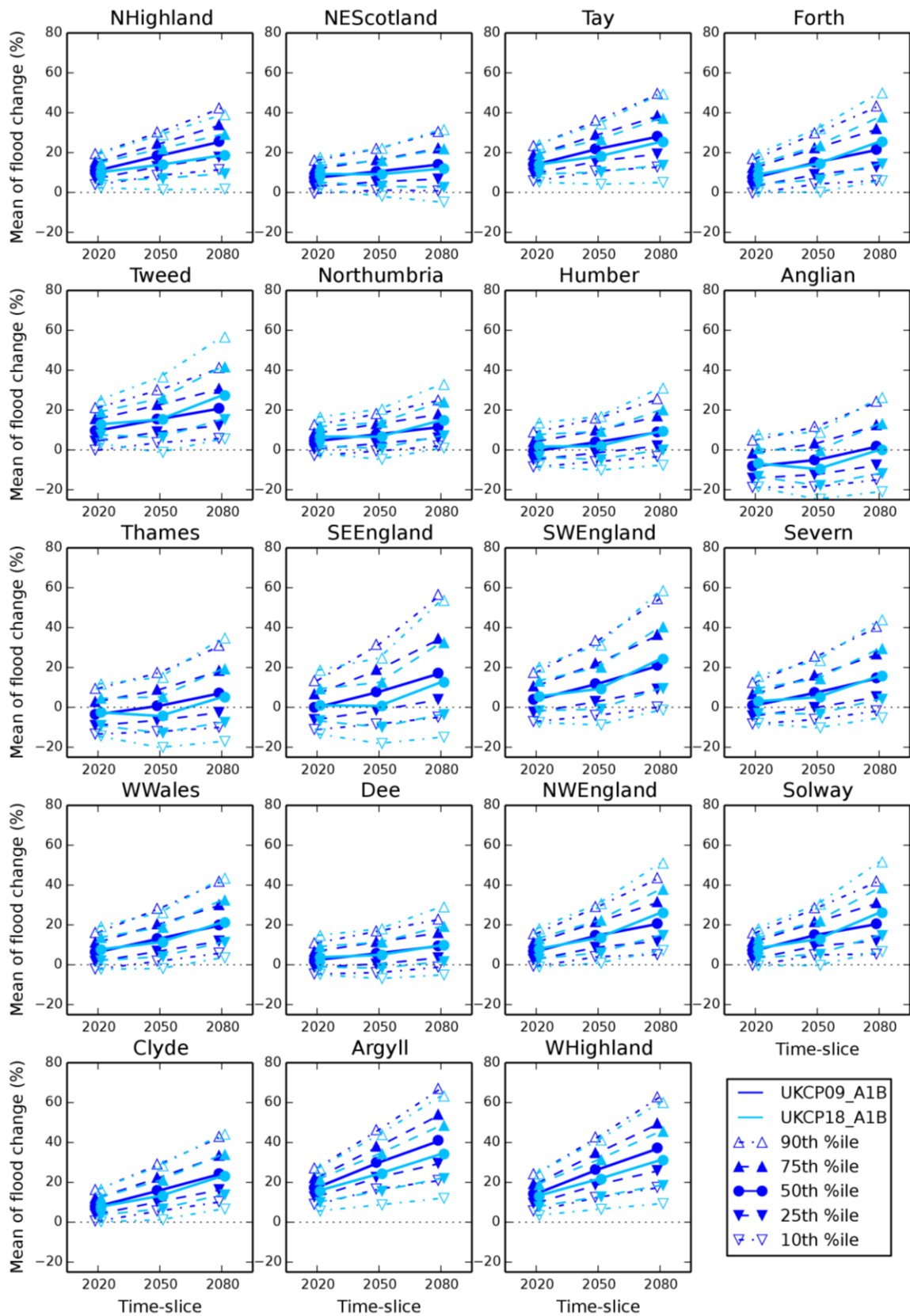


Figure 3.21 Plots comparing the regional means of changes in 20-year return period flood peaks using UKCP18 and UKCP09 probabilistic projections for 3 time slices (2020s, 2050s and 2080s) under A1B emissions, without the extra uncertainty allowances (Medium-August T/PE scenario). Each plot shows 5 percentiles of change (10th, 25th, 50th, 75th and 90th)

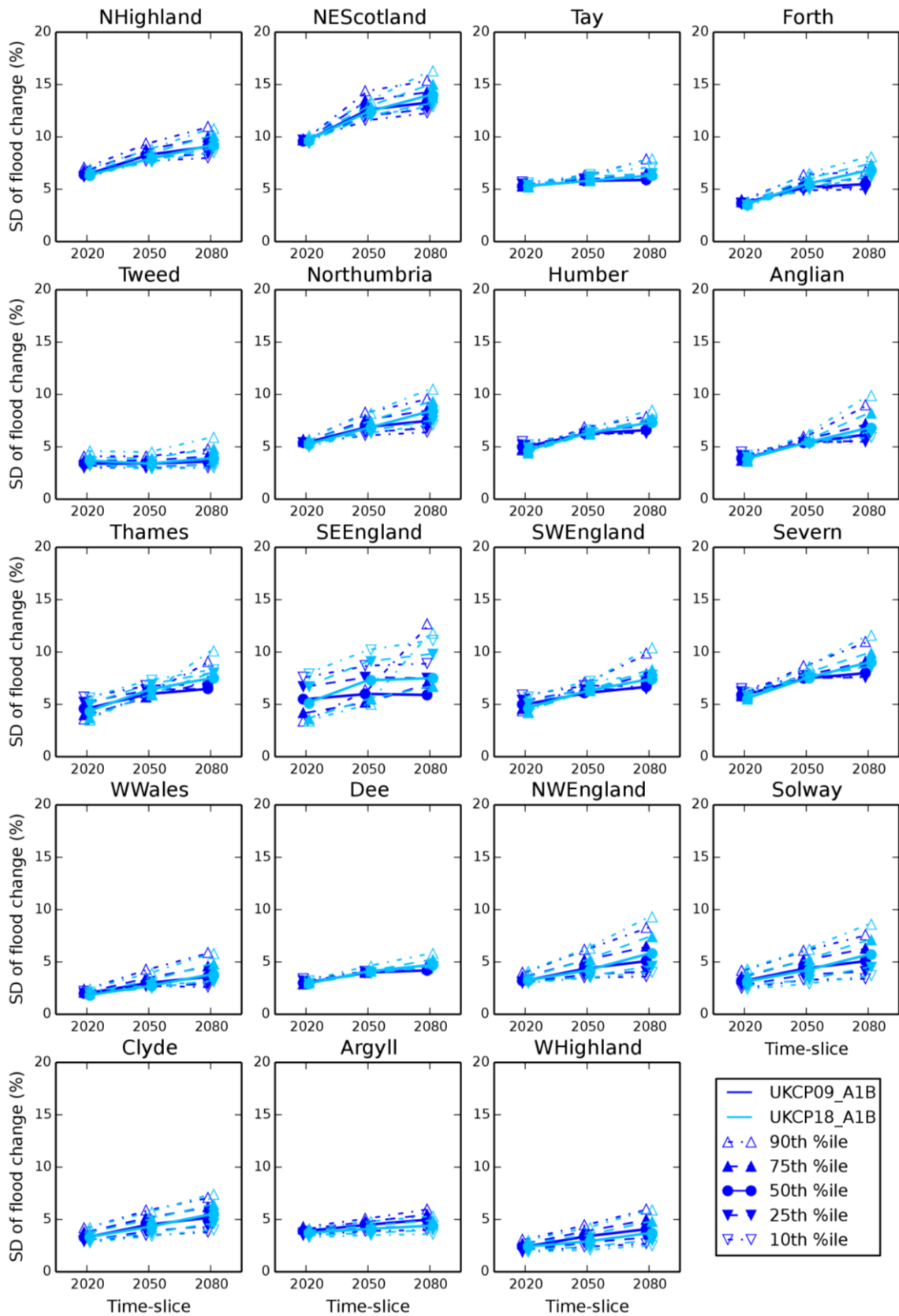


Figure 3.22 Plots comparing the regional SDs of changes in 20-year return period flood peaks using UKCP18 and UKCP09 probabilistic projections for 3 time slices (2020s, 2050s and 2080s) under A1B emissions, without the extra uncertainty allowances (Medium-August T/PE scenario). Each plot shows 5 percentiles of change (10th, 25th, 50th, 75th and 90th)

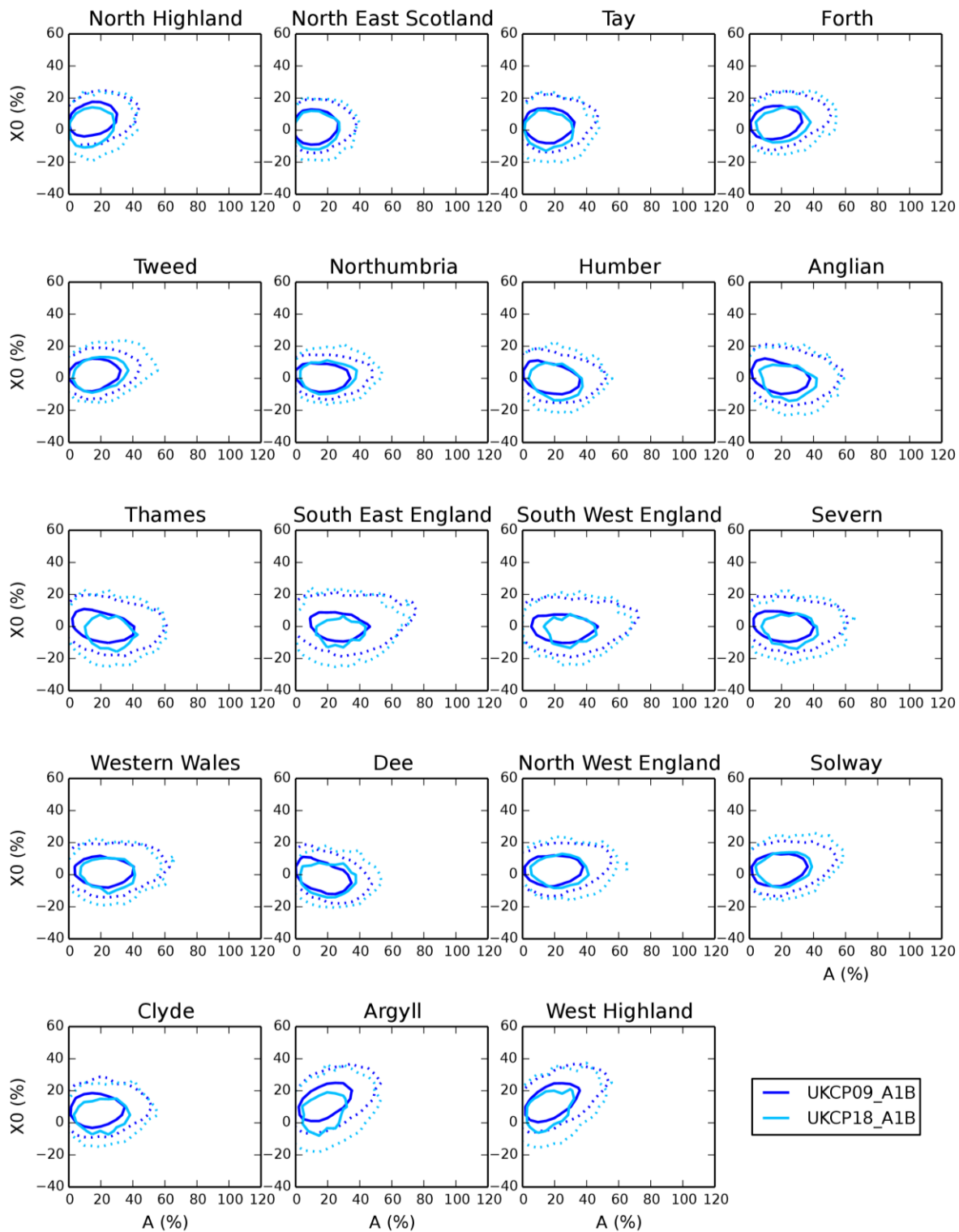


Figure 3.23 Contour plots comparing the UKCP18 and UKCP09 projections in terms of P harmonic mean (X_0) versus amplitude (A) for each river basin region, for the 2080s (A1B emissions). Contours delineate densities of 0.2% and 1.8% of projections per 5% \times 5% sensitivity domain square (dotted and solid lines respectively), where there is an ensemble of 10,000 projections for UKCP09 and 3,000 for UKCP18

3.4.2 Comparing new regional values with existing guidance

Values from the existing regional guidance on flood peaks and climate change for England and Wales (derived from FD2648; EA2016a,b and Welsh Government 2016) are compared with regional mean values derived from the new grid-based modelling combined with the UKCP09 projections (including the extra uncertainty allowances). The comparison covers the 10th, 50th and 90th percentile (Lower, Central and Upper) values for the 2020s, 2050s and 2080s. The new regional values are taken for 50-year return period flood peaks and rounded to the nearest 5%; values for the 2020s and 2050s use the A1B emissions scenario, while the 10th, 50th and 90th percentile values for the 2080s use B1, A1B and A1F1 emissions respectively. The comparison shows that, for most regions, the new regional values are very close to the values provided by the existing guidance (Table 3.2). Larger differences are coloured. The main exceptions to this are the Anglian and Tweed regions.

For the Anglian region, the new regional values are consistently lower than the existing guidance values, especially for the later time slice. This is likely to be because the new grid-based modelling gives mainly Mixed, Enhanced-Medium and Enhanced-High types in the Anglian region, whereas the FD2648 decision trees gave both Neutral and Sensitive types as well as Mixed and Enhanced-High (Kay and others, 2011b). Therefore, overall the changed balance of types with the new modelling gives a lower impact. Of particular influence could be the fact that the FD2648 decision trees only identified an Enhanced family, rather than being able to separately distinguish Enhanced-Low, -Medium and -High response types, and the Enhanced-High average response type was used to represent this Enhanced family, therefore likely increasing the regional mean impacts derived in FD2648.

The Thames and West Wales regions also have new regional values that are lower than the existing guidance value for the latest time slice and highest percentile. This is also likely to be due to some differences in the regional balance of response types between the FD2648 decision trees and the new grid-based modelling, combined with using the Enhanced-High average response type to represent all Enhanced catchments in FD2648.

For the Tweed region, the new regional values are consistently higher than the existing guidance values, especially for the later time slices and the 90th percentile. This is likely to be because the new grid-based modelling generally gives Enhanced types in the Tweed region, whereas the FD2020 catchment-based modelling gave very few Enhanced types within the 45 modelled Scottish catchments. As a result, the decision trees produced to estimate the response types of other Scottish catchments could not include the identification of Enhanced types (Kay and others, 2011b).

A similar comparison of existing regional guidance for Scotland (derived from R10023PUR; SEPA 2016) to regional mean values derived from the new grid-based modelling with the UKCP09 projections is presented in Table 3.3. Larger differences are coloured. In this case, the comparison only covers the 10th, 50th and 90th percentile values for the 2050s and 2080s, and the new regional values are rounded to the nearest 1%. As for England and Wales, values for the 2050s use the A1B emissions scenario, while the 10th, 50th and 90th percentile values for the 2080s use B1, A1B and A1F1 emissions respectively. The comparison shows a great deal of similarity between the new regional values and the existing guidance in western regions of Scotland. However, in eastern regions of Scotland the new regional values are consistently higher than the existing guidance values, especially for the later time slices and the 90th percentile. The reason for this is the same as for the Tweed in the comparison for England and Wales; the decision trees produced to

estimate the response types of Scottish catchments could not include identification of Enhanced types (Kay and others, 2011b).

It should be noted that the decision trees previously used to estimate the response types of gauged catchments (Kay and others, 2011a,b) have considerable uncertainty associated with them. Each branch of a decision tree was associated with a 'most likely' response type, given a particular set of rules applied to a range of catchment properties, but most branches also have some likelihood of alternative response types; only the information on the most likely response type was applied in FD2648. Also, the rules and probabilities of the decision trees will depend to some extent on the set of catchments used to produce them. Furthermore, the decision trees could only be applied to gauged catchments, so the weighting of types within a region may have been biased by the gauging station locations. The new grid-based modelling provides response surfaces for every 1km river cell; it does not need to use decision trees and is not affected by gauging station locations.

Table 3.4 is the same as Table 3.2 but compares values from the existing regional guidance for England and Wales with equivalent regional mean values produced from the new grid-based modelling combined with the UKCP18 projections (including the extra uncertainty allowances). Larger differences are coloured. The comparison shows that, for most regions, the new regional values are very similar to the existing guidance (consistent with the comparison of the UKCP18 and UKCP09 projections on the sensitivity domain; Figure 3.23). The main exceptions to this are Anglian, Thames, SE England and West Wales, where the new regional values are often lower than the existing guidance values, particularly for the 2080s. At least part of the reason for differences in the high (low) percentile values for the 2080s could be because the A1F1 (B1) emissions scenario was used for the existing guidance based on UKCP09 projections, but for UKCP18 the RCP8.5 (RCP4.5) emissions scenario is used instead, as the nearest equivalent, since the only SRES scenario available in UKCP18 is A1B (section 2.5). For the Tweed region, the new regional values are higher than the existing guidance values, for the reasons discussed for Table 3.2.

Table 3.5 is the same as Table 3.3 but compares values from the existing regional guidance for Scotland with equivalent regional mean values produced from the new grid-based modelling combined with the UKCP18 projections (including the extra uncertainty allowances). Larger differences are coloured. As for England and Wales, the comparison shows a lot of similarity between the new regional values and the existing guidance, particularly in western regions of Scotland. However, in eastern regions of Scotland, the new regional values are consistently higher than the existing guidance values, especially for the later time slices and the 90th percentile. The reasons for these differences are as discussed for Table 3.3.

Note that for these comparisons the new regional mean values use the UKCP09 river basin regions (Figure 2.4a) for spatial consistency with the existing guidance. However, as mentioned previously, overlaying the projections on response surfaces uses the river basin regions corresponding to each respective set of projections for consistency with the calculation of the projections. This is considered to be the fairest way to compare the newly-derived impacts with the existing guidance, given the (relatively small) differences in the river basin regions (Figure 2.4 and Table 2.3).

Table 3.2 Comparison of existing guidance for England and Wales with new regional values derived using grid-based modelling and the UKCP09 projections

	Existing (UKCP09)			New (UKCP09)			Diffs (New-Existing)		
	2020s	2050s	2080s	2020s	2050s	2080s	2020s	2050s	2080s
Solway									
Upper (90th)	20	30	60	20	35	65	0	5	5
Central (50th)	10	20	25	15	20	25	5	0	0
Lower (10th)	5	10	10	5	10	10	0	0	0
NW England									
Upper (90th)	20	35	70	25	35	70	5	0	0
Central (50th)	15	25	30	15	20	30	0	-5	0
Lower (10th)	10	10	10	5	10	10	-5	0	0
Dee									
Upper (90th)	20	30	45	20	25	40	0	-5	-5
Central (50th)	10	15	20	10	15	15	0	0	-5
Lower (10th)	5	5	5	5	5	5	0	0	0
Severn									
Upper (90th)	25	40	70	20	35	65	-5	-5	-5
Central (50th)	10	20	25	10	15	25	0	-5	0
Lower (10th)	0	5	5	0	5	5	0	0	0
SW England									
Upper (90th)	25	40	85	25	40	85	0	0	0
Central (50th)	10	20	30	10	20	30	0	0	0
Lower (10th)	5	5	10	0	5	5	-5	0	-5
Tweed									
Upper (90th)	20	25	45	30	40	70	10	15	25
Central (50th)	10	15	20	20	25	30	10	10	10
Lower (10th)	0	5	5	10	15	15	10	10	10
Northumbria									
Upper (90th)	20	30	50	25	30	45	5	0	-5
Central (50th)	10	15	20	15	20	25	5	5	5
Lower (10th)	5	5	10	10	10	15	5	5	5
Humber									
Upper (90th)	20	30	50	20	25	45	0	-5	-5
Central (50th)	10	15	20	10	15	20	0	0	0
Lower (10th)	5	5	10	0	5	5	-5	0	-5
Anglian									
Upper (90th)	25	35	65	15	25	45	-10	-10	-20
Central (50th)	10	15	25	5	5	10	-5	-10	-15
Lower (10th)	0	0	5	-10	-10	-5	-10	-10	-10
Thames									
Upper (90th)	25	35	70	20	30	60	-5	-5	-10
Central (50th)	10	15	25	10	15	20	0	0	-5
Lower (10th)	-5	0	5	0	0	0	5	0	-5
SE England									
Upper (90th)	25	50	105	30	45	100	5	-5	-5
Central (50th)	10	20	35	15	20	30	5	0	-5
Lower (10th)	-5	0	5	5	5	10	10	5	5
West Wales									
Upper (90th)	25	40	75	25	35	65	0	-5	-10
Central (50th)	15	25	30	15	20	25	0	-5	-5
Lower (10th)	5	10	15	5	10	10	0	0	-5

Table 3.3 Comparison of existing guidance for Scotland with new regional values derived using grid-based modelling and the UKCP09 projections

	Existing (UKCP09)		New (UKCP09)		Diffs (New-Existing)	
	2050s	2080s	2050s	2080s	2050s	2080s
N Highland						
Upper (90th)	29	50	37	60	8	10
Central (50th)	16	23	25	32	9	9
Lower (10th)	7	7	15	15	8	8
W Highland						
Upper (90th)	42	>60	49	86	7	N/A
Central (50th)	25	36	33	43	8	7
Lower (10th)	11	12	18	20	7	8
NE Scotland						
Upper (90th)	21	33	32	48	11	15
Central (50th)	12	14	20	23	8	9
Lower (10th)	2	2	10	9	8	7
Argyll						
Upper (90th)	42	>60	50	87	8	N/A
Central (50th)	26	37	34	45	8	8
Lower (10th)	11	12	21	21	10	9
Tay						
Upper (90th)	27	50	47	77	20	27
Central (50th)	14	20	32	39	18	19
Lower (10th)	6	4	20	18	14	14
Clyde						
Upper (90th)	32	60	36	66	4	6
Central (50th)	18	27	22	31	4	4
Lower (10th)	7	8	12	12	5	4
Forth						
Upper (90th)	29	54	40	70	11	16
Central (50th)	16	21	25	32	9	11
Lower (10th)	6	5	14	13	8	8
Solway						
Upper (90th)	30	60	35	66	5	6
Central (50th)	17	22	21	27	4	5
Lower (10th)	7	6	11	10	4	4
Tweed						
Upper (90th)	24	45	40	69	16	24
Central (50th)	13	17	25	31	12	14
Lower (10th)	4	5	13	13	9	8

Table 3.4 Comparison of existing guidance for England and Wales with new regional values derived using grid-based modelling and the UKCP18 projections

	Existing (UKCP09)			New (UKCP18)			Diffs (New-Existing)		
	2020s	2050s	2080s	2020s	2050s	2080s	2020s	2050s	2080s
Solway									
Upper (90th)	20	30	60	25	35	75	5	5	15
Central (50th)	10	20	25	15	20	30	5	0	5
Lower (10th)	5	10	10	5	5	10	0	-5	0
NW England									
Upper (90th)	20	35	70	25	40	75	5	5	5
Central (50th)	15	25	30	15	20	35	0	-5	5
Lower (10th)	10	10	10	5	10	10	-5	0	0
Dee									
Upper (90th)	20	30	45	25	25	45	5	-5	0
Central (50th)	10	15	20	10	15	15	0	0	-5
Lower (10th)	5	5	5	5	0	5	0	-5	0
Severn									
Upper (90th)	25	40	70	25	30	65	0	-10	-5
Central (50th)	10	20	25	10	15	25	0	-5	0
Lower (10th)	0	5	5	0	0	5	0	-5	0
SW England									
Upper (90th)	25	40	85	30	40	80	5	0	-5
Central (50th)	10	20	30	15	15	30	5	-5	0
Lower (10th)	5	5	10	0	0	5	-5	-5	-5
Tweed									
Upper (90th)	20	25	45	35	45	85	15	20	40
Central (50th)	10	15	20	20	25	35	10	10	15
Lower (10th)	0	5	5	10	10	15	10	5	10
Northumbria									
Upper (90th)	20	30	50	30	30	55	10	0	5
Central (50th)	10	15	20	20	20	25	10	5	5
Lower (10th)	5	5	10	10	5	10	5	0	0
Humber									
Upper (90th)	20	30	50	25	25	50	5	-5	0
Central (50th)	10	15	20	10	10	20	0	-5	0
Lower (10th)	5	5	10	0	0	5	-5	-5	-5
Anglian									
Upper (90th)	25	35	65	20	20	45	-5	-15	-20
Central (50th)	10	15	25	5	0	10	-5	-15	-15
Lower (10th)	0	0	5	-5	-15	-10	-5	-15	-15
Thames									
Upper (90th)	25	35	70	25	25	55	0	-10	-15
Central (50th)	10	15	25	10	5	15	0	-10	-10
Lower (10th)	-5	0	5	0	-10	-5	5	-10	-10
SE England									
Upper (90th)	25	50	105	35	40	80	10	-10	-25
Central (50th)	10	20	35	15	15	25	5	-5	-10
Lower (10th)	-5	0	5	0	-5	0	5	-5	-5
West Wales									
Upper (90th)	25	40	75	25	35	60	0	-5	-15
Central (50th)	15	25	30	15	20	30	0	-5	0
Lower (10th)	5	10	15	5	5	10	0	-5	-5

Table 3.5 Comparison of existing guidance for Scotland with new regional values derived using grid-based modelling and the UKCP18 projections

	Existing (UKCP09)		New (UKCP18)		Diffs (New-Existing)	
	2050s	2080s	2050s	2080s	2050s	2080s
N Highland						
Upper (90th)	29	50	36	58	7	8
Central (50th)	16	23	21	25	5	2
Lower (10th)	7	7	8	8	1	1
W Highland						
Upper (90th)	42	>60	47	82	5	N/A
Central (50th)	25	36	27	37	2	1
Lower (10th)	11	12	12	13	1	1
NE Scotland						
Upper (90th)	21	33	32	50	11	17
Central (50th)	12	14	18	21	6	7
Lower (10th)	2	2	7	4	5	2
Argyll						
Upper (90th)	42	>60	48	83	6	N/A
Central (50th)	26	37	28	38	2	1
Lower (10th)	11	12	13	14	2	2
Tay						
Upper (90th)	27	50	45	75	18	25
Central (50th)	14	20	28	36	14	16
Lower (10th)	6	4	13	13	7	9
Clyde						
Upper (90th)	32	60	35	67	3	7
Central (50th)	18	27	19	30	1	3
Lower (10th)	7	8	7	10	0	2
Forth						
Upper (90th)	29	54	41	75	12	21
Central (50th)	16	21	24	34	8	13
Lower (10th)	6	5	9	12	3	7
Solway						
Upper (90th)	30	60	37	74	7	14
Central (50th)	17	22	19	32	2	10
Lower (10th)	7	6	6	10	-1	4
Tweed						
Upper (90th)	24	45	47	86	23	41
Central (50th)	13	17	25	37	12	20
Lower (10th)	4	5	8	13	4	8

3.5 Indicator of hydrological model uncertainty

Figure 3.24 shows the indicator of hydrological model uncertainty for each of the 94 modelled catchments (section 2.8), and regionalised for each 1km river cell. Figure 3.24a shows that 63 of the 94 catchments have medium hydrological model uncertainty (there is some agreement between the models), and 26 catchments have low hydrological model uncertainty (all models predicting response types in the same group as G2G). The latter tend to be in the west. Only 5 of the 94 catchments have been classified as having high hydrological model uncertainty; these are located in eastern Scotland and south-eastern England.

Consequently, the majority of 1km river cells (72%) have medium hydrological model uncertainty (Figure 3.24b). There are some areas in eastern Scotland and south-eastern England where some 1km river cells (4%) have been classified as having high hydrological model uncertainty. The remaining 1km river cells (24%) have low hydrological model uncertainty, and these tend to be in the west.

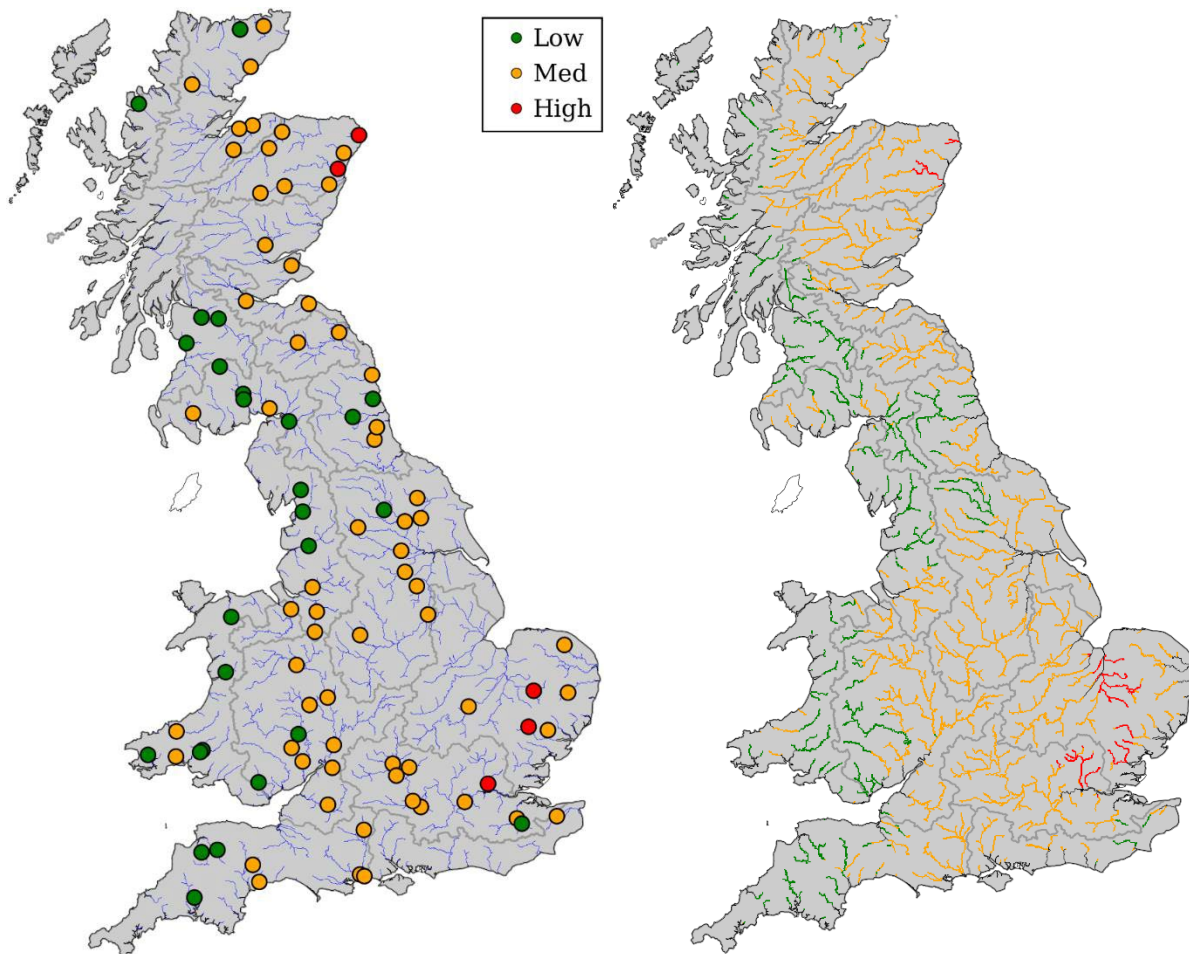


Figure 3.24 showing a) 94 modelled catchments (left) and b) regionalised for each 1km river cell, for the 20-year return period and Medium-August T/PE scenario (right)

To see the influence of each model on the uncertainty indicator, it was re-calculated leaving out each model in turn (Figure 3.25). When CLASSIC-GB is not considered, some river cells in the east change to low uncertainty (green). When GR4J is not considered, some river cells in northern England and the Midlands change to low uncertainty (green). When PDM/CLASSIC are not considered, the changes in uncertainty indicator are less obvious, suggesting that the PDM/CLASSIC results are less different to the G2G results and so have less influence on the uncertainty indicator. Table 3.6 shows the influence of each model on the uncertainty indicator in terms of the percentage of river cells in each category; the highest percentage of river cells with low uncertainty occurs without GR4J, while the lowest percentage of river cells with high uncertainty occurs without CLASSIC-GB.

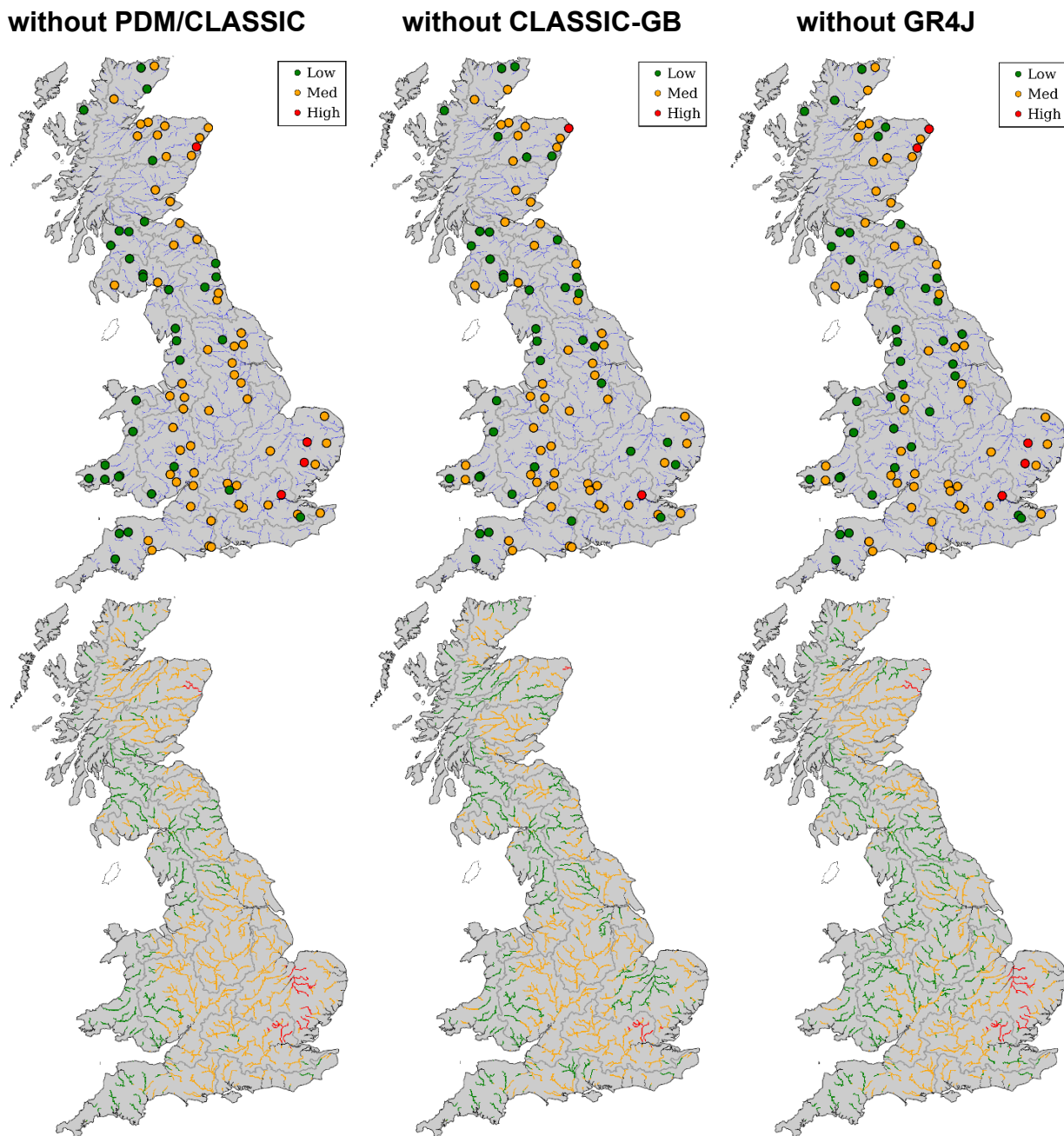


Figure 3.25 Indicator of hydrological modelling uncertainty for the 94 modelled catchments (top) and regionalised for each 1km river cell (bottom), leaving out one set of model results in turn

Table 3.6 Percentage of river cells with each level of uncertainty

	Including all models	without PDM/CLASSIC	without CLASSIC-GB	without GR4J
Low (green)	24	29	41	45
Medium (amber)	72	67	58	51
High (red)	4	4	1	4

4 Conclusions

4.1 Summary

By applying an existing sensitivity framework (from FD2020) using a grid-based hydrological model, this project has provided a nationally consistent assessment of the sensitivity of flood peaks across Great Britain to climatic changes (section 3.1).

The UK CEH web tool (Appendix D) enables a user to explore the change in a flood peak to a range of future scenarios and return periods. These results have been used to inform [peak river flow climate change allowances by management catchment](#), giving, for the first time, higher resolution changes in peak river flow and thereby giving a greater representation of spatial variability than preceding regionalised climate allowances.

While it would not be possible to give a detailed description of individual results within this report, the results show that the change in peak river flow under climate change is highly influenced by catchment sensitivity, with Enhanced High and Sensitive response types showing the greatest positive change in peak river flow, and Damped Extreme showing the lowest, or even a negative change in peak river flow.

The impacts under the UKCP18 projections are similar to the impacts derived using the older UKCP09 projections with the new grid-based modelling, and to the existing guidance, based on UKCP09 and catchment-based modelling plus decision trees (section 3.4).

4.2 Discussion

The sensitivity framework developed in FD2020, applied here and in FD2648, relies on 2 main methods/assumptions:

1. a single harmonic (cosine) function representing the monthly pattern of P and T changes
2. the change factor method; monthly (percentage or absolute) changes in a climate variable (P, T and PE) are applied to a baseline time series of that variable, to produce modified time series

The former reduces the number of dimensions of the sensitivity domain, making the analysis tractable (two driving variables/axis and a third response variable/surface colour). The latter allows the consistent application of the sets of climatic changes represented by the sensitivity domain (section 2.2). However, the analysis of Kay and others (2014c), comparing impacts derived from overlaying climate projections on response surfaces with impacts derived from direct top-down modelling, showed that these simplifications led to some underestimation of impacts on flood peaks, which varied by response type. The extra uncertainty allowances derived in FD2020 (section 2.7) were designed to correct the mean impact, but no attempt was made to alter the uncertainty ranges, which were typically found to be broader from direct impact modelling.

While enabling consistency of application, the change factor method gives perturbed climate series that are inevitably similar to the baseline series in terms of ordering and relative size of events (Cloke and others, 2013; Vormoor and others, 2017). It also assumes that changes in more extreme precipitation follow those of mean monthly precipitation. Reynard and others (2017) and Kay and others (2014c) note that “more information on how future changes in rainfall could develop (e.g. changes varying with

intensity) may also suggest refinements to the two dimensions used to characterise rainfall changes in the sensitivity-based approach, as the sensitivity domain is necessarily a simplification of the temporal patterns of change". Broderick and others (2019), who apply a similar sensitivity framework to that applied here but for catchments in the Republic of Ireland, note that "...small, catchments with a shorter memory and more linear rainfall-runoff response are also likely to be affected by changing patterns at (sub)daily scales, particularly for extreme events." Kay and Jones (2012) showed that the range of impacts from ensembles was broader when full time series methods were used (that is, direct use of Regional Climate Model (RCM) data or weather generator data) rather than the change factor method, although the median impacts were similar from each method.

Vormoor and others (2017) developed a technique to test the influence of temporal sequencing of events on response surfaces. They make a small set of alternative baseline time series by scaling future RCM time series to allow for mean changes, then use each baseline with the delta change method to make a set of alternative response surfaces representing changes in mean, low and high flows. Their analysis of differences in the response surfaces suggests that the temporal sequencing makes little difference for mean flows, is slightly more important for high flows (mean of annual maxima), but makes the most difference for low flows (mean of 7-day annual minima). However, their sensitivity domain only includes changes in annual mean precipitation and temperature, so the influence of precipitation seasonality changes is included in their alternative response surface range. Here, the single sensitivity domain includes changes in the seasonality of precipitation, therefore a lower influence would be expected for remaining temporal sequencing effects. The analysis of Vormoor and others (2017) also only covered one catchment in Norway, with a mixed snowmelt/rainfall regime; the effect in British catchments could be quite different as snow is much less important in the vast majority of the country.

Keller and others (2018) developed this type of analysis further by looking at how response surfaces of changes in the mean annual maximum flood differed between 3 methods, for a catchment in Switzerland. The 3 methods were: i) the RCM-scaling approach of Vormoor and others (2017), ii) using weather generator data and quantile mapping, and iii) incorporating changes in precipitation seasonality using a harmonic function (as applied here). The results showed that changes in annual maxima were typically larger from the latter 2 methods than the former. The authors recommend combining several sensitivity-based methods, as each has its own strengths and weaknesses. However, the alternative methods are more reliant on RCM data to define certain aspects/parameters, making them less general for subsequent application.

It is possible to use weather generator data within a sensitivity-based approach applied with catchment models (for example, Bastola and others, 2011, Steinschneider and others, 2015, Kim and others, 2018, Broderick and others 2019), but applying this with a national-scale grid-based model is difficult as weather generators are typically designed for single-site (or occasionally multi-site) application rather than to produce spatially coherent gridded data across very large regions (Peleg and others, 2017). Furthermore, it is not straightforward to theoretically assess what parameters of a weather generator should be modified to produce time series with the required statistics to represent a sensitivity domain. Guo and others (2017) developed an inverse approach to address this problem, but only applied it with a single-site weather generator for a very small catchment (29km²) in Australia. An additional issue is that if an ensemble of weather generator runs (or one very long run) is used for each point on the sensitivity domain (for example, Steinschneider and others, 2015, Kim and others, 2018, Broderick and others, 2019) then this adds considerably to the hydrological model run time required. Alternatively, if a single weather generator run is used for each point on the sensitivity domain (for example, Bastola and

others, 2011), then this is likely to produce 'noisy' response surfaces due to the presence of natural variability between runs at different points; neither of these options is ideal.

A further potential source of uncertainty is the hydrological model. Although it is typically considered that the climate models provide the main source of uncertainty when projecting the impacts of climate change on river flows, especially for high flows (for example, Gosling and others, 2011, Kay and others, 2009, New and others, 2007, Wilby and Harris 2006), recent research has shown that hydrological model uncertainty can still be significant (Steinschneider and others, 2015, Broderick and others, 2019). An initial investigation of differences in response surfaces from different hydrological models, for a limited set of catchments, has been used here to provide a simple indicator of possible hydrological model uncertainty (section 3.5). However, the approach taken to develop the indicator assumes that the response type results from all 4 hydrological models applied are equally valid (section 2.8); this may not be the case if models vary significantly in terms of performance in simulating a baseline period, or if a model shows any systematic bias in its response. Indicator development could potentially use baseline model performance to weight model response types differently. However, even if a model performs well in a baseline period, it does not necessarily mean that it will perform reliably under altered climatic conditions. Here, the GR4J model tends strongly towards more enhanced response types and the CLASSIC-GB model tends towards more damped response types (Figure A.2), despite both models performing relatively well in a baseline simulation (Appendix A.2). Leaving out either model when deriving the indicator of hydrological model uncertainty did lead to some differences in the spatial pattern of the indicator (Figure 3.25). It is currently unclear precisely what is causing the differences in response for these models, but it is likely to be related to aspects of model structure. The work of Broderick and others (2019) also showed that GR4J tended towards more enhanced responses than another catchment-based model, when applied for 35 catchments in the Republic of Ireland using a sensitivity framework approach.

Another potential source of uncertainty is the time step of the hydrological model, and/or the time step of the driving data used by the model. The grid-based hydrological modelling in this project used daily 1km precipitation data (CEH-GEAR; section 2.1) for the baseline run (1961 to 2001), and although the model itself operates on a sub-daily (15 minute) time step, the flood frequency analysis was based on annual maxima (AM) of simulated daily mean flows (section 2.3). Similarly, for the catchment-based modelling in FD2020, 109 of the 155 catchments used daily precipitation data (derived from rain gauge data for 1961 to 2001) and a daily model time step, although 46 (typically smaller) catchments used hourly precipitation data (generally for a shorter baseline period) and an hourly model time step. However, the subsequent flood frequency analysis for all catchments was based on peaks-over-threshold (POT) extracted from simulated daily mean flows. While the use of AM versus POT is not expected to make a significant difference to the modelled response surfaces (especially for lower return periods), it is possible that sub-daily peak flows may respond differently to climate change than daily peak flows. This was investigated by Kim and others (2018), who used a sensitivity-based approach for a mesoscale catchment in South Korea. They found that using daily rather than hourly peak flows underestimated the effect of climate change.

An important point to make here is that, while there is substantial uncertainty associated with the potential impacts of climate change on flood peaks, which is derived from a range of sources, the corresponding uncertainty in flood extents could be less due to physical and topographic constraints (Collet and others, 2018). However, this will vary significantly depending on at-site characteristics.

4.3 Possible future work

Based on section 4.2, future work could include some or all of the options listed below. However, it should be noted that most of these would significantly increase the computational demands of the sensitivity-based approach. Therefore, initial analyses should use a small but representative sample of catchments across Britain, with a catchment-based hydrological model (or models), to assess the relative importance of different factors in estimating the impacts of climate change on flood peaks.

- **Assess the importance of temporal sequencing within the applied sensitivity framework:** The approach of Vormoor and others (2017) could be adapted to allow for the seasonality changes included in the sensitivity domain applied here, to enable an assessment of the influence of remaining temporal sequencing differences on response surfaces. However, this would require selecting future regional climate model (RCM) time series to apply (for example, from the UKCP18 12km or 2.2km RCM ensembles), and the results may depend on the choice of RCM and future time period. Using RCM time series to directly drive the grid-based hydrological model would also allow the extra uncertainty allowances to be further investigated, including possibly producing specific gridded allowances (rather than using values based on the response type of each 1km river cell).
- **Apply multiple different sensitivity-based methods:** Similar to Keller and others (2018), essentially the same sensitivity domain could be applied, but with a range of different ways used to derive time series corresponding to each point of the domain. For example, RCM-scaling (above) or a weather generator could be used.
- **Develop a more complex sensitivity domain:** This could involve introducing additional dimensions to the sensitivity domain, to allow precipitation changes to vary with intensity, for example. This may be particularly important to capture intensification of summer storms (Kendon and others, 2014), but presentation of the resulting response surfaces would be more difficult.
- **Further investigate the potential level of hydrological model uncertainty:** Model a greater number of catchments with a range of hydrological models, and critically assess differences in modelled response surfaces versus differences in model structure and baseline performance.
- **Use baseline hourly rainfall data and look at changes in hourly peak flows:** For example the 1km gridded hourly precipitation data set (CEH-GEAR1hr; Lewis and others, 2018), which has the same daily totals as the 1km CEH-GEAR data. It covers a much shorter period than daily CEH-GEAR, only 26 years (1990–2015) initially, so cannot immediately replace CEH-GEAR (used here for 1961 to 2001 - 40 full water years - to allow reasonably high return period flows to be estimated). However, CEH-GEAR1hr could be used to investigate potential differences in response of hourly versus daily peak flows, in different types of catchment. This could assess whether impacts on daily peaks underestimate impacts on sub-daily peaks. It could potentially provide guidance on where, or what type, of catchment is particularly affected. Hourly data would also better enable modelling for grid points with smaller catchment areas than the 100km² threshold applied here.

The application of the sensitivity framework with a grid-based national-scale hydrological model, and overlaying the resulting response surfaces with the UKCP18 climate projections, has provided a nationally consistent and up-to-date assessment of the sensitivity and vulnerability of flood peaks across Great Britain to climate change. Further work would add to this by providing more information on the robustness of the results to

various assumptions/simplifications, and provide guidance on prioritising future developments.

References

- BASTOLA, S., MURPHY, C. AND SWEENEY, J., 2011. The sensitivity of fluvial flood risk in Irish catchments to the range of IPCC AR4 climate change scenarios. *Science of Total Environment*. 409: 5403–5415.
- BELL, V.A., KAY, A.L., COLE, S.J., JONES, R.G., MOORE, R.J. AND REYNARD, N.S., 2012. How might climate change affect river flows across the Thames Basin? An area-wide analysis using the UKCP09 Regional Climate Model ensemble. *Journal of Hydrology*. 442–443: 89–104.
- BELL, V.A., KAY, A.L., DAVIES, H.N. AND JONES, R.G., 2016. An assessment of the possible impacts of climate change on snow and peak river flows across Britain. *Climate Change*. 136: 539–553.
- BELL, V.A., KAY, A.L., JONES, R.G., MOORE, R.J. AND REYNARD, N.S., 2009. Use of soil data in a grid-based hydrological model to estimate spatial variation in changing flood risk across the UK. *Journal of Hydrology*. 377(3–4): 335–350.
- BRODERICK, C., MURPHY, C., WILBY, R.L., MATTHEWS, T., PRUDHOMME, C. AND ADAMSON, M., 2019. Using a scenario-neutral framework to avoid potential maladaptation to future flood risk. *Water Resources Research*. 55 (2):1079-1104.
- CLOKE, H.L., WETTERALL, F., HE, Y., FREER, J.E. AND PAPPENBERGER, F., 2013. Modelling climate change impact on floods with ensemble climate projections. *Quarterly Journal of the Royal Meteorological Society*. 139: 282–297.
- COLLET, L., BEEVERS, L. AND STEWART, M.D., 2018. Decision-making and flood risk uncertainty: statistical data set analysis for flood risk assessment. *Water Resources Research*. 54: 7291- 7308.
- CRANSTON, M., MAXEY, R., TAVENDALE, A., BUCHANAN, P., MOTION, A., COLE, S., ROBSON, A., MOORE, R.J. AND MINETT, A., 2012. Countrywide flood forecasting in Scotland: challenges for hydrometeorological model uncertainty and prediction, in: MOORE, R.J., COLE, S.J. AND ILLINGWORTH, A.J. (Eds.) *Weather radar and hydrology*. Proceedings Exeter Symposium, April 2011. IAHS Publication. 351: pp.538-542.
- CROOKS, S.M., KAY, A.L., DAVIES, H.N. AND BELL, V.A., 2014. From Catchment to National Scale Rainfall-Runoff Modelling: Demonstration of a Hydrological Modelling Framework. *Hydrology*. 1(1): 63–88.
- CROOKS, S.M. AND NADEN, P.S., 2007. CLASSIC: A semi-distributed modelling system. *Hydrology and Earth System Sciences*. 11(1): 516–531.
- DESER, C., KNUTTI, R., SOLOMON, S. AND OTHERS, 2012. Communication of the role of natural variability in future North American climate. *Nature Climate Change*. 2: 775–779.
- ENVIRONMENT AGENCY, 2016a. Adapting to Climate Change: Advice for Flood and Coastal Erosion Risk Management Authorities. Environment Agency, April 2016, 25. <https://www.gov.uk/government/publications/adapting-to-climate-change-for-risk-management-authorities> (accessed March 2020).
- ENVIRONMENT AGENCY, 2016b. Flood risk assessments: Climate change allowances. <https://www.gov.uk/guidance/flood-risk-assessments-climate-change-allowances> (accessed March 2020).

- FRONZEK, S., CARTER, T.R., RAISANEN, J., RUOKOLAINEN, L. AND LUOTO, M., 2010. Applying probabilistic projections of climate change with impact models: a case study for sub-arctic palsa mires in Fennoscandia. *Climate Change* 99: 515–534.
- GOSLING, S.N., TAYLOR, R.G. AND OTHERS, 2011. A comparative analysis of projected impacts of climate change on river runoff from global and catchment-scale hydrological models. *Hydrology and Earth System Sciences*. 15: 279–294.
- GUO, D., WESTRA, S. AND MAIER, H.R., 2017. Use of a scenario-neutral approach to identify the key hydro-meteorological attributes that impact runoff from a natural catchment. *Journal of Hydrology*. 354:317-330.
- HOUGH, M.N. AND JONES, R.J.A., 1997. The United Kingdom Meteorological Office rainfall and evaporation calculation system: MORECS version 2.0--an overview. *Hydrology and Earth System Sciences*. 1(2): 227–239.
- IPCC, 2000. Special Report on Emissions Scenarios (SRES): A special report of Working Group III of the Intergovernmental Panel on Climate Change. Cambridge University Press, Cambridge, UK, 599pp.
- KAY, A.L., CROOKS, S., DAVIES, H.N., PRUDHOMME, C. AND REYNARD, N.S., 2011a. Practicalities for implementing regionalised allowances for climate change on flood flows. Report to Department for Environment, Food and Rural Affairs, Technical Report FD2648, CEH Wallingford, May 2011, 209pp.
- KAY, A.L., CROOKS, S.M., DAVIES, H.N. AND REYNARD, N.S., 2011b. An assessment of the vulnerability of Scotland's river catchments and coasts to the impacts of climate change: Work Package 1 Report. Report to Scottish Environment Protection Agency, project R10023PUR, CEH Wallingford, August 2011, 219pp.
- KAY, A.L., CROOKS, S.M., DAVIES, H.N., PRUDHOMME, C. AND REYNARD, N.S., 2014a. Probabilistic impacts of climate change on flood frequency using response surfaces. I: England and Wales. *Regional Environmental Change*. 14(3): 1215–1227.
- KAY, A.L., CROOKS, S.M., DAVIES, H.N. AND REYNARD, N.S., 2014b. Probabilistic impacts of climate change on flood frequency using response surfaces. II: Scotland. *Regional Environmental Change*. 14(3): 1243–1255.
- KAY, A.L., CROOKS, S.M. AND REYNARD, N.S., 2014c. Using response surfaces to estimate impacts of climate change on flood peaks: assessment of uncertainty. *Hydrological Processes*. 28(20): 5273–5287.
- KAY, A.L., DAVIES, H.N., BELL, V.A. AND JONES, R.G., 2009. Comparison of uncertainty sources for climate change impacts: flood frequency in England. *Climatic Change*. 92(1–2): 41–63.
- KAY, A.L. AND JONES, R.G., 2012. Comparison of the use of alternative UKCP09 products for modelling the impacts of climate change on flood frequency. *Climatic Change*. 114(2): 211–230.
- KELLER, L., ROSSLER, O., MARTIUS, O. AND WEINGARTNER, R., 2018. Comparison of scenario-neutral approaches for estimation of climate change impacts on flood characteristics. *Hydrological Processes*. 33: 535-550.
- KELLER, V.D.J., TANGUY, M. AND OTHERS, 2015. CEH-GEAR: 1 km resolution daily and monthly areal rainfall estimates for the UK for hydrological and other applications. *Earth Systems Science Data*. 7: 143–155.

- KENDON, E.J., ROBERTS, N.M., FOWLER, H.J. AND OTHERS, 2014. Heavier summer downpours with climate change revealed by weather forecast resolution model. *Nature Climate Change*. 4: 570–576.
- KIM, D., CHUN, J.A. AND AIKINS, C.M., 2018. An hourly-scale scenario-neutral flood risk assessment in a mesoscale catchment under climate change. *Hydrological Processes*. 32: 3416-3430.
- LEWIS, E., QUINN, N., BLENKINSOP, S., FOWLER, H.J., FREER, J., TANGUY, M., HITT, O., COXON, G., BATES, P. AND WOODS, R., 2018. A rule based quality control method for hourly rainfall data and a 1 km resolution gridded hourly rainfall dataset for Great Britain: CEH-GEAR1hr. *Journal of Hydrology*. 564: 930-943.
- LOWE, J.A., BERNIE, D., BETT, P., BRICHENO, L., BROWN, S., CALVERT, D., CLARK, R., EAGLE, K., EDWARDS, T., FOSSER, G., FUNG, F., GOHAR, L., GOOD, P., GREGORY, J., HARRIS, G., HOWARD, T., KAYE, N., KENDON, E., KRIJNEN, J., MAISEY, P., MCDONALD, R., MCINNES, R., MCSWEENEY, C., MITCHELL, J.F.B., MURPHY, J., PALMER, M., ROBERTS, C., ROSTRON, J., SEXTON, D., THORNTON, H., TINKER, J., TUCKER, S., YAMAZAKI, K., AND BELCHER, S., 2018. UKCP18 Science Overview report. Met Office Hadley Centre, Exeter, UK.
<https://www.metoffice.gov.uk/pub/data/weather/uk/ukcp18/science-reports/UKCP18-Overview-report.pdf> (Accessed November 2022)
- MASLIN, M. AND AUSTIN, P., 2012. Climate models at their limit? *Nature*. 486: 183–184.
- MAXEY, R., CRANSTON, M., TAVENDALE, A. AND BUCHANAN, P., 2012. The use of deterministic and probabilistic forecasting in countrywide flood guidance in Scotland, in: BHS Eleventh National Symposium, Hydrology for a Changing World. pp.01–07. doi:10.7558/bhs.2012.ns33.
- MET OFFICE HADLEY CENTRE, 2018. UKCP18 probabilistic projections by UK river basins for 1961-2099. Centre for Environmental Data Analysis
<http://catalogue.ceda.ac.uk/uuid/10538cf7a8d84e5e872883ea09a674f3> (accessed November 2022)
- MONTEITH, J.L., 1965. Evaporation and environment. *Symposia of the Society for Experimental Biology*. 19: 205–234.
- MORRIS, D.G. AND FLAVIN, R.W., 1990. A digital terrain model for hydrology, in: *Proceedings of the 4th International Symposium on Spatial Data Handling, Zurich, Switzerland, 23–27 July 1990*, pp.250–262.
- MURPHY, J.M., SEXTON, D.M.H., JENKINS, G.J., BOOTH, B.B.B., BROWN, C.C., CLARK, R.T., COLLINS, M., HARRIS, G.R., KENDON, E.J., BETTS, R.A., BROWN, S.J., HUMPHREY, K.A., MCCARTHY, M.P., MCDONALD, R.E., STEPHENS, A., WALLACE, C., WARREN, R., WILBY, R. AND WOOD, R.A., 2009. UK Climate Projections Science Report: Climate change projections. Met Office Hadley Centre, Exeter, UK.
http://cedadocs.ceda.ac.uk/1320/1/climate_projections_full_report.pdf (accessed November 2022)
- NEW, M., LOPEZ, A., DESSAI, S. AND WILBY, R., 2007. Challenges in using probabilistic climate change information for impact assessments: an example from the water sector. *Philosophical Transactions of the Royal Society A*. 365: 2117–2131.
- LOUDIN, L., HERVIEU, F., MICHEL, C., PERRIN, C., ANDREASSIAN, V., ANCTIL, F., LOUMANGNE C., 2005. Which potential evapotranspiration input for a lumped rainfall-

runoff model?: Part 2 - Towards a simple and efficient potential evapotranspiration model for rainfall-runoff modelling. *Journal of Hydrology*. 303: 290-306.

PELEG, N., FATICHI, S., PASCHALIS, A., MOLNAR, P. AND BURLANDO, P., 2017. An advanced stochastic weather generator for simulating 2-D high-resolution climate variables. *Journal of Advances of Modeling Earth Systems*. 9: 1595–1627.

PERRIN, C., MICHEL, C. AND ANDRÉASSIAN, V., 2003. Improvement of a parsimonious model for streamflow simulation. *Journal of Hydrology*. 279(1): 275-289.

PERRY, M., HOLLIS, D. AND ELMS, M., 2009. The generation of daily gridded datasets of temperature and rainfall for the UK. *Climate Memorandum No.24*, National Climate Information Centre, Met Office, Exeter, UK.

https://www.metoffice.gov.uk/binaries/content/assets/metofficegovuk/pdf/weather/learn-about/uk-past-events/papers/cm24_generation_of_daily_gridded_datasets.pdf (accessed November 2022)

PRICE, D., HUDSON, K., BOYCE, G., SCHELLEKENS, J., MOORE, R.J., CLARK, P., HARRISON, T., CONNOLLY, E. AND PILLING, C., 2012. Operational use of a grid-based model for flood forecasting. *Water Management* 165(2): 65–77.

PRUDHOMME, C., CROOKS S., KAY, A.L. AND REYNARD, N.S., 2013a. Climate change and river flooding: part 1 Classifying the sensitivity of British catchments. *Climatic Change*. 119(3-4): 933-948.

PRUDHOMME, C., KAY, A.L., CROOKS S. AND REYNARD, N.S., 2013b. Climate change and river flooding: Part 2 sensitivity characterisation for British catchments and example vulnerability assessments. *Climatic Change*. 119(3-4): 949-964.

PRUDHOMME, C., WILBY, R.L., CROOKS, S., KAY, A.L. AND REYNARD, N.S., 2010. Scenario-neutral approach to climate change impact studies: application to flood risk. *Journal of Hydrology*. 390: 198-209.

REYNARD, N.S., CROOKS, S., KAY, A.L. AND PRUDHOMME, C., 2009. Regionalised impacts of climate change on flood flows. Report to Department for Environment, Food and Rural Affairs, Technical Report FD2020, CEH Wallingford, November 2009, 113pp.

REYNARD, N.S., KAY, A.L., ANDERSON, M., DONOVAN, B. AND DUCKWORTH, C., 2017. The evolution of climate change guidance for flood risk management. *Progress in Physical Geography*. 41(2): 222–237.

ROBSON, A.J. AND REED, D.W., 1999. Statistical procedures for flood frequency estimation. Vol. 3, *Flood Estimation Handbook*. Institute of Hydrology, Wallingford, UK.

RUDD, A.C., KAY, A.L. AND BELL, V.A. (2019). National-scale analysis of future river flow and soil moisture droughts: potential changes in drought characteristics. *Climatic Change*. 156: 323-340.

SEPA, 2016. *Flood Modelling Guidance for Responsible Authorities Version 1.1*. Scottish Environment Protection Agency.

https://www.sepa.org.uk/media/219653/flood_model_guidance_v2.pdf (accessed March 2020).

SEPA (2019). *Climate change allowances for flood risk assessment in land use planning*. Scottish Environment Protection Agency. Available at:

https://www.sepa.org.uk/media/426913/lups_cc1.pdf (accessed March 2020).

STEINSCHNEIDER, S., WI, S. AND BROWN, C., 2015. The integrated effects of climate and hydrologic uncertainty on future flood risk assessments. *Hydrological Processes*. 29: 2823-2839.

TANGUY, M., DIXON, H. AND OTHERS, 2016. Gridded estimates of daily and monthly areal rainfall for the United Kingdom (1890-2015) [CEH-GEAR]. NERC Environmental Information Data Centre. <https://catalogue.ceh.ac.uk/documents/33604ea0-c238-4488-813d-0ad9ab7c51ca>

VAN VUUREN, D.P., EDMONDS, J., KAINUMA, M. AND OTHERS, 2011. The representative concentration pathways: an overview. *Climatic Change*. 109: 5-31.

VORMOOR, K., ROSSLER, O., BURGER, G., BRONSTERT, A. AND WEINGARTNER, R., 2017. When timing matters – considering changing temporal structures in runoff response surfaces. *Climatic Change*, 142: 213-226.

WEISS, M., 2011. Future water availability in selected European catchments: a probabilistic assessment of seasonal flows under the IPCC A1B emission scenario using response surfaces. *Natural Hazards and Earth System Sciences*. 11: 2163–2171

Welsh Government. (2016) Climate change allowances and flood consequence assessments (CL-03-16). <https://gov.wales/climate-change-allowances-and-flood-consequence-assessments-cl-03-16> (accessed March 2020).

Welsh Government. (2017) Adapting to climate change: Advice for flood and coastal erosion risk management authorities in Wales.

<https://gov.wales/sites/default/files/publications/2019-06/adapting-to-climate-change-guidance-for-flood-and-coastal-erosion-risk-management-authorities-in-wales.pdf> (accessed March 2020).

WETTERHALL, F., GRAHAM, L.P., ANDREASSON, J., ROSBERG, J. AND YANG, W., 2011. Using ensemble climate projections to assess probabilistic hydrological change in the Nordic region. *Natural Hazards and Earth System Sciences*. 11: 2295–2306.

WILBY, R.L. AND HARRIS, I., 2006. A framework for assessing uncertainties in climate change impacts: Low-flow scenarios for the River Thames, UK. *Water Resource Research*. 42: W02419.

Appendix A: Indicator of hydrological model uncertainty

A.1 Modelled response types

Hydrological model uncertainty is investigated for 94 of the 154 catchments modelled in FD2020; those with catchment area $\geq 150\text{km}^2$ (Table A.1). For these catchments, the G2G modelled response types are compared to those from the original FD2020 catchment-based models (CLASSIC and PDM), plus modelled response types from the grid-based model CLASSIC-GB (5km resolution) and the catchment-based model GR4J (for changes in 20-year return period flood peaks under the Medium-August T/PE scenario) – see Box A.1.

However, an issue with direct comparison to FD2020 modelled response types is that the driving data used in FD2020 (in 2008) is not the same as that used by more recent modelling, for which the CEH-GEAR 1km gridded daily precipitation data (Keller and others, 2015, Tanguy and others, 2016) are applied. CEH-GEAR uses a different method for spatial interpolation from rain gauge data than previously, and uses correction factors derived from more readily available monthly data. Therefore, the CLASSIC and PDM daily catchments are re-run with the new rainfall data (the PDM hourly catchments cannot be re-run since there is not, as yet, an hourly version of CEH-GEAR covering the required period).

Re-running CLASSIC with the new data (after also recalibrating the routing parameters) results in changes in the response types for some catchments, typically towards more enhanced responses (Table A.1), particularly for more northerly catchments. However, it should be noted that there have also been some other (relatively minor) changes to the setup of CLASSIC in the last decade (for example, using more up-to-date land-cover data), which complicates the comparison. There are fewer differences in response types when PDM (daily) is re-run (Table A.1), but there has been no re-calibration for parameters in PDM.

Table A.1 List of the 94 catchments, with the hydrological model used in FD2020 (CLASSIC, PDM daily or PDM hourly) and the response types both from FD2020 and when re-run with the new rainfall data. *PDM hourly was not re-run

Catchment number	River	Location	FD2020	New data	Model
02001	Helmsdale	Kilphedir	DpH	DpH	PDM dly
03003	Oykel	Easter Turnaig	DpL	*	PDM hly
07001	Findhorn	Shenachie	DpL	*	PDM hly
07002	Findhorn	Forres	DpE	DpE	PDM dly
07004	Nairn	Firhall	EnM	*	PDM hly
08004	Avon	Delnashaugh	DpE	DpE	PDM dly
08006	Spey	Boat o Brig	DpL	EnL	CLASSIC
10002	Ugie	Inverugie	DpH	DpH	PDM dly
10003	Ythan	Ellon	Neu	*	PDM hly
11001	Don	Parkhill	DpH	Mix	CLASSIC
12002	Dee	Park	DpH	EnM	CLASSIC
12003	Dee	Polhollick	DpH	Mix	CLASSIC
12007	Dee	Mar Lodge	DpE	*	PDM hly
14001	Eden	Kemback	DpL	DpL	PDM dly
15006	Tay	Ballathie	Neu	EnH	CLASSIC
17005	Avon	Polmonthill	DpH	DpH	PDM dly

Catchment number	River	Location	FD2020	New data	Model
20001	Tyne	East Linton	Mix	Mix	PDM dly
21009	Tweed	Norham	Mix	EnM	CLASSIC
21013	Gala Water	Galashiels	Mix	*	PDM hly
22001	Coquet	Morwick	DpH	DpH	PDM dly
22006	Blyth	Hartford Bridge	Mix	*	PDM hly
23001	Tyne	Bywell	DpH	Mix	CLASSIC
24005	Browney	Burn Hall	Mix	*	PDM hly
24009	Wear	Chester le Street	Mix	Mix	CLASSIC
27003	Aire	Beal Weir	DpH	Mix	CLASSIC
27007	Ure	Westwick Lock	DpH	Mix	CLASSIC
27009	Ouse	Skelton	DpH	Mix	CLASSIC
27021	Don	Doncaster	DpH	DpL	PDM dly
27041	Derwent	Buttercrambe	Mix	Mix	CLASSIC
27043	Wharfe	Addingham	DpH	DpH	PDM dly
27049	Rye	Ness	EnL	Mix	PDM dly
28008	Dove	Rocester Weir	DpL	*	PDM hly
28015	Idle	Mattersey	Sen	Sen	PDM dly
28022	Trent	North Muskham	Mix	EnL	CLASSIC
33019	Thet	Melford Bridge	EnM	EnM	PDM dly
33026	Bedford Ouse	Offord	Mix	EnM	CLASSIC
34003	Bure	Ingworth	Mix	Mix	PDM dly
34006	Waveney	Needham Mill	EnM	EnM	PDM dly
36005	Brett	Hadleigh	EnH	EnH	PDM dly
36008	Stour	Westmill	EnL	*	PDM hly
37001	Roding	Redbridge	DpH	DpH	PDM dly
39001	Thames	Kingston	Mix	Mix	CLASSIC
39007	Blackwater	Swallowfield	Mix	*	PDM hly
39008	Thames	Eynsham	Mix	EnL	CLASSIC
39016	Kennet	Theale	Mix	EnL	CLASSIC
39081	Ock	Abingdon	Mix	EnL	CLASSIC
39105	Thame	Wheatley	EnL	EnL	PDM dly
40003	Medway	Teston	Mix	Mix	CLASSIC
40005	Beult	Stile Bridge	Mix	*	PDM hly
40011	Great Stour	Horton	EnL	EnL	PDM dly
43005	Avon	Amesbury	EnH	EnH	PDM dly
43007	Stour	Throop	EnL	EnL	PDM dly
43021	Avon	Knapp Mill	Mix	EnL	CLASSIC
45003	Culm	Wood Mill	DpL	*	PDM hly
45005	Otter	Dotton	DpL	DpL	PDM dly
47001	Tamar	Gunnislake	EnL	EnL	CLASSIC
50002	Torrige	Torrington	Neu	Neu	PDM dly
50006	Mole	Woodleigh	DpL	DpL	PDM dly
53018	Avon	Bathford	Mix	Mix	CLASSIC
54001	Severn	Bewdley	EnL	EnL	CLASSIC
54008	Teme	Tenbury	EnL	EnL	PDM dly
54018	Rea Brook	Hookagate	EnL	EnL	PDM dly
54027	Frome	Ebley Mill	EnL	*	PDM hly
54057	Severn	Haw Bridge	Mix	EnL	CLASSIC
55002	Wye	Belmont	DpL	EnL	CLASSIC
55023	Wye	Redbrook	EnL	EnM	CLASSIC
55029	Monnow	Grosmont	EnL	EnL	PDM dly
57005	Taff	Pontypridd	Neu	*	PDM hly

Catchment number	River	Location	FD2020	New data	Model
60002	Cothi	Felin Mynachdy	DpL	*	PDM hly
60003	Taf	Clog-y-Fran	DpH	*	PDM hly
60010	Tywi	Nantgaredig	Mix	EnL	CLASSIC
61001	Western Cleddau	Prendergast Mill	DpL	DpL	PDM dly
62001	Teifi	Glan Teifi	EnL	EnM	CLASSIC
64001	Dyfi	Dyfi Bridge	Neu	Neu	PDM dly
66011	Conwy	Cwm Llanerch	DpL	DpL	PDM dly
67033	Dee	Chester Suspension Br	Mix	EnL	CLASSIC
68001	Weaver	Ashbrook	Neu	Neu	PDM dly
68005	Weaver	Audlem	EnM	EnM	PDM dly
69037	Mersey	Westy	EnL	Mix	CLASSIC
71001	Ribble	Samlesbury	DpH	EnL	CLASSIC
72004	Lune	Caton	Neu	EnL	CLASSIC
73005	Kent	Sedgwick	Neu	Neu	PDM dly
76007	Eden	Sheepmount	Neu	EnL	CLASSIC
78003	Annan	Brydekirk	DpH	DpH	PDM dly
79002	Nith	Friars Carse	DpL	DpL	PDM dly
79003	Nith	Hall Bridge	DpL	DpL	PDM dly
79005	Cluden Water	Fiddlers Ford	Neu	*	PDM hly
81002	Cree	Newton Stewart	DpH	DpH	PDM dly
83005	Irvine	Shewalton	DpL	DpL	PDM dly
84012	White Cart Water	Hawkhead	Neu	Neu	PDM dly
84013	Clyde	Daldowie	DpL	Mix	CLASSIC
94001	Ewe	Poolewe	Neu	Neu	PDM dly
96001	Halladale	Halladale	DpE	*	PDM hly
97002	Thurso	Halkirk	DpH	DpL	PDM dly

The G2G, PDM/CLASSIC (re-run), CLASSIC-GB and GR4J modelled response types are mapped in Figure A.1 and listed in Table A.2. These modelled response types are used to produce a spatial indicator of hydrological model uncertainty (see main text section 2.8).

Figure A.2 summarises Table A.2, providing the percentage of the 94 catchments with each response type for each model. This shows that the GR4J model tends strongly towards more enhanced types, whereas the CLASSIC-GB model tends towards more damped types. These differences require further investigation, but they are likely to be related to aspects of the model structures.

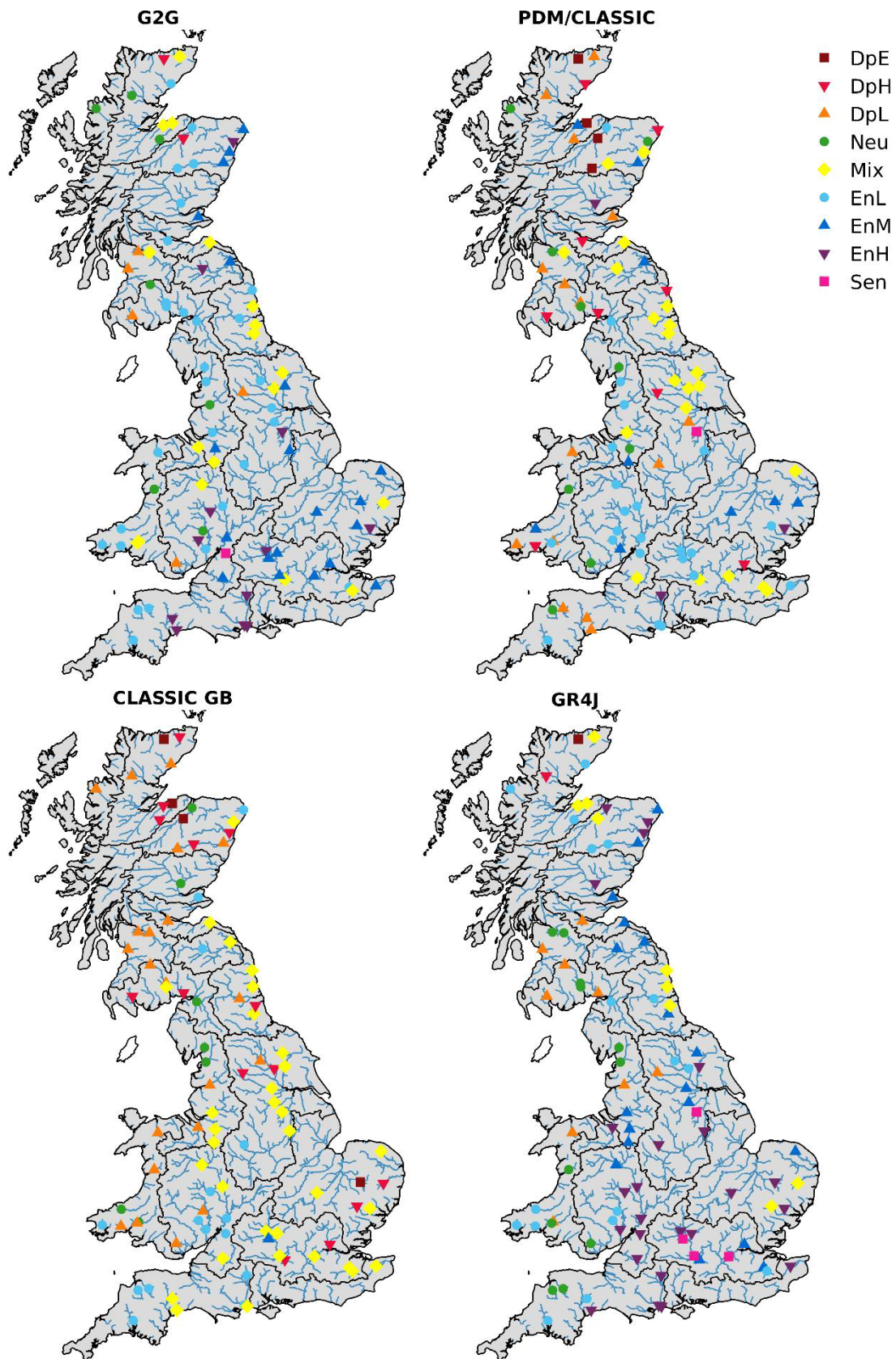


Figure A.1 Comparison of G2G, PDM/CLASSIC (re-run), CLASSIC-GB and GR4J modelled response types (20-year return period flood peaks and Medium-August T/PE scenario) for 94 catchments

Table A.2 List of modelled response types for the 94 catchments modelled with G2G, PDM/CLASSIC (re-run), CLASSIC-GB and GR4J (20-year return period and Medium-August T/PE scenario).

		PDM/ CLASSIC	CLASSIC- GB	GR4J	Catchment number	G2G	PDM/ CLASSIC	CLASSIC- GB	GR4J
02001	EnL	DpH	DpL	EnL	40003	EnL	Mix	Mix	EnM
03003	Neu	DpL	DpL	DpH	40005	Mix	Mix	Mix	EnL
07001	Neu	DpL	DpH	EnL	40011	EnM	EnL	Mix	EnH
07002	Mix	DpE	DpE	Mix	43005	EnH	EnH	EnL	EnH
07004	Mix	EnM	DpH	Mix	43007	EnH	EnL	EnL	EnH
08004	DpH	DpE	DpE	Mix	43021	EnH	EnL	Mix	EnH
08006	EnL	EnL	Neu	EnH	45003	EnH	DpL	Mix	EnL
10002	EnM	DpH	EnL	EnM	45005	EnH	DpL	Mix	EnH
10003	EnH	Neu	Mix	EnH	47001	EnL	EnL	EnL	EnL
11001	EnM	Mix	DpH	EnH	50002	EnL	Neu	EnL	Neu
12002	EnM	EnM	DpL	EnM	50006	EnL	DpL	EnL	Neu
12003	EnL	Mix	DpH	EnL	53018	EnM	Mix	Mix	EnH
12007	EnL	DpE	DpL	EnL	54001	EnL	EnL	Mix	EnH
14001	EnM	DpL	EnL	EnM	54008	EnH	EnL	EnL	EnH
15006	EnL	EnH	Neu	EnH	54018	Mix	EnL	Mix	EnM
17005	EnL	DpH	DpL	DpL	54027	Sen	EnL	EnL	EnH
20001	Mix	Mix	Mix	EnM	54057	EnM	EnL	EnL	EnH
21009	EnM	EnM	Mix	EnM	55002	Neu	EnL	DpL	EnL
21013	EnH	Mix	EnL	EnM	55023	EnL	EnM	EnL	EnH
22001	EnL	DpH	Mix	Mix	55029	EnH	EnL	EnL	EnL
22006	Mix	Mix	Mix	Mix	57005	DpL	Neu	DpL	Neu
23001	EnL	Mix	DpL	EnL	60002	Mix	DpL	Neu	DpL
24005	Mix	Mix	Mix	EnM	60003	EnL	DpH	DpL	EnL
24009	Mix	Mix	DpH	Mix	60010	Mix	EnL	DpL	Neu
27003	EnL	Mix	Mix	EnM	61001	EnL	DpL	EnL	EnL
27007	EnL	Mix	DpL	EnL	62001	EnL	EnM	Neu	EnL
27009	Mix	Mix	DpH	EnL	64001	Neu	Neu	DpL	Neu
27021	EnL	DpL	Mix	EnM	66011	EnL	DpL	DpL	DpL
27041	EnM	Mix	Mix	EnH	67033	Mix	EnL	DpL	EnH
27043	DpL	DpH	DpH	DpL	68001	EnM	Neu	Mix	EnM
27049	Mix	Mix	Mix	EnM	68005	Mix	EnM	Mix	EnM
28008	EnL	DpL	EnL	EnH	69037	EnL	Mix	Mix	EnM
28015	EnH	Sen	Mix	Sen	71001	Neu	EnL	DpL	DpL
28022	EnM	EnL	Mix	EnH	72004	EnL	EnL	Neu	Neu
33019	EnM	EnM	DpE	EnH	73005	EnL	Neu	Neu	Neu
33026	EnM	EnM	Mix	EnH	76007	EnL	EnL	Neu	EnL
34003	EnM	Mix	Mix	EnM	78003	EnL	DpH	DpH	DpL
34006	Mix	EnM	DpH	Mix	79002	EnL	DpL	DpL	Neu
36005	EnH	EnH	Mix	EnH	79003	Neu	DpL	DpL	DpL
36008	EnM	EnL	DpH	Mix	79005	EnL	Neu	Mix	Neu
37001	EnM	DpH	DpH	EnM	81002	DpL	DpH	DpH	DpL
39001	EnM	Mix	Mix	Sen	83005	DpL	DpL	DpL	DpL
39007	Mix	Mix	DpH	EnM	84012	DpL	Neu	DpL	Neu
39008	EnH	EnL	Mix	EnH	84013	Mix	Mix	DpL	Neu
39016	EnM	EnL	Mix	Sen	94001	Neu	Neu	DpL	EnL
39081	EnM	EnL	EnM	Sen	96001	DpH	DpE	DpE	DpE
39105	EnM	EnL	Mix	EnH	97002	Mix	DpL	DpH	Mix

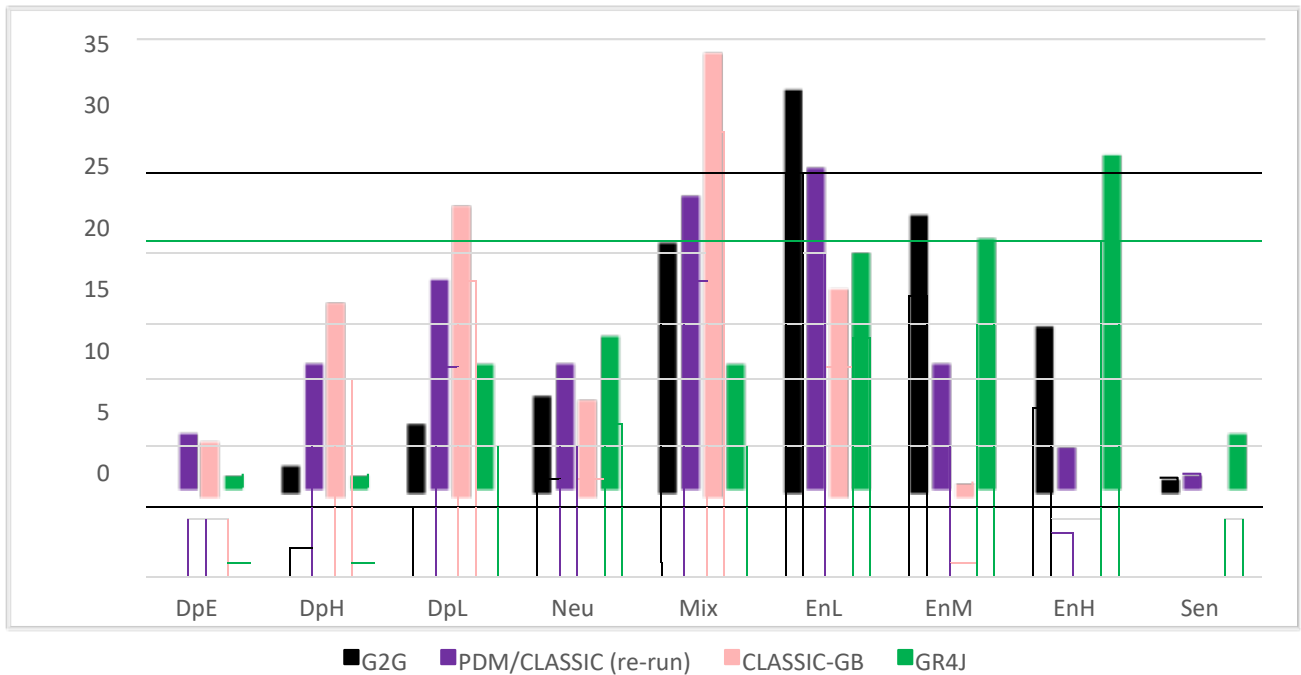


Figure A.2 The percentage of the 94 catchments with each response type, for each model (20-year return period and Medium-August T/PE scenario)

A.2 Baseline model performance

Baseline performance of G2G, PDM/CLASSIC, CLASSIC-GB (5km) and GR4J is assessed using 3 measures to quantify different aspects of the agreement between modelled and observed flows. This includes the Nash-Sutcliffe model efficient to determine the goodness of fit of hydrological models, the overflow volume bias and fitting the flood frequency (ffr) curve to annual maxima using a generalized logistic distribution, where the fit is averaged over 2-, 5- and 10-year return periods.

Table A.3 summarises the performance of each model, using the median of each measure across the 94 catchments, and shows that overall performance is relatively similar. Figure A.3 presents the catchment values of the 3 performance measures for each model, along with the modelled response types and hydrological model uncertainty indicator. This does not show any clear relationship between model performance and whether or not different models respond similarly or differently to climatic changes (that is, the spread of modelled response types).

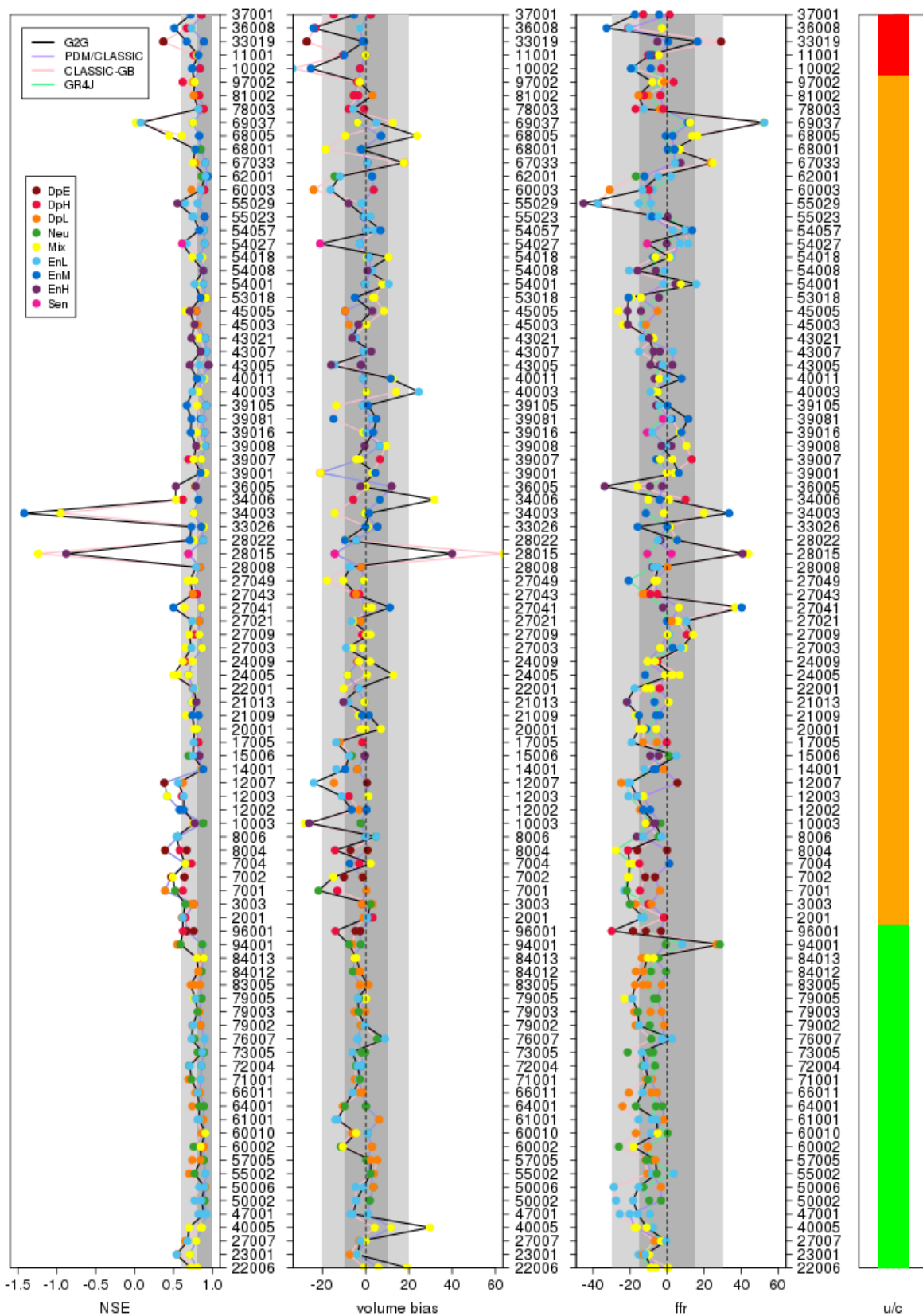


Figure A.3 The baseline model performance (NSE, volume bias and ffr) compared to the modelled response types (dot colour) and uncertainty indicator (right-hand panel) for 94 catchments, for G2G, PDM/CLASSIC (re-run), CLASSIC-GB and GR4J. The grey shading indicates very good (mid-grey) and good (light grey) performance bands for each performance measure

Table A.3 Median model performance, over the 94 catchments, for each model and each performance measure. Note that the PDM calibrations focused in part on flood frequency fit, therefore the better performance for ffr at the (marginal) expense of NSE

	G2G	PDM/CLASSIC	CLASSIC-GB	GR4J
NSE	0.74	0.69	0.76	0.85
volume bias	-3.04	-0.60	-4.22	-1.01
ffr	-10.15	-3.35	-11.60	-7.51

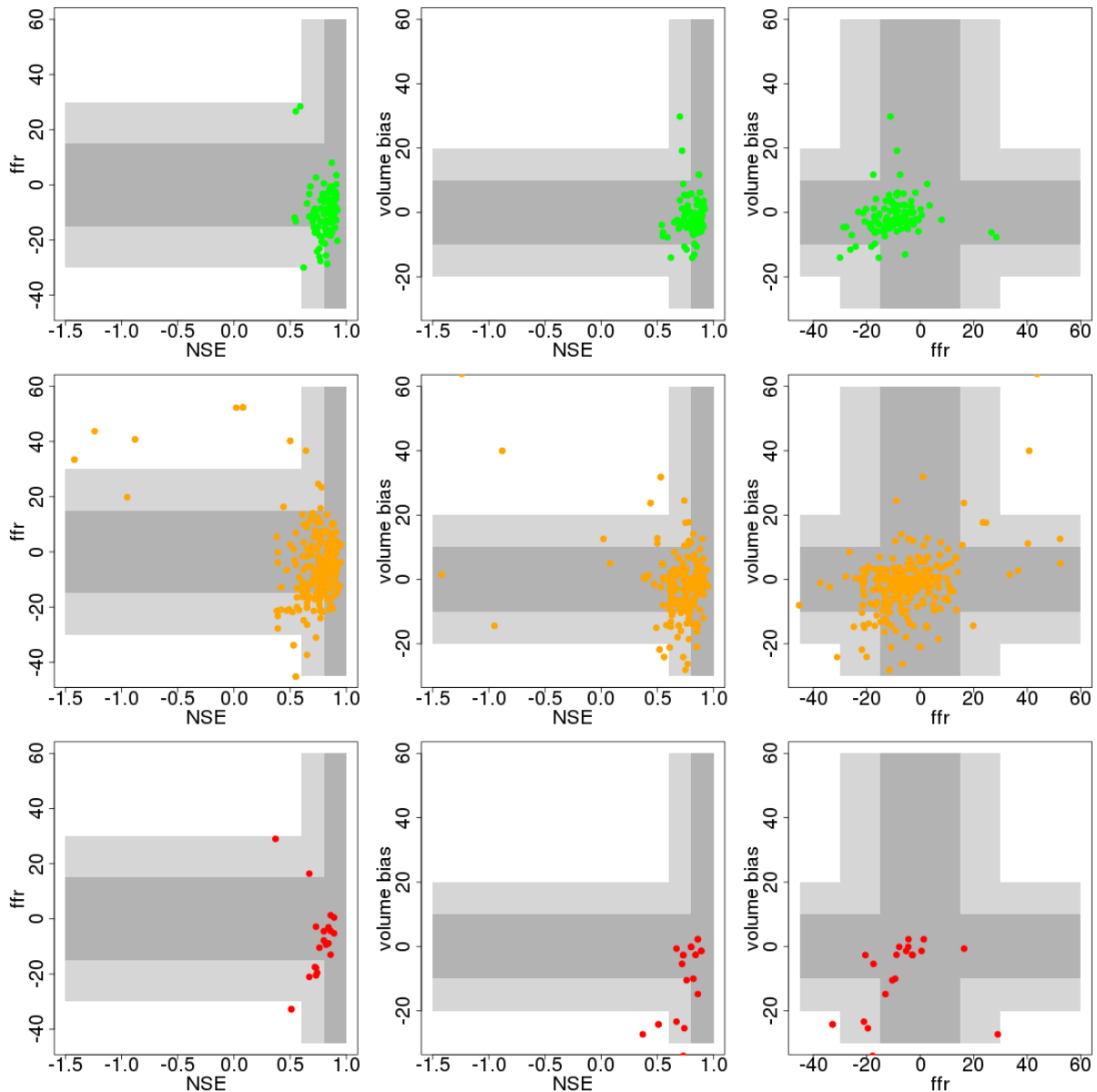


Figure A.4 Comparison of model performance measures (NSE, volume bias, ffr) for 94 catchments, separated by uncertainty indicator value (Low (green) – top; Medium (amber) – middle; High (red) - bottom). As in Figure A.3, the grey shading indicates very good (mid-grey) and good (light grey) performance bands for each performance measure

Figure A.4 presents plots of model performance stratified by the hydrological model uncertainty indicator, and shows that the two are not strongly related. Note that, in most cases where the gridded models (G2G and CLASSIC-GB) perform much worse than the catchment models (PDM/CLASSIC, GR4J), this is due to significant artificial influences on flows, which can be accounted for in catchment-specific calibration. Examples include 28015, for which the [NRFA flow regime description](#) states “reservoir(s) in the catchment together with significant abstraction and effluent returns affect runoff”; 34003 for which runoff is “influenced by groundwater abstraction/recharge” with “some returns from public and agricultural uses”; and 69037 which experiences “abstraction, augmentation and regulation” with “runoff probably substantially modified, at least temporally”. These catchments are the outliers visible in the medium (amber) uncertainty indicator plots of Figure A.4.

Box A.1: Hydrological models

To calculate the uncertainty indicator, output from 5 hydrological models was used; G2G, PDM, CLASSIC, CLASSIC-GB and GR4J. Below is a short summary of each model, more detail can be found in the references given.

G2G: The Grid-to-Grid model (Bell and others, 2009) is a national-scale distributed rainfall-runoff model with a 1km resolution over Great Britain. It runs at a 15-minute time step. Model parameters are set using digital data sets (for example, soil types, land cover).

PDM: The Probability Distributed Model (Moore, 1985, 2007) is a lumped rainfall-runoff model with 3 conceptual stores; a soil moisture store, and fast and slow flow stores. For small, hydrologically-responsive catchments (area < 50km²) it is typically run using hourly input data, otherwise it can be run using daily data.

CLASSIC: The Climate and Land-use Scenario Simulation In Catchments model (Crooks and Naden, 2007) is a semi-distributed grid-based rainfall-runoff model typically used for larger catchments and run with a daily time step. The grid to outlet structure is such that the simulated run-off from each grid square is routed directly to the catchment outlet rather than through successive grid cells. The total discharge at the outlet is given, adding together the routed run-off from each grid square. Most model parameters are set using digital data sets (for example, soil types).

CLASSIC-GB: A national-scale distributed hydrological model that uses a runoff-production scheme based on CLASSIC. It can be run at different spatial resolutions (Crooks and others, 2014) and simulates daily flow using a resolution-dependent time step.

GR4J: A daily lumped catchment model (Perrin and others, 2003) produced by IRSTEA in France. The model has 4 free parameters calibrated using gauged daily river flows.

G2G, CLASSIC and CLASSIC-GB require inputs of gridded rainfall and potential evaporation (PE), whereas PDM and GR4J require catchment-average values. All of the models except GR4J use (essentially) the same temperature-based snow module (Bell and others, 2016, Bell and Moore 1999), for which daily minimum and maximum temperature are required. GR4J does not currently include a snow module.

References

- BELL, V.A., KAY, A.L., DAVIES, H.N., JONES, R.G., 2016. An assessment of the possible impacts of climate change on snow and peak river flows across Britain. *Climatic Change*. 136: 539–553.
- BELL, V.A., KAY, A.L., JONES, R.G., MOORE, R.J., REYNARD, N.S., 2009. Use of soil data in a grid-based hydrological model to estimate spatial variation in changing flood risk across the UK. *Journal of Hydrology*. 377(3–4): 335–350.
- BELL, V.A., MOORE, R.J., 1999. An elevation dependent snowmelt model for upland Britain. *Hydrological Processes*. 13: 1887–1903.
- CROOKS, S.M., KAY, A.L., DAVIES, H.N., BELL, V.A., 2014. From Catchment to National Scale Rainfall-Runoff Modelling: Demonstration of a Hydrological Modelling Framework. *Hydrology*. 1(1): 63–88.
- CROOKS, S.M., NADEN, P.S., 2007. CLASSIC: a semi-distributed modelling system. *Hydrology and Earth System Sciences*. 11(1): 516-531.
- MOORE, R.J., 1985. The probability-distributed principle and runoff production at point and basin scales. *Hydrological Sciences Journal*. 30(2): 273-297.
- MOORE R.J., 2007. The PDM rainfall-runoff model. *Hydrology and Earth Systems Sciences*. 11(1): 483-499.
- PERRIN, C., MICHEL, C., ANDRÉASSIAN, V., 2003. Improvement of a parsimonious model for streamflow simulation. *Journal of Hydrology*. 279(1-4): 275–289.

Appendix B: Response types

B.1 Mapping response types

The G2G modelled response types are mapped in Figure B.1 for changes in 10-, 20- and 50- year return period flood peaks, using the 3 T/PE scenarios (Medium-August, Low-August, High-January). There is significant similarity between the maps (see main report).

These similarities and differences are summarised by bar charts showing the balance of response types over each river basin region. Figure B.2 and Figure B.3 compare return periods for the Low-August and High-January T/PE scenarios respectively.

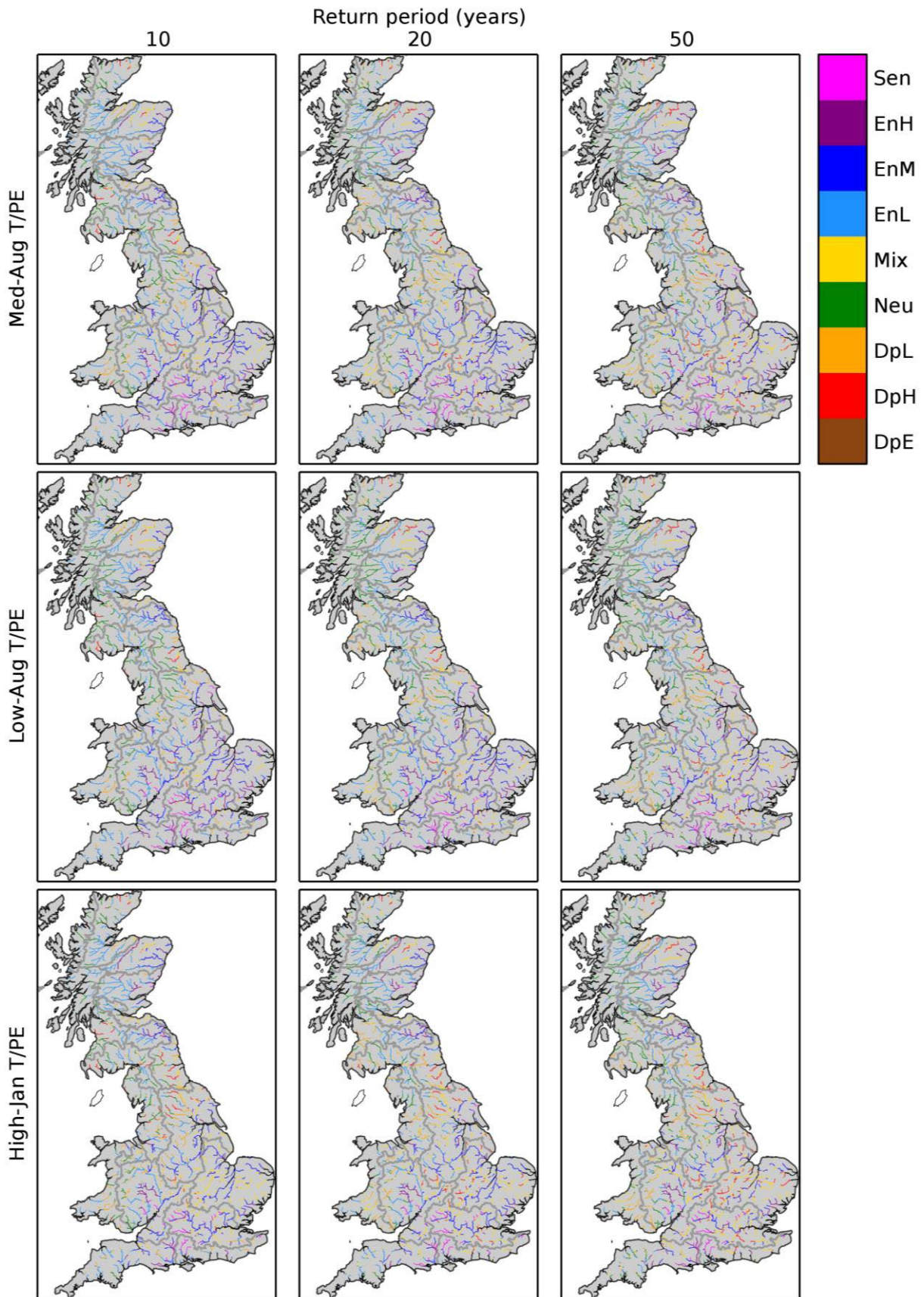


Figure B.1 Maps of the response type of modelled response surfaces, for changes in 10-, 20- and 50-year return period flood peaks (left to right) using the 3 T/PE scenarios (Medium-August, Low-August, High-January; top to bottom)

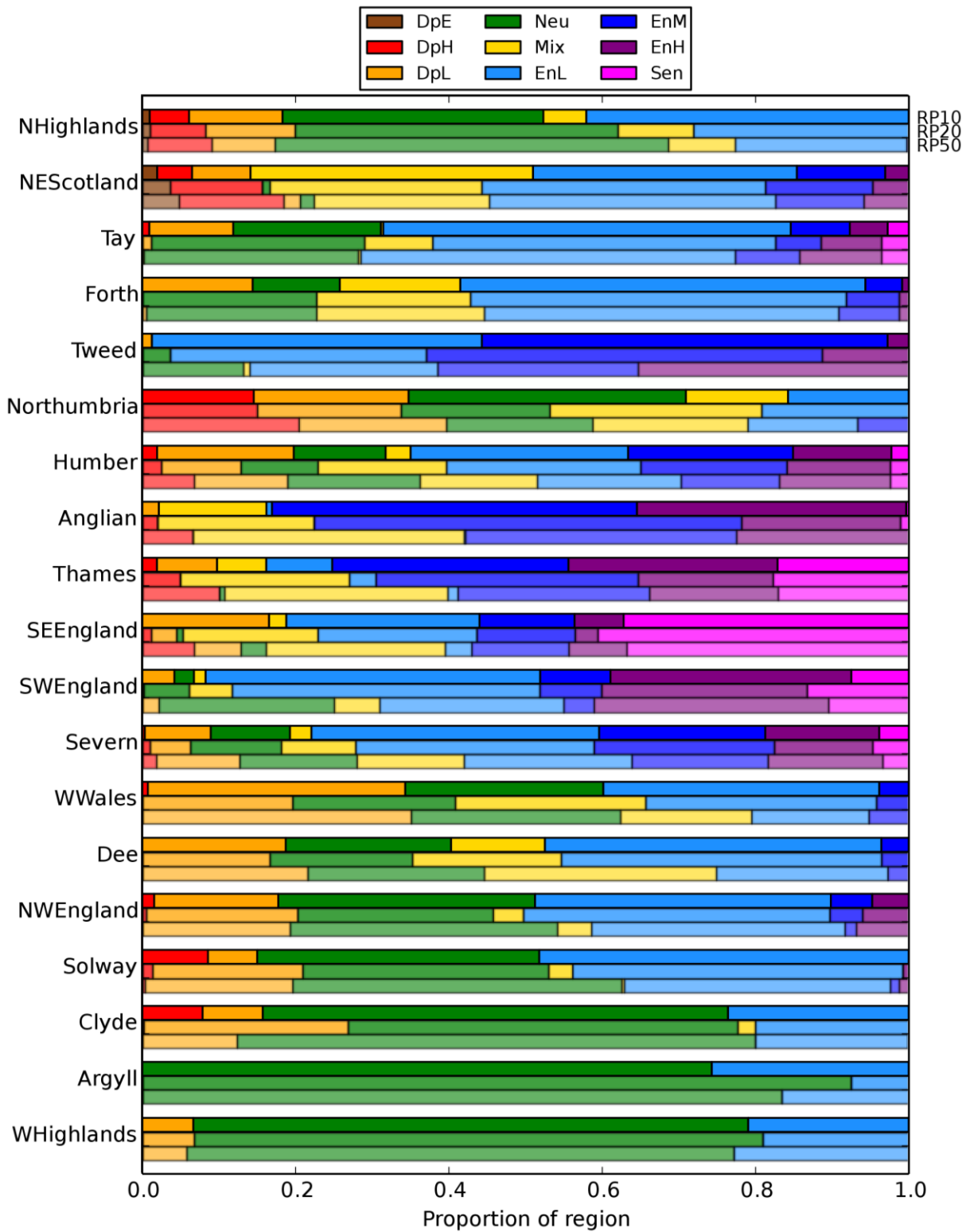


Figure B.2 Stacked bar charts showing the balance of response types over the 19 river basin regions, for changes in flood peaks at three return periods (10-, 20 and 50- years), for the Low-August T/PE scenario

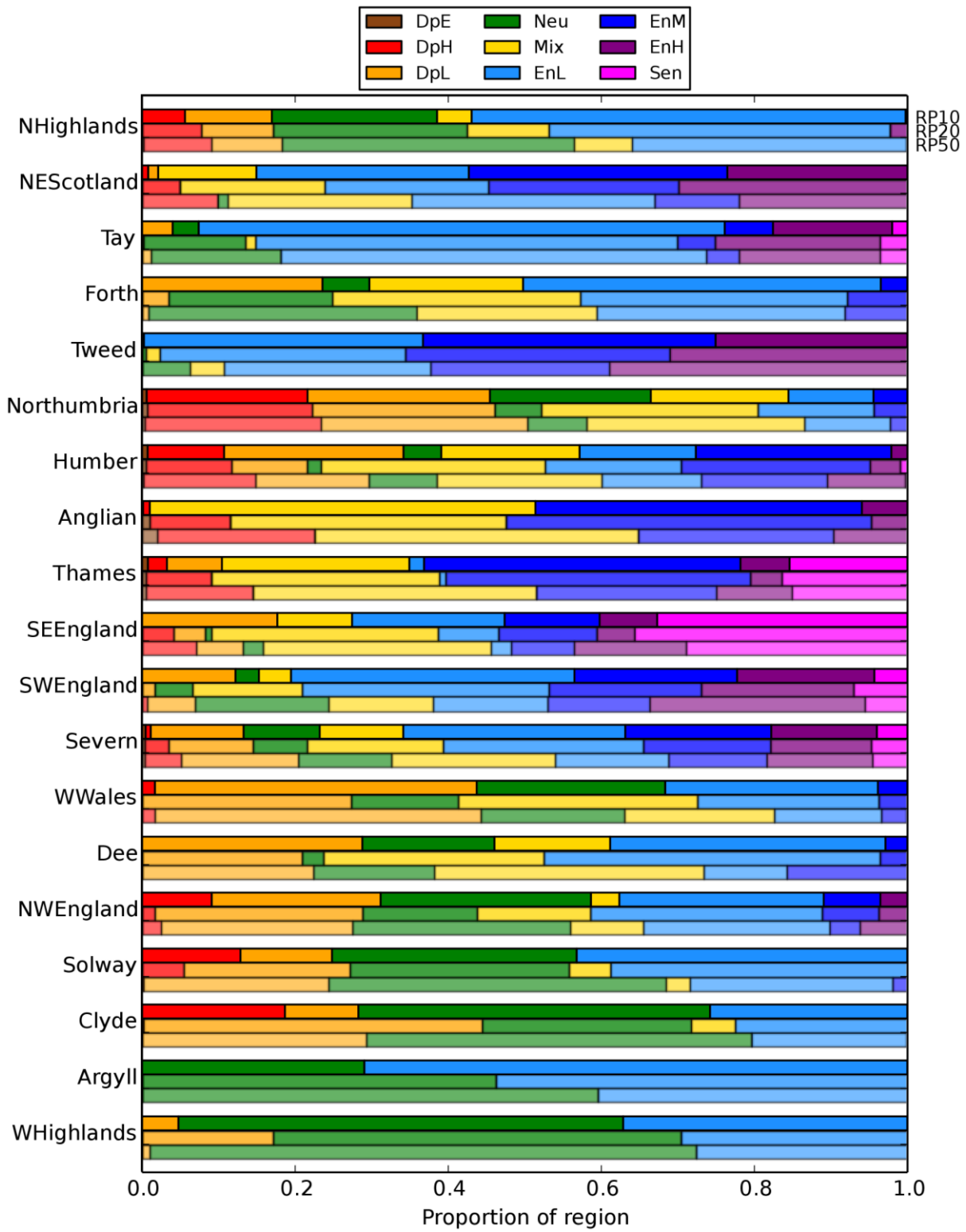


Figure B.3 As Figure B.2 but for the High-January T/PE scenario

B.2 Checking for new response types

Figures B.4 to B.12 show Taylor diagrams comparing the modelled response surfaces for each 1km river cell to the average response surfaces of the corresponding type, for 3 return periods (10-, 20- and 50-years) and for the 3 T/PE scenarios (Medium-August, Low-August and High-January). As expected, for each response type, the modelled response surfaces correspond to points on the Taylor diagrams that lie near where the correlation and standard deviation equal one. River points identified as having a Damped-Extreme (Brown), Damped-High (Red) or Sensitive response type (Magenta) show the largest intra-group variability (the points are not all very close to each other). The Taylor diagrams look similar across all return periods and T/PE scenarios, although with a tendency to greater intra-group variability for the higher return period.

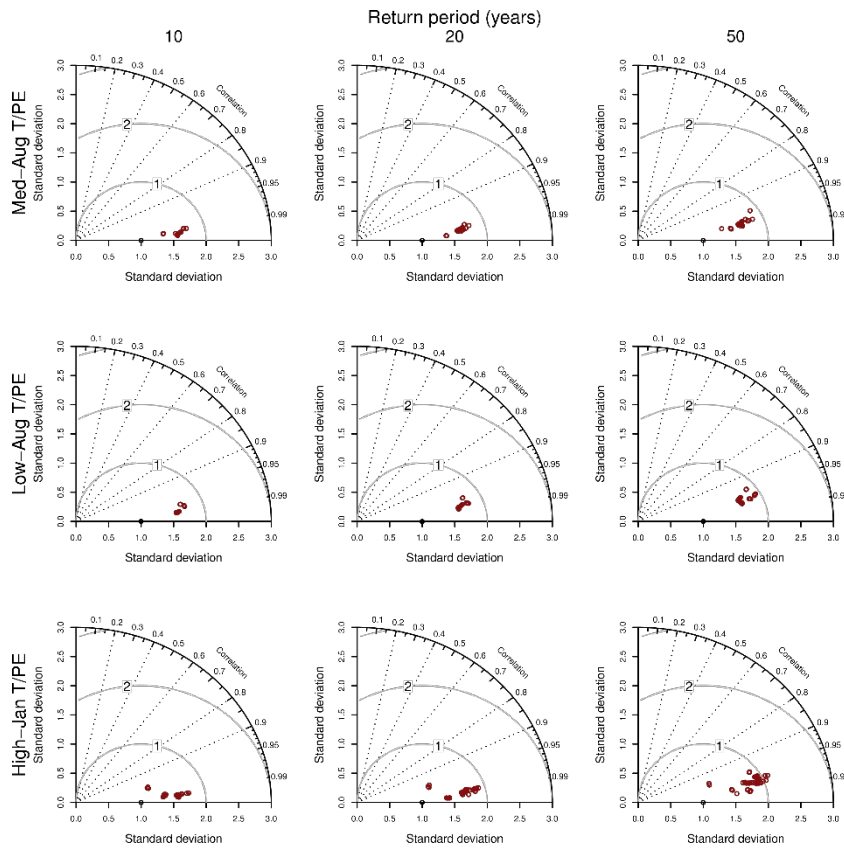


Figure B.4 Taylor diagrams comparing the modelled response surfaces for every 1km river cell identified as Damped-Extreme with the Damped-Extreme average response surface as reference.

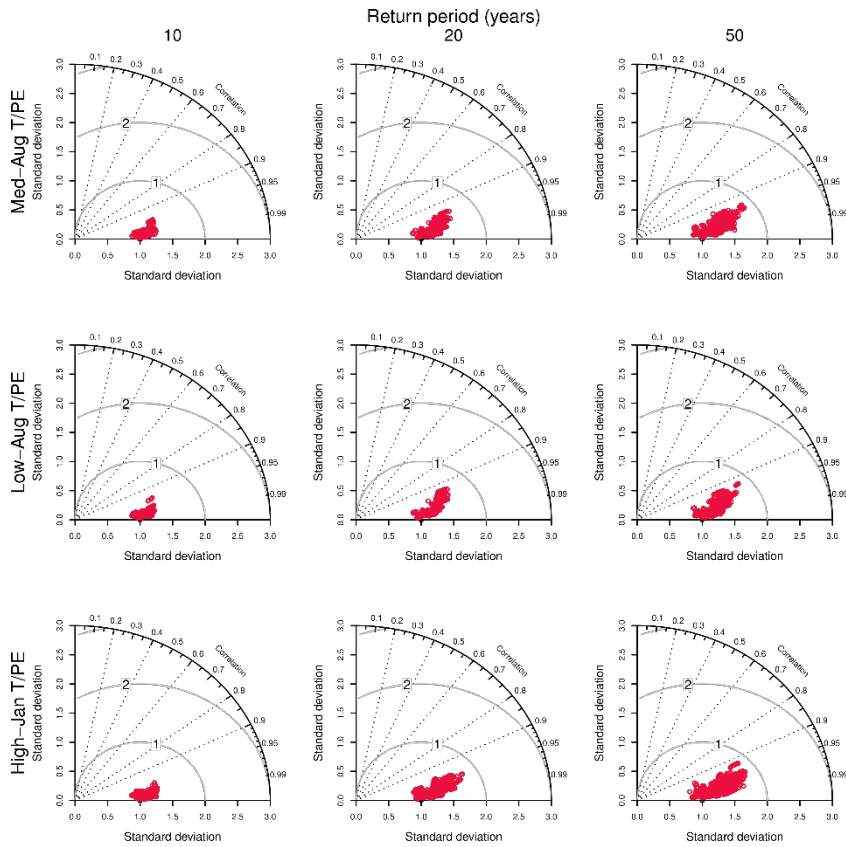


Figure B.5 As Figure B.4 but for Damped-High

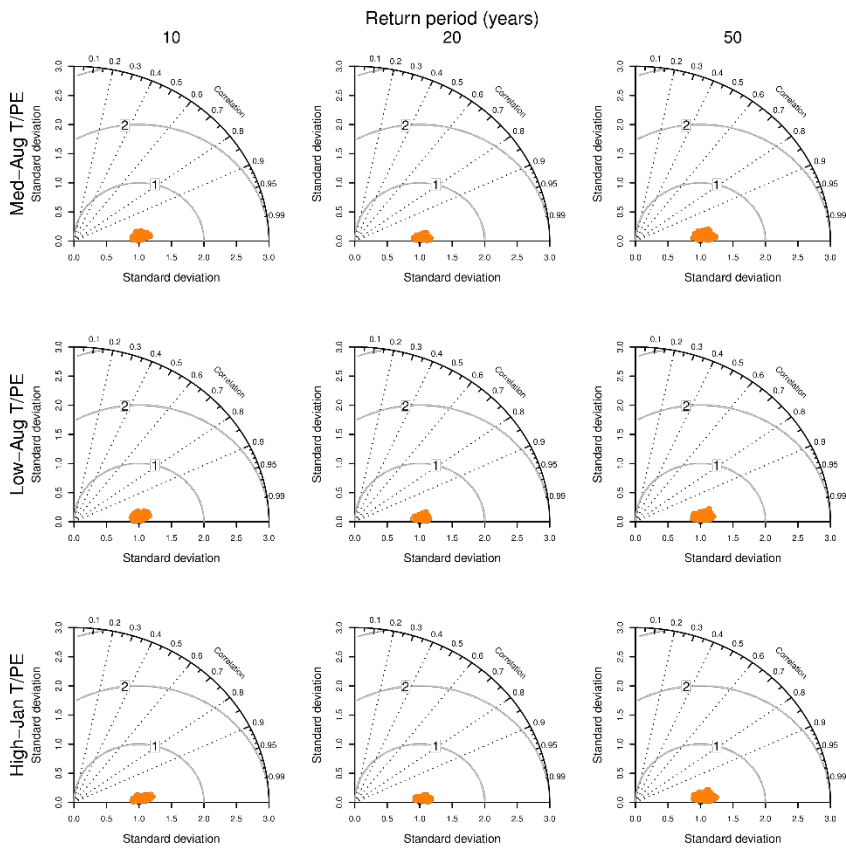


Figure B.6 As Figure B.4 but for Damped-Low

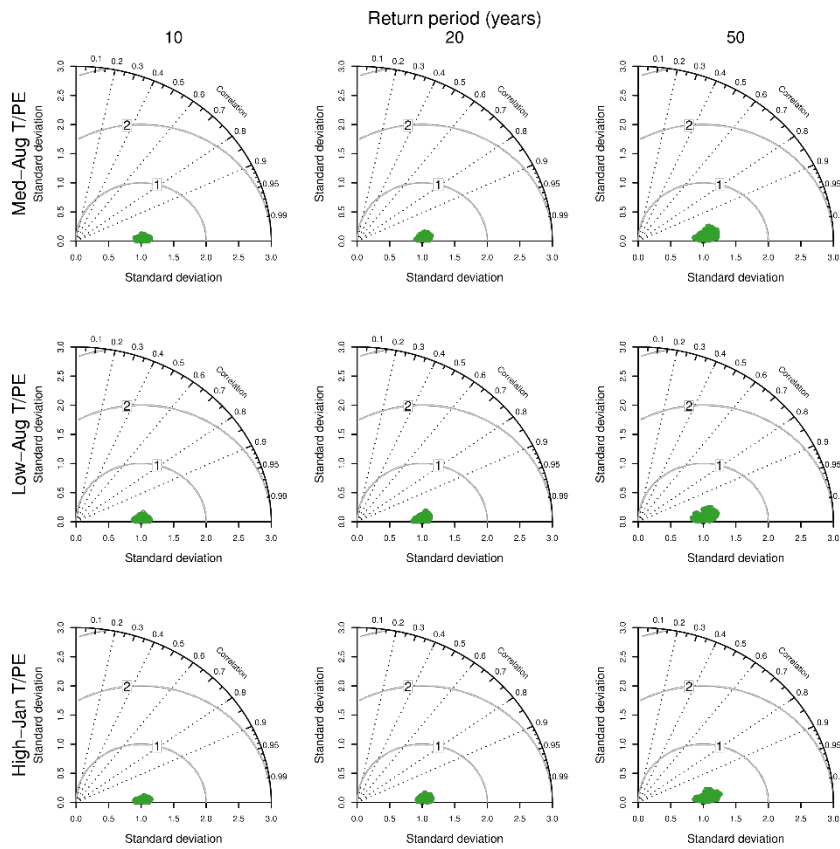


Figure B.7 As figure B.4 but for Neutral

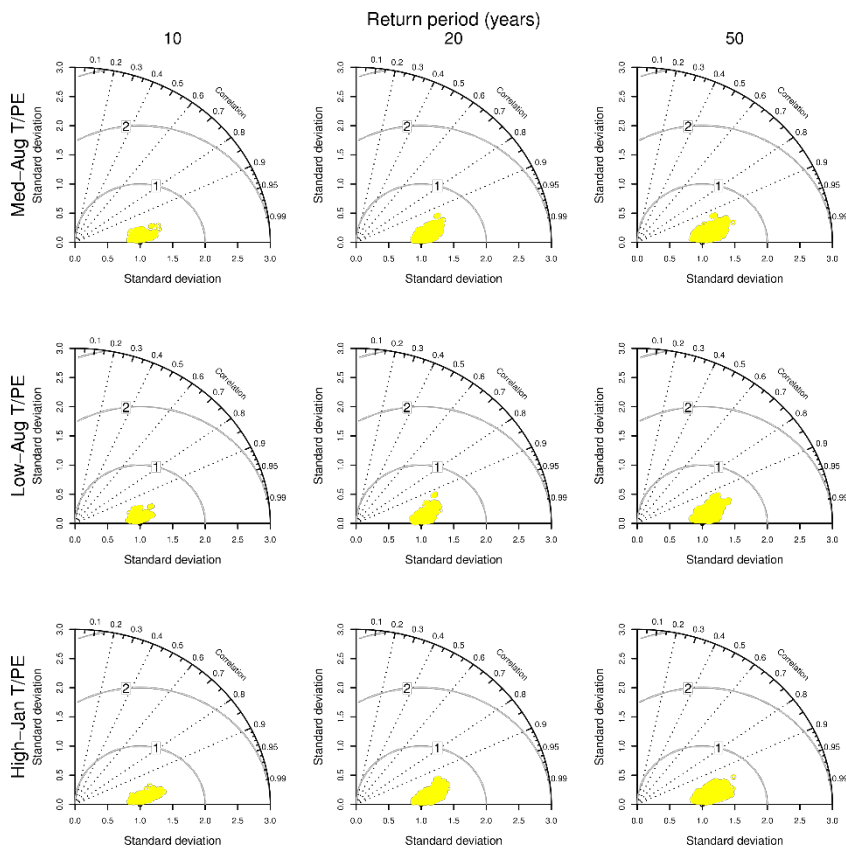


Figure B.8 As Figure B.4 but for Mixed

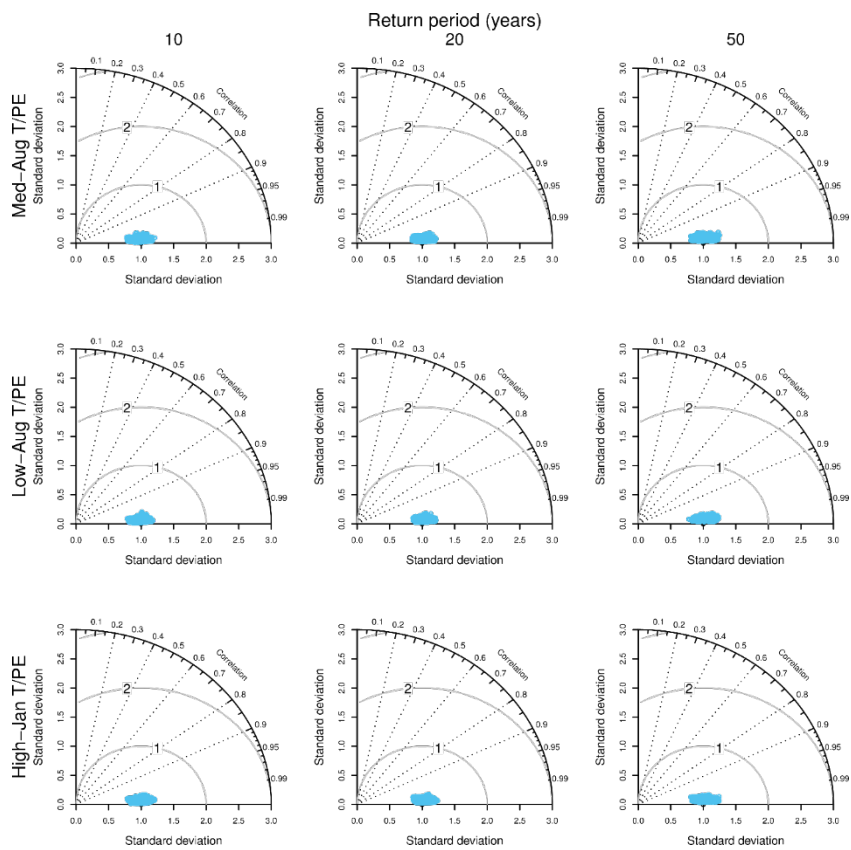


Figure B.9 As Figure B.4 but for Enhanced-Low

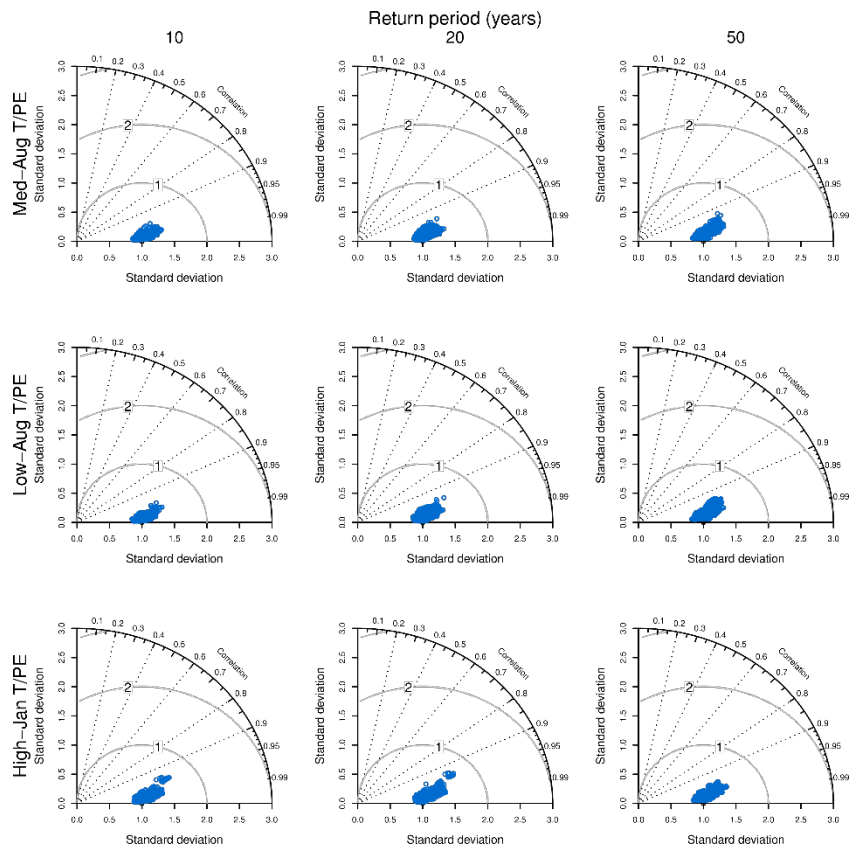


Figure B.10 As Figure B.4 but for Enhanced-Medium

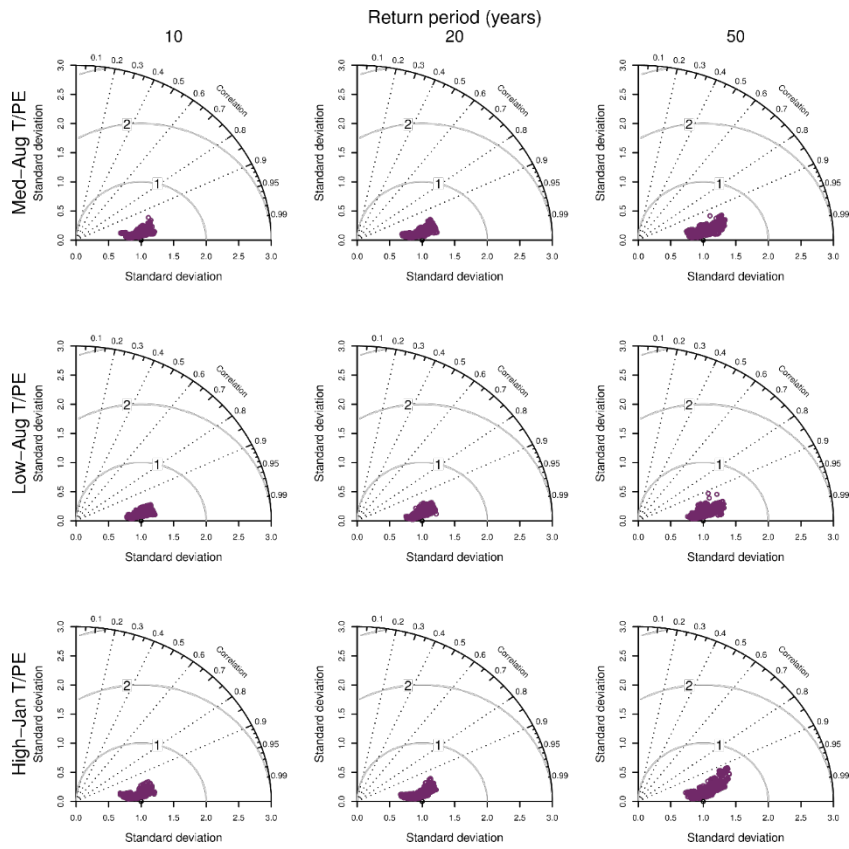


Figure B.11 As Figure B.4 but for Enhanced-High

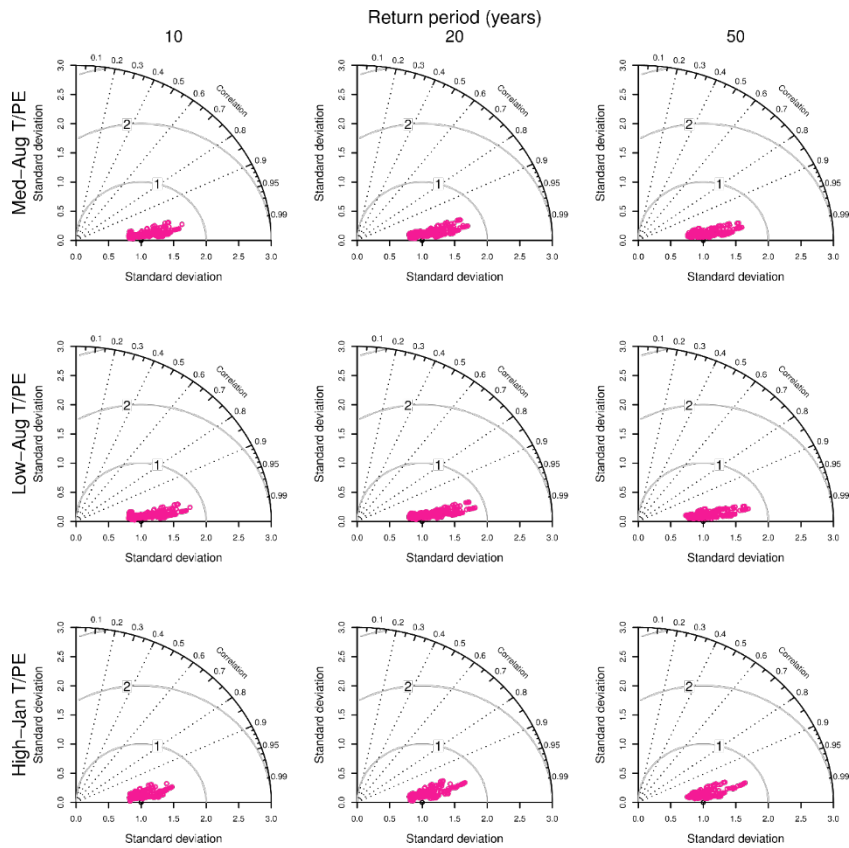


Figure B.12 As Figure B.4 but for Sensitive

Appendix C: Consistency of sensitivity domain with climate change projections

Figures C1 to C9 show contour plots and histograms describing how the precipitation and temperature changes used within the sensitivity domains relates to the UKCP18 climate change projections for temperature and rainfall at regional and UK scale.

C.1 Precipitation change projections

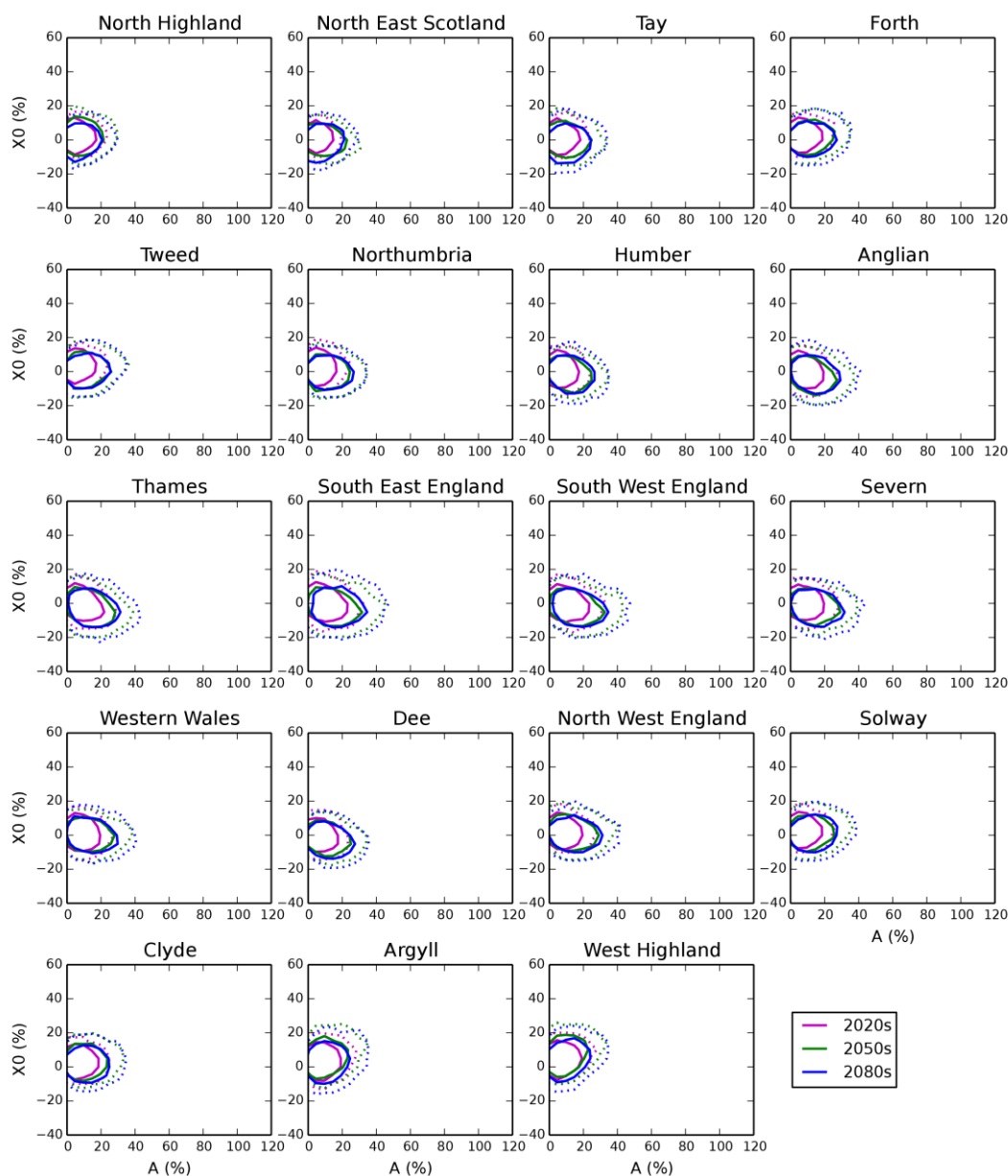


Figure C.1 Contour plots showing UKCP18 P harmonic mean (X_0) versus amplitude (A) for each river basin region, for RCP2.6 emissions for the 2020s, 2050s and 2080s (magenta, green and blue respectively). Contours delineate densities of 5 and 50 projections per 5% \times 5% sensitivity domain square (dotted and solid lines respectively)

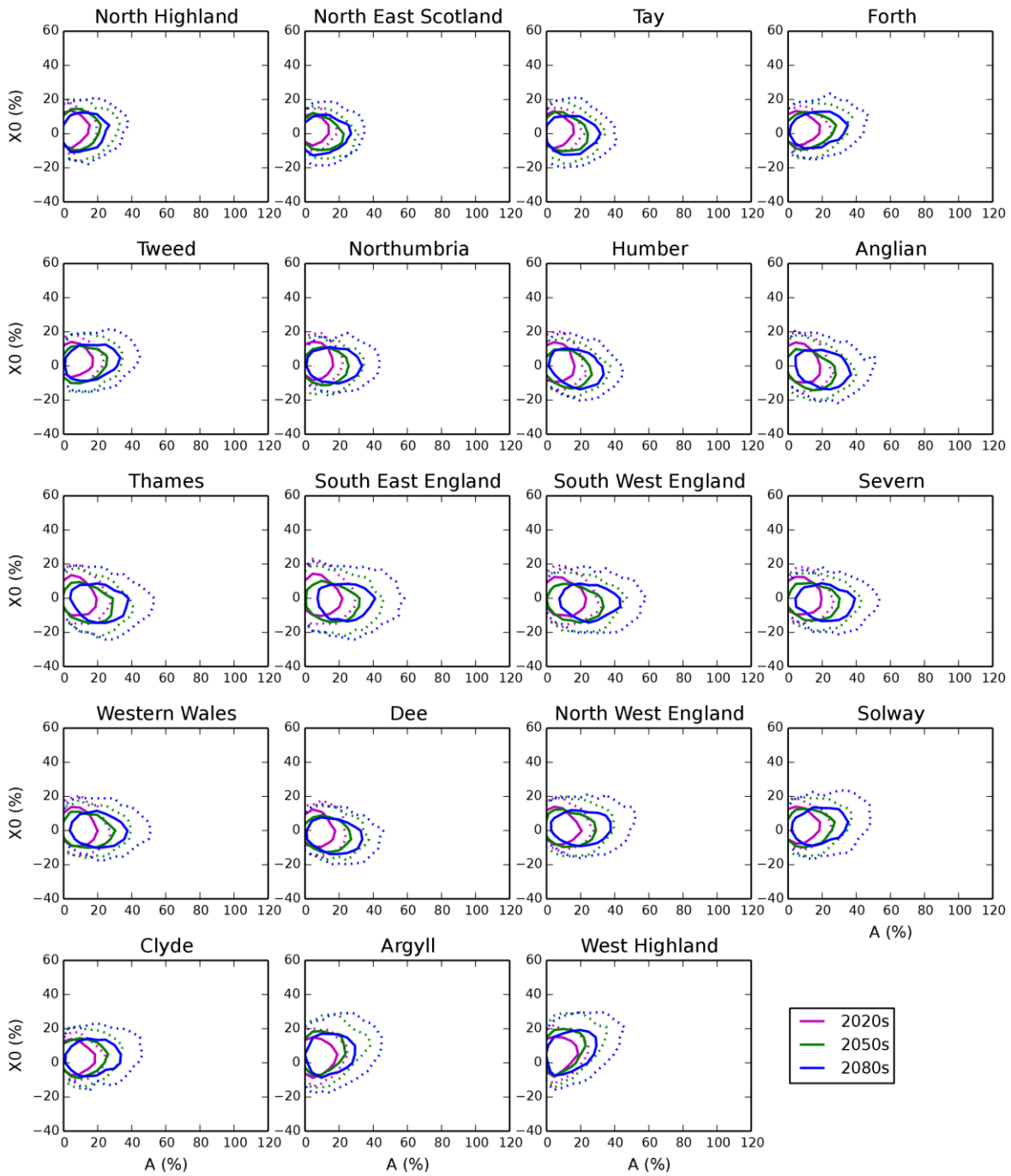


Figure C.2 As Figure C.1 but for RCP4.5

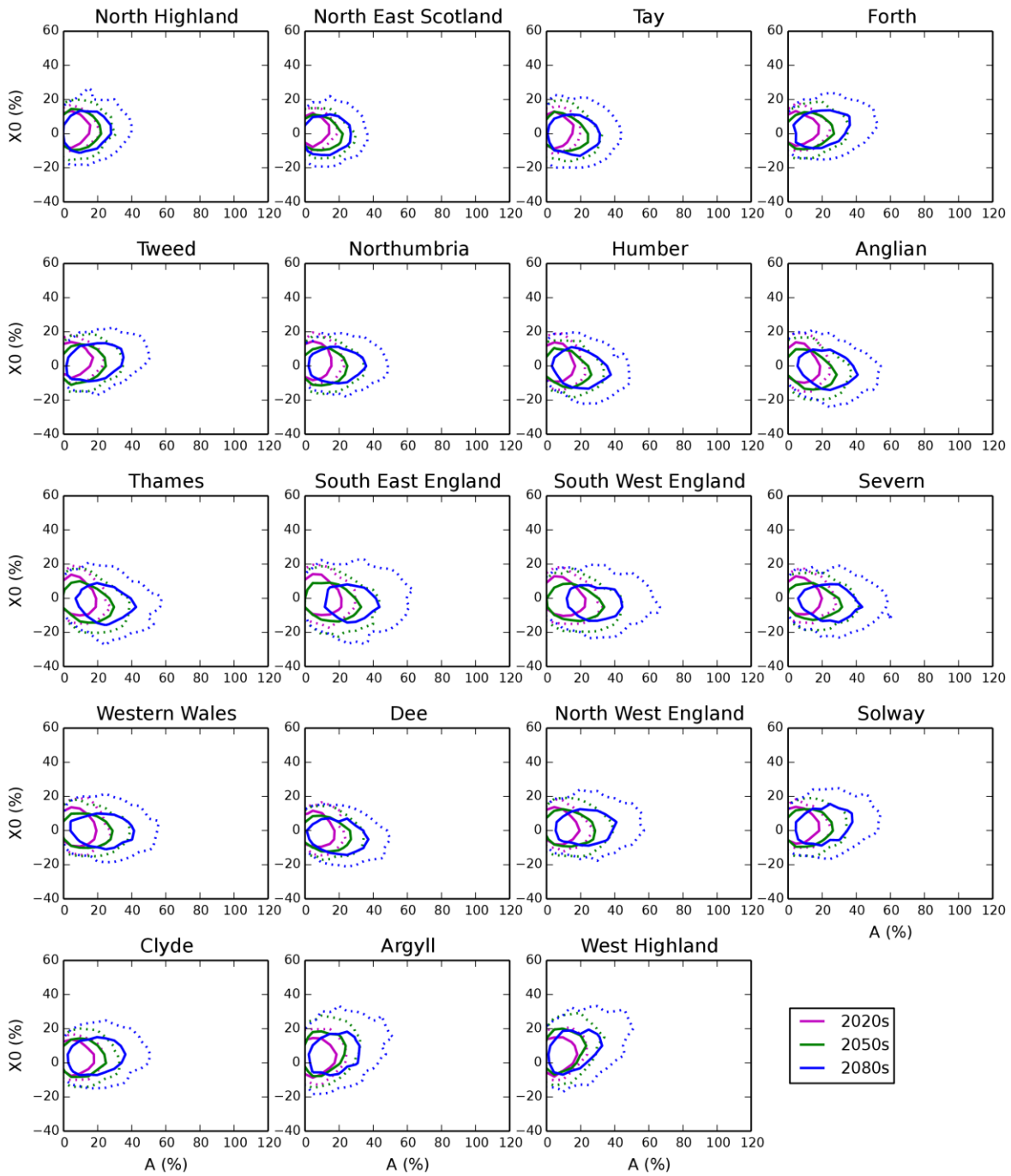


Figure C.3 As Figure C.1 but for RCP6.0

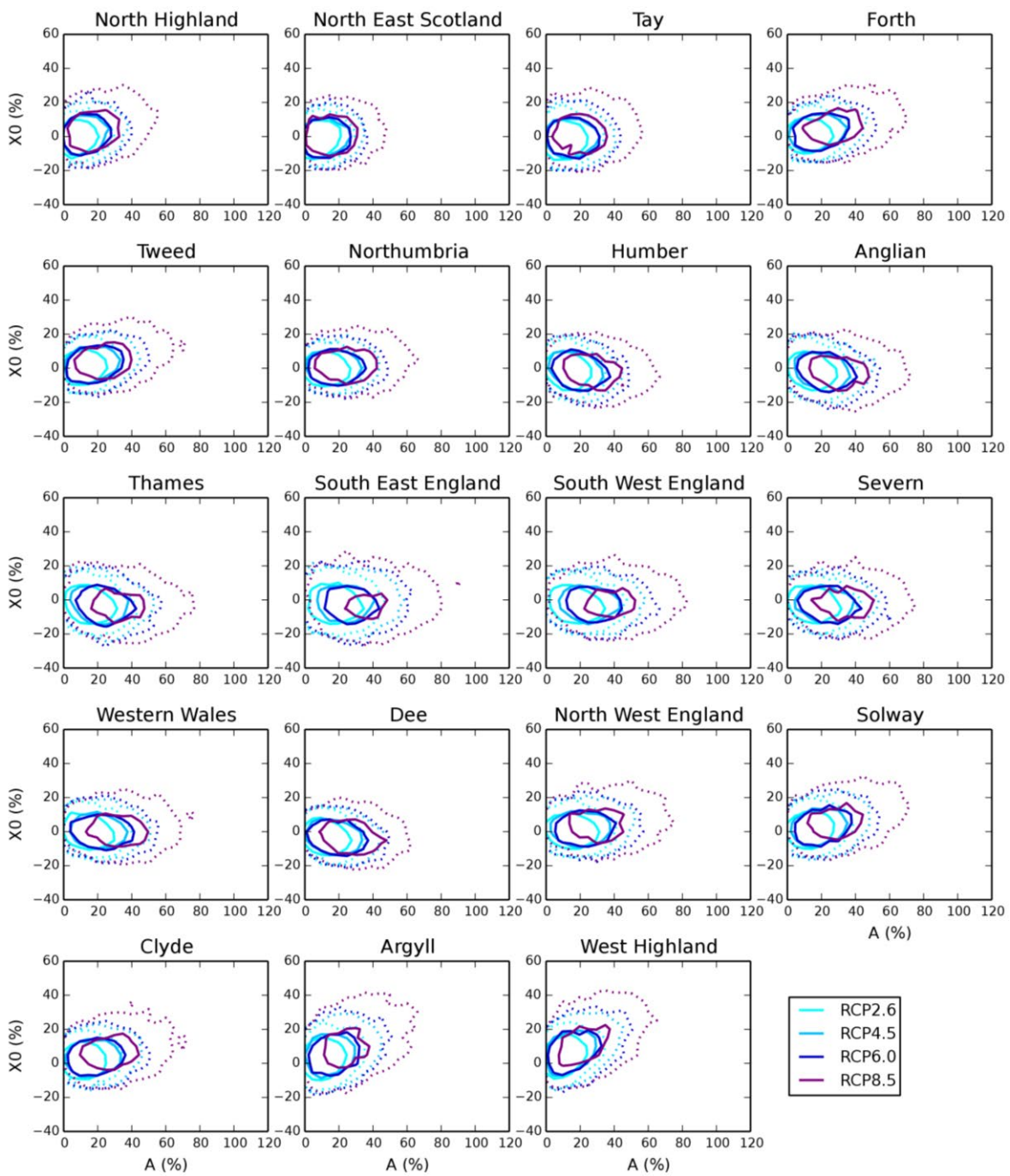


Figure C.4 Contour plots showing UKCP18 P harmonic mean (X_0) versus amplitude (A) for each river basin region, for the 2080s under RCP2.6, RCP4.5, RCP6.0 and RCP8.5 emissions (magenta, green and blue respectively). Contours delineate densities of 5 and 50 projections per 5% \times 5% sensitivity domain square (dotted and solid lines respectively).

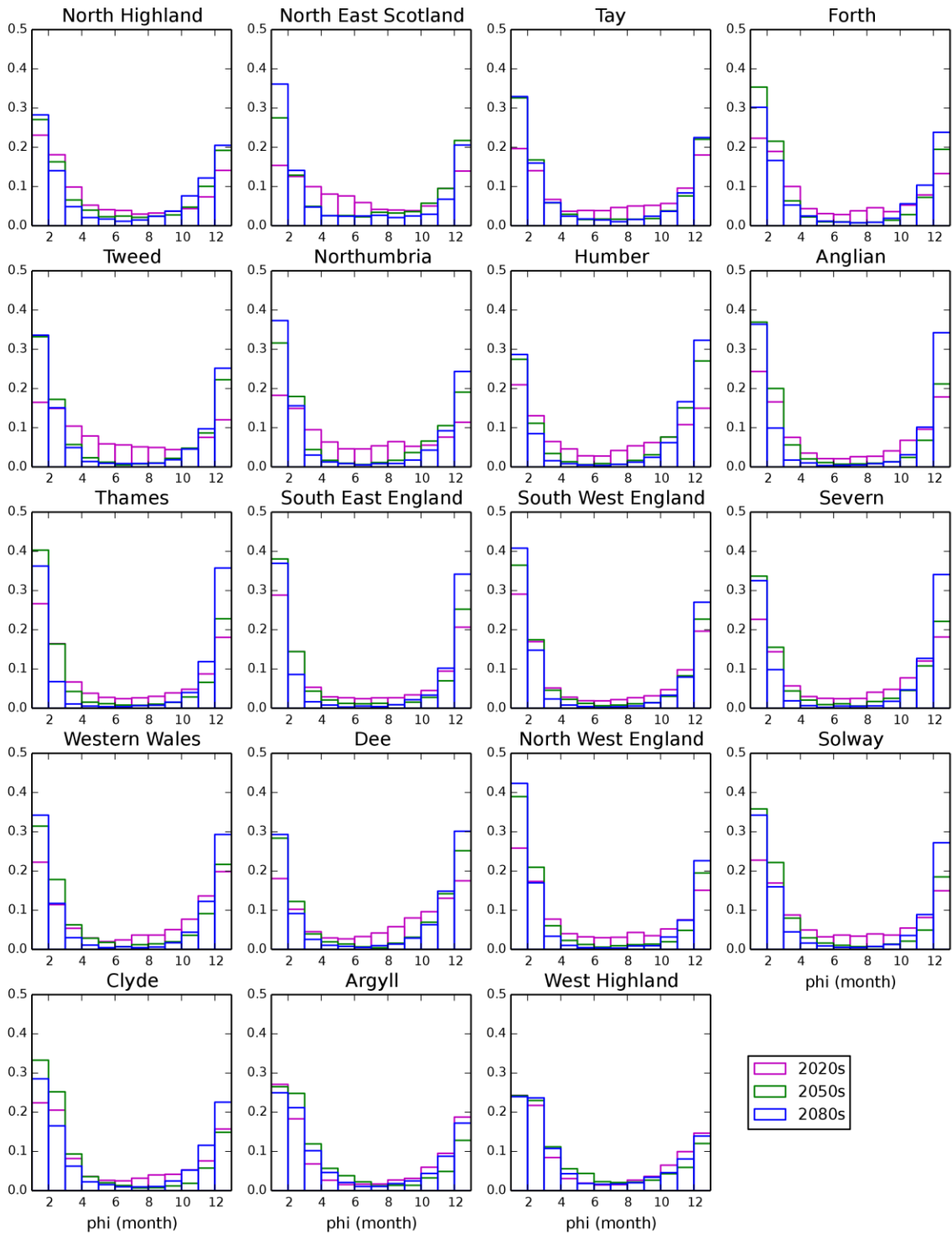


Figure C.5 Histograms showing the distribution of the UKCP18 P harmonic phase (Φ) for each river basin region, for RCP2.6 emissions for the 2020s, 2050s and 2080s (magenta, green and blue respectively)

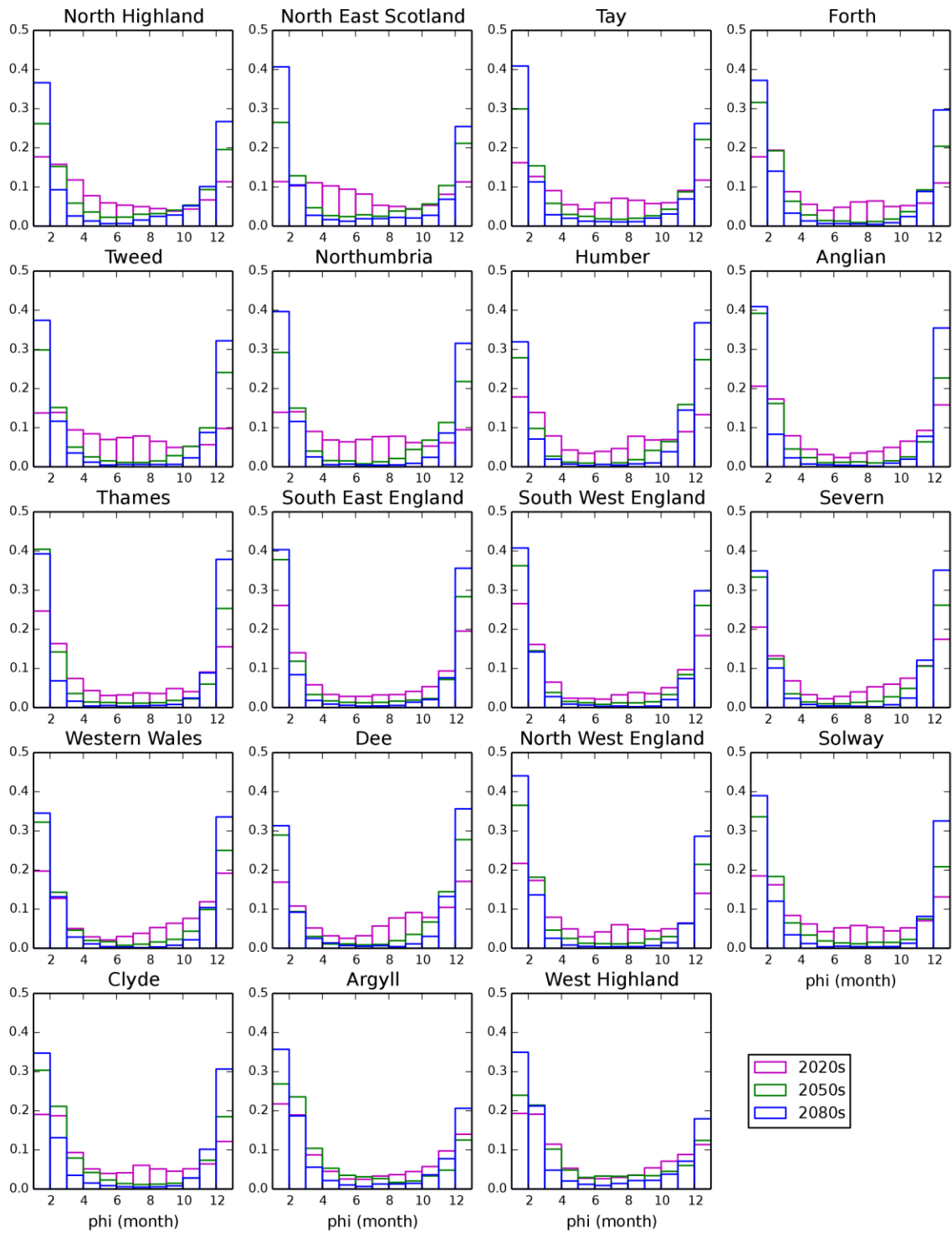


Figure C.6 As Figure C.5 but for RCP4.

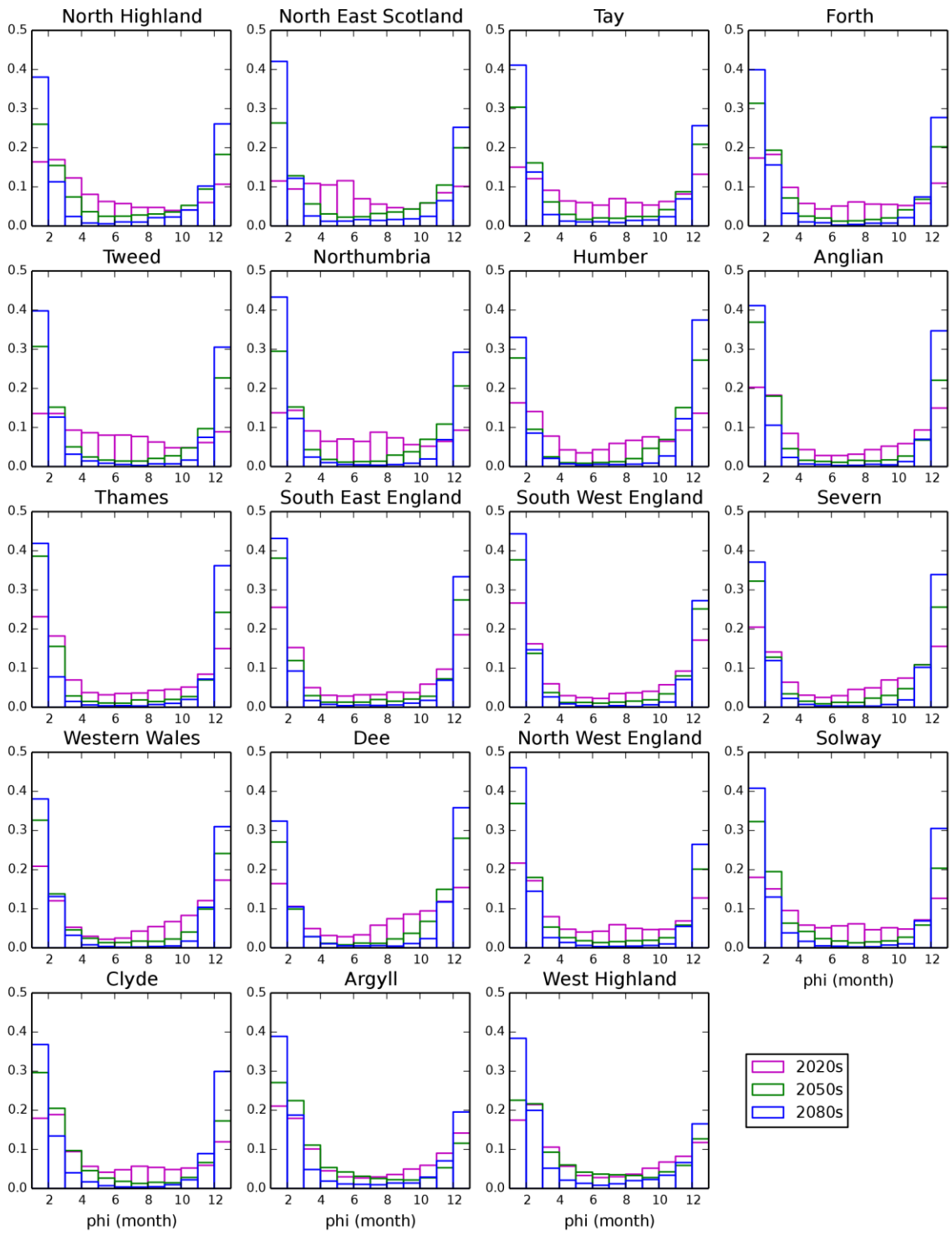


Figure C.7 As Figure C.5 but for RCP6.0

C.2 Temperature change projections

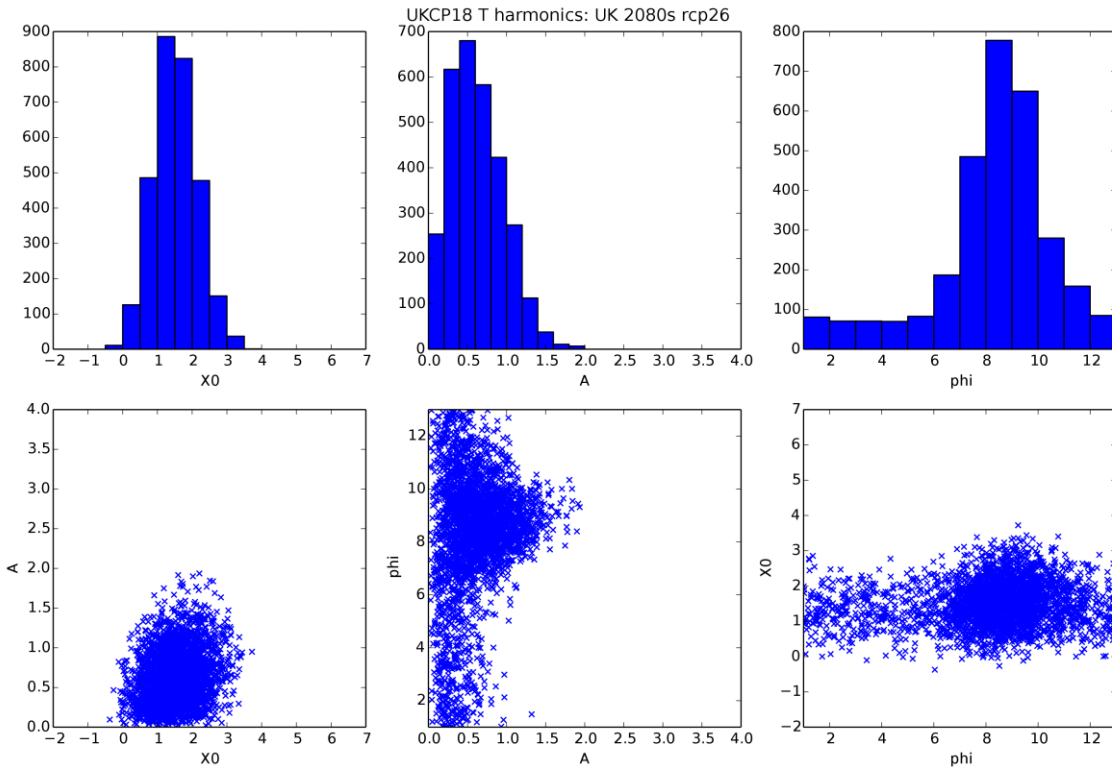


Figure C.8 Distribution of the 3 harmonic function parameters (X_0 , A , ϕ) from the UKCP18 probabilistic temperature change projections for the UK, for the 2080s under RCP2.6 emissions

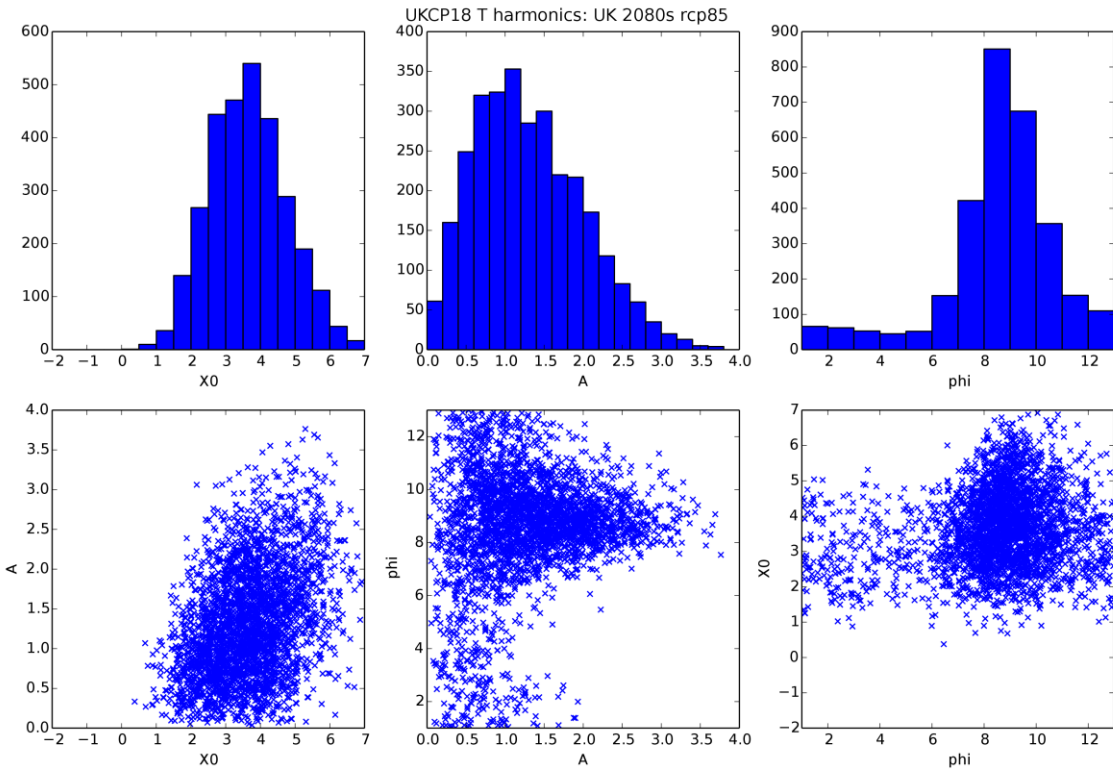


Figure C.9 As Figure C.8 but for RCP8.5 emissions

Appendix D: Web tool for exploring results

An interactive web tool has been developed to produce and explore the results (<https://eip.ceh.ac.uk/hydrology/cc-impacts/>). A river cell (catchment area $\geq 100\text{km}^2$) can be selected from a map of Great Britain, and then corresponding information and figures are shown (Figure D.1).

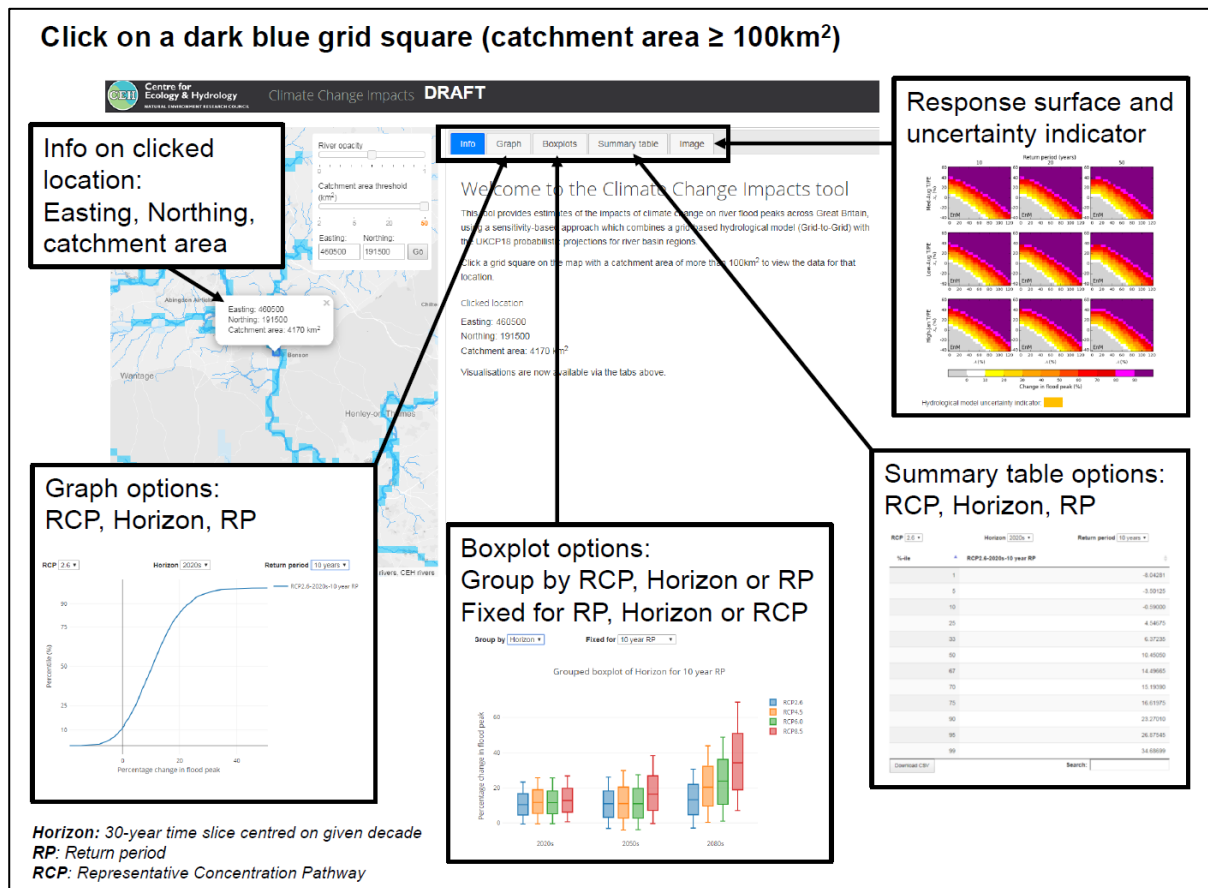


Figure D.1 Components of the climate change impacts web tool

There are 5 tabs:

- 1. Info tab** – provides a brief introduction to the tool, with instructions on selecting a grid square with a catchment area $\geq 100\text{km}^2$. It then gives the Easting, Northing and catchment area of the selected river cell (or a message asking the user to select another cell, if a cell without data is selected). See example in Figure D.2.
- 2. Graph tab** – shows the cumulative distribution function of the percentage change in flood peaks for the selected river cell, for a choice of 4 emissions scenarios (RCP2.6, 4.5, 6.0, 8.5), 3 time horizons (2020s, 2050s, 2080s) and 3 return periods (10-, 20- and 50-years). See example in Figure D.3.

3. **Boxplot tab** – allows comparison of the range of percentage changes in flood peaks for the selected river cell, for different emissions scenarios, time slices and return periods. See examples in Figure D.4. The whiskers show the 10th–90th percentile range.
4. **Summary table tab** – provides a data table with key percentiles of change in flood peaks for the selected river cell, which can be downloaded as a .csv file. See example in Figure D.5.
5. **Image tab** – shows the modelled response surfaces for the selected river cell, for the 3 return periods and 3 T/PE scenarios. The hydrological model uncertainty indicator (green/amber/red) for the selected river cell is also shown. See example in Figure D.6.

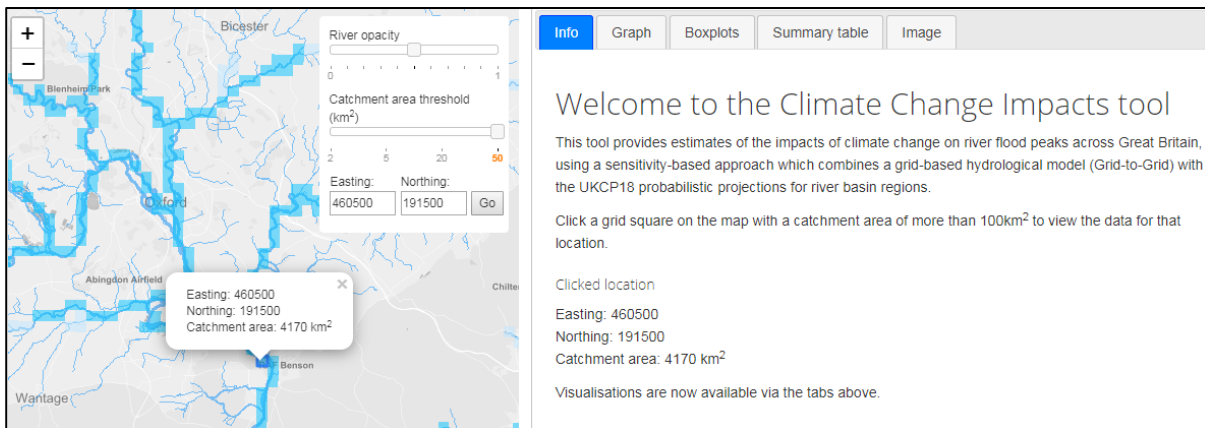


Figure D.2 Example Info, showing the Easting, Northing and catchment area of the selected river cell

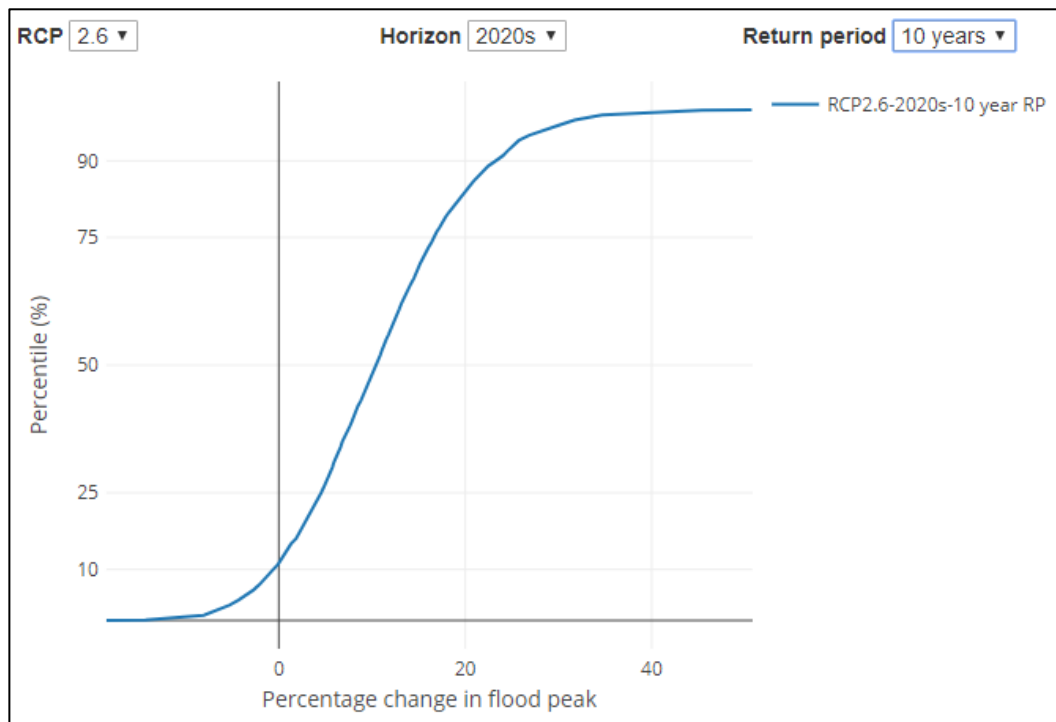
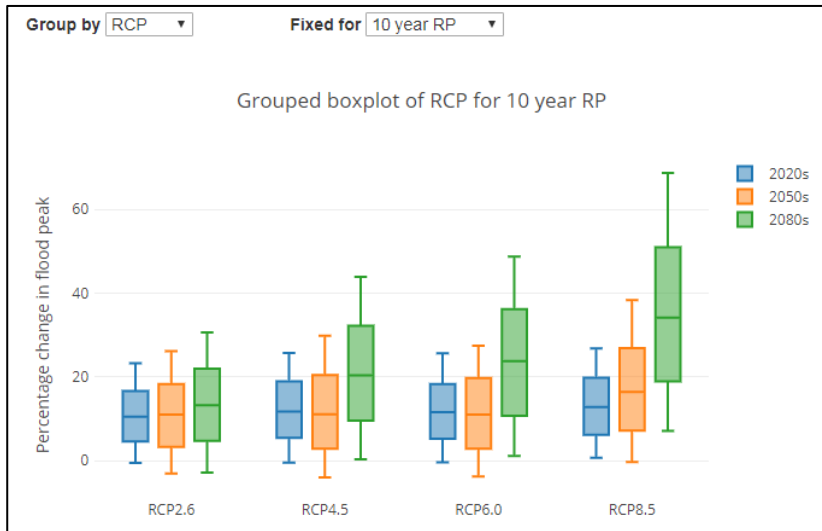
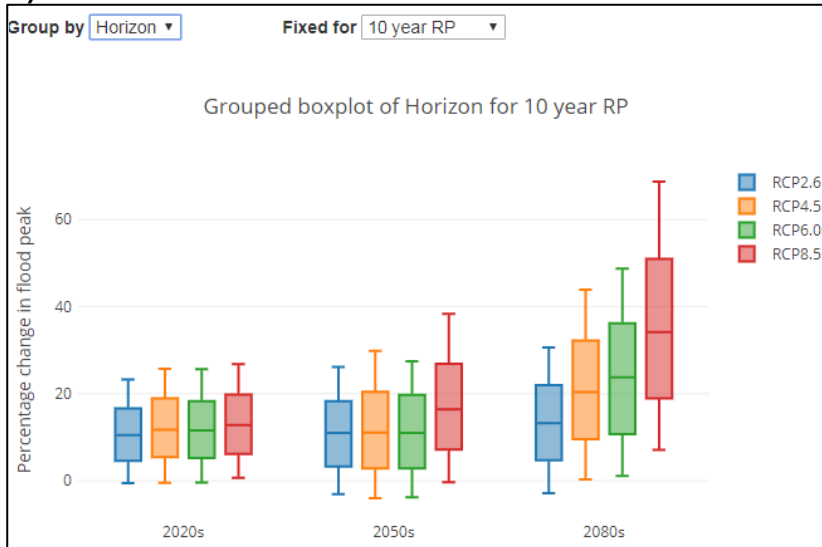


Figure D.3 Example graph, for the selected river cell, showing the cumulative distribution function of the percentage change in 10-year return period flood peaks for the 2020s under RCP2.6 emissions scenario

a)



b)



c)

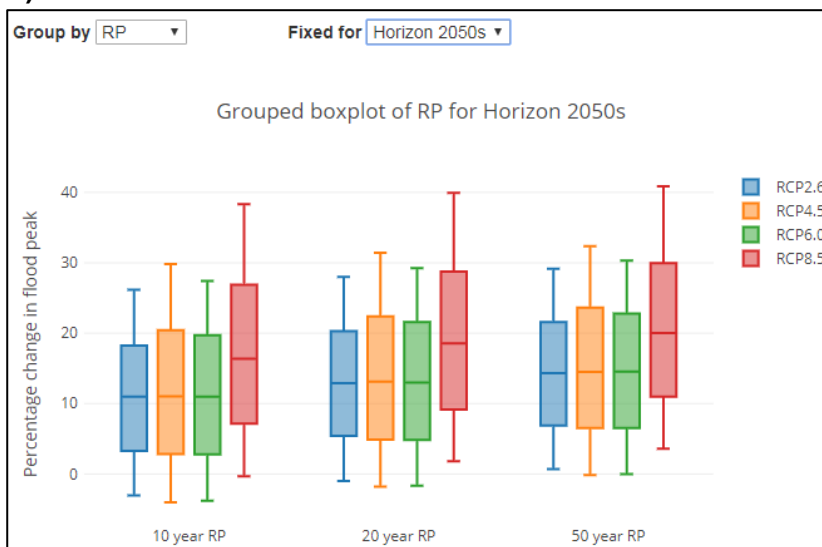


Figure D.4 Example boxplots, for the selected river cell, comparing the range of percentage changes in flood peaks: a) grouped by RCP and fixed for 10-year RP return period flood peaks, b) grouped by horizon and fixed for 10-year return period flood peaks c) grouped by flood return period and fixed by 2050s horizon

RCP 2.6 Horizon 2020s Return period 10 years

%-ile ▲ RCP2.6-2020s-10 year RP

1	-8.04281
5	-3.50125
10	-0.59000
25	4.54675
33	6.37235
50	10.45050
67	14.49665
70	15.19390
75	16.61975
90	23.27010
95	26.87545
99	34.68699

Download CSV Search:

Figure D.5 Example summary table, for the selected river cell, showing key percentiles for the percentage change in 10-year return period flood peaks for the 2020s under RCP2.6 emissions

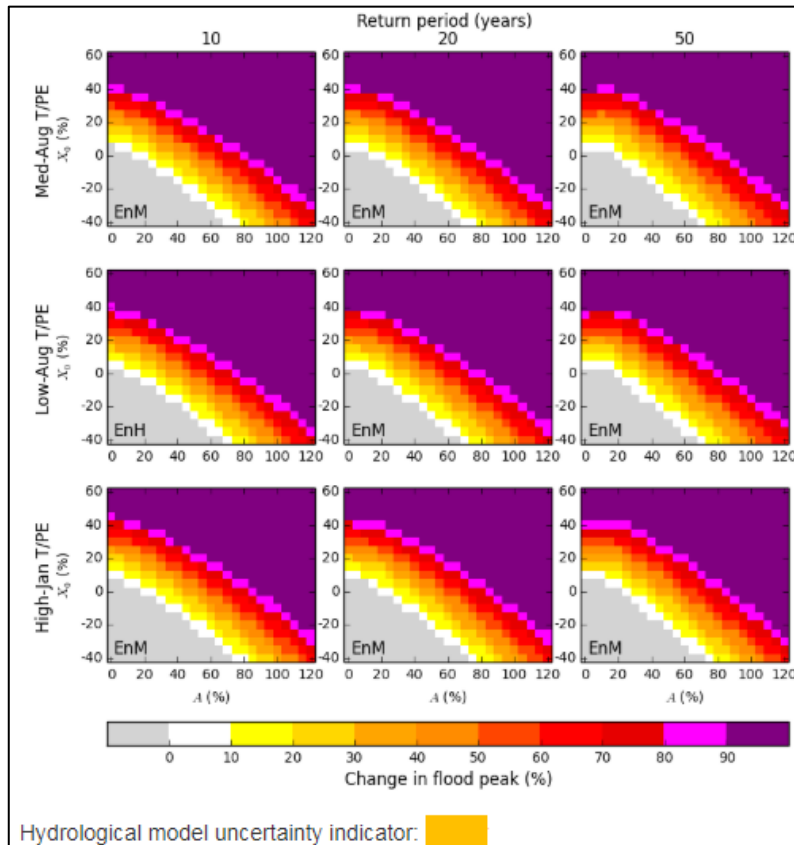


Figure D.6 Example image, for the selected river cell, showing the modelled response surfaces and the hydrological model uncertainty indicator

Would you like to find out more about us or your environment?

Then call us on

03708 506 506 (Monday to Friday, 8am to 6pm)

Email: enquiries@environment-agency.gov.uk

Or visit our website

www.gov.uk/environment-agency

incident hotline

0800 807060 (24 hours)

floodline

0345 988 1188 (24 hours)

Find out about call charges (<https://www.gov.uk/call-charges>)

Environment first

Are you viewing this onscreen? Please consider the environment and only print if absolutely necessary. If you are reading a paper copy, please don't forget to reuse and recycle.